

August 2023

## Cellular Heat Responses of Desert Mammals Promote Survival in Extreme Conditions

Janessa Montenegro  
*University of Nevada, Las Vegas*

Follow this and additional works at: <https://digitalscholarship.unlv.edu/thesesdissertations>



Part of the [Biology Commons](#)

---

### Repository Citation

Montenegro, Janessa, "Cellular Heat Responses of Desert Mammals Promote Survival in Extreme Conditions" (2023). *UNLV Theses, Dissertations, Professional Papers, and Capstones*. 4845.  
<http://dx.doi.org/10.34917/36948196>

This Thesis is protected by copyright and/or related rights. It has been brought to you by Digital Scholarship@UNLV with permission from the rights-holder(s). You are free to use this Thesis in any way that is permitted by the copyright and related rights legislation that applies to your use. For other uses you need to obtain permission from the rights-holder(s) directly, unless additional rights are indicated by a Creative Commons license in the record and/or on the work itself.

This Thesis has been accepted for inclusion in UNLV Theses, Dissertations, Professional Papers, and Capstones by an authorized administrator of Digital Scholarship@UNLV. For more information, please contact [digitalscholarship@unlv.edu](mailto:digitalscholarship@unlv.edu).

CELLULAR HEAT RESPONSES OF DESERT MAMMALS PROMOTE SURVIVAL IN  
EXTREME CONDITIONS

By

Janessa Montenegro

Bachelor of Science – Biological Sciences  
University of Nevada, Las Vegas  
2020

A thesis submitted in partial fulfillment  
of the requirements for the

Master of Science - Biological Sciences

School of Life Sciences  
College of Sciences  
The Graduate College

University of Nevada, Las Vegas  
August 2023



## Thesis Approval

The Graduate College  
The University of Nevada, Las Vegas

July 5, 2023

This thesis prepared by

Janessa Montenegro

entitled

Cellular Heat Responses of Desert Mammals Promote Survival in Extreme Conditions

is approved in partial fulfillment of the requirements for the degree of

Master of Science - Biological Sciences  
School of Life Sciences

Allyson Hindle, Ph.D.  
*Examination Committee Chair*

Sean Neiswenter, Ph.D.  
*Examination Committee Member*

Mo Weng, Ph.D.  
*Examination Committee Member*

Gary Kleiger, Ph.D.  
*Graduate College Faculty Representative*

Alyssa Crittenden, Ph.D.  
*Vice Provost for Graduate Education &  
Dean of the Graduate College*

## Abstract

Increasing temperatures with the potential for heat stress is among the future threats facing many mammals. Cellular mechanisms to maintain homeostasis in the face of heat stress likely differ across species based on naturally tolerated intracellular variability. In some mammals, the homeostatic set point in cells has a narrow range. Other species tolerate more varied intracellular conditions, including in temperature. Heat stress responses of cultured dermal fibroblasts from several mammals were compared to detect cell proliferation and cellular death (chapter 2). Cells from heat-tolerant species (13-lined ground squirrel, dromedary camel, round-tailed ground squirrel, and white-tailed antelope squirrel) were compared with cells from species with narrow observed body temperature ranges (human, rat, and southern white rhinoceros) to determine whether cell stress responses were consistent with known physiological flexibility. Consistent with predictions from organismal phenotypes, fibroblasts of presumed heat tolerant mammals were able to maintain cell proliferation at 41°C over many days compared to fibroblasts from heat sensitive mammals. Organismal phenotypes were not, however, consistent with cellular death levels. The mechanisms in response to heat stress were investigated to detect protein abundance and heat-stress gene expression patterns (HSF1, ERN1, PRKAA2, and CDKN1A) underlying resilience to heat stress versus patterns reflecting sensitivity (chapter 3). Immediate induction of ERN1 in the dromedary camels were identified. This study also identified patterns in HSF1 expression in rats, ERN1 expression in the southern white rhinoceros, PRKAA2 expression in the round-tailed ground squirrels, southern white rhinoceros and rat, and CDKN1A expression in the southern white rhinoceros over shorter scaled time

durations of heat exposure at 41°C. Cells from rat, antelope ground squirrel, and 13-lined ground squirrel were analyzed via proteomics following a 6- and 24h heat exposure. Differentially expressed proteins provided better insight into species-specific response mechanisms to heat stress.

## Acknowledgements

I would like to thank my advisor Dr. Allyson G. Hindle for her guidance and support throughout this project. Allyson has challenged me to critically think outside of a molecular based view and more from a physiological standpoint.

My lab experience was accented by lab members in Allyson's lab. I would like to extend my appreciation to Allyson's previous post-doctoral researcher, Dr. Carla B. Madelaire, and current graduate student, Amy C. Klink, who have worked on this project and have also guided me throughout the process. Thank you to Thomas J. Crippen and Sebastiano Cupani, who are also graduate students in Allyson's lab, for their support. In addition, I would also like to acknowledge the undergraduate students who have assisted me with cell maintenance and RNA extractions: Hannah Gould, Nathan Vu, Micaah Douglas, and Josie Martinez.

I would like to express my gratitude to my other committee members, Dr. Sean Neiswenter, Dr. Gary Kleiger, and Dr. Mo Weng for their guidance and advice in directing this project.

I would like to thank my parents and sister for their strong support and encouragement. Their continuous support of my endeavors has helped me stay focused and motivated to keep moving forward in my education and career.

## Table of Contents

Abstract.....	iii
Acknowledgements .....	v
List of Tables .....	viii
List of Figures .....	viii
Chapter 1: Introduction.....	1
Background .....	1
Research Objectives.....	9
Research questions and hypotheses .....	13
Chapter 2: Cell sensitivity matches organism sensitivity.....	15
Background .....	15
Methods.....	18
Results.....	26
Discussion .....	34
Chapter 3: Mechanisms of resilience at the cellular level .....	40
Introduction.....	40
Methods.....	43
Results.....	50
Discussion .....	78

Chapter 4 .....	85
Summary of findings .....	85
Limitations .....	86
Future directions.....	87
Significance .....	89
Appendix .....	90
References.....	120
Curriculum Vitae .....	135



## List of Tables

Table 1. Passage number of primary dermal fibroblasts used for LDH and crystal violet assays, and qPCR.....	90
Table 2. Optimal cell number plated for viability and proliferation assays.....	92
Table 3. Crystal violet absorbance values.....	93
Table 4. Normalized viability data. ....	97
Table 5. Repeated measures ANOVA table for cell proliferation data. ....	102
Table 6. Repeated measures ANOVA table for cell viability data. ....	103
Table 7. Linear mixed effects analysis on cell proliferation and cell viability data. ....	104
Table 8. SYBR Green primers developed for qPCR gene expression assays. ....	105
Table 9. Outliers excluded from qPCR analysis.....	108
Table 10. T-test results comparing relative fold change of expression between 0- and 0.5 hours.....	109
Table 11. Wilcoxon test results comparing relative fold change of expression between 0- and 0.5 hours.....	110
Table 12. One-way ANOVA test results comparing the mean expression at 0.5 hours at 41°C for HSF1. ....	110
Table 13. Three-level nested ANOVA analyzing HSF1 expression differences at 0.5 hours at 41°C for heat tolerant and heat sensitive phenotypes of different species. ...	110
Table 14. Repeated measures ANOVA results for HSF1 gene expression patterns...	110
Table 15. Linear mixed effects analysis on HSF1, ERN1, PRKAA2, and CDKN1A gene expression.....	111

Table 16. One-way ANOVA test results comparing the mean expression at 0.5 hours at 41°C for ERN1.....	112
Table 17. Three-level nested ANOVA analyzing ERN1 expression differences at 0.5 hours at 41°C for heat tolerant and heat sensitive phenotypes of different species. ...	113
Table 18. Repeated measures ANOVA results for ERN1 gene expression patterns. .	113
Table 19. One-way ANOVA test results comparing the mean expression at 0.5 hours at 41°C for PRKAA2. ....	114
Table 20. Nested ANOVA analyzing PRKAA2 expression differences at 0.5 hours at 41°C for heat tolerant and heat sensitive phenotypes of different species. ....	114
Table 21. Repeated measures ANOVA results for PRKAA2 gene expression patterns. ....	114
Table 22. One-way ANOVA test results comparing the mean expression at 0.5 hours at 41°C for CDKN1A.....	116
Table 23. Nested ANOVA analyzing CDKN1A expression differences at 0.5 hours at 41°C for heat tolerant and heat sensitive phenotypes of different species. ....	116
Table 24. Repeated measures ANOVA results for CDKN1A gene expression patterns. ....	116
Table 25. Significant induction of HSPs demonstrating desert-dwelling and species-specific mechanisms. ....	117
Table 26. Selected variables generated by Random Forest.....	118
Table 27. Selected variables with 75% or higher appearance rate. ....	119

## List of Figures

Figure 1. Schematic of experimental design for chapter 2.....	23
Figure 2. Relative frequency (%) distribution exhibiting the effect of chronic heat exposure (41°C) on cell proliferation of presumed heat tolerant mammals. ....	27
Figure 3. Relative frequency (%) distribution exhibiting the effect of chronic heat exposure (41°C) on cell proliferation of presumed heat sensitive mammals. ....	28
Figure 4. Relative frequency (%) distribution exhibiting the effect of chronic heat exposure (41°C) for 2-8 days on cell proliferation of all presumed (A) heat tolerant and (B) heat sensitive mammals.....	29
Figure 5. Relative frequency (%) distribution exhibiting the effect of chronic heat exposure (41°C) on cell viability of presumed heat tolerant mammals. ....	31
Figure 6. Relative frequency (%) distribution exhibiting the effect of chronic heat exposure (41°C) on cell viability of presumed heat sensitive mammals. ....	32
Figure 7. Relative frequency (%) distribution exhibiting the effect of chronic heat exposure (41°C) for 2-8 days on cell viability of all presumed (A) heat tolerant and (B) heat sensitive mammals.....	33
Figure 8. Schematic of experimental design for chapter 3.....	44
Figure 9. The effect of heat stress (41°C) did not cause an immediate induction of HSF1 at 0.5 hours. ....	50
Figure 10. The effect of heat stress (41°C) did not cause significant differences in the mean expression of HSF1, ERN1, and PRKAA2 at 0.5 hours. ....	52
Figure 11. The effect of heat exposure (41°C) on HSF1 expression in squirrels and camel.....	53

Figure 12. The effect of heat exposure (41°C) on HSF1 expression in rat, rhino, and human. ....	54
Figure 13. The effect of heat exposure (41°C) on HSF1 expression in presumed (A) heat tolerant and (B) heat sensitive mammals. ....	55
Figure 14. The effect of heat stress (41°C) caused an immediate induction of ERN1 at 0.5 hours in the 13-lined ground squirrel and dromedary camel. ....	56
Figure 15. The effect of heat exposure (41°C) on ERN1 expression in squirrels and camel.....	57
Figure 16. The effect of heat exposure (41°C) on ERN1 expression in rat, rhino, and human. ....	58
Figure 17. The effect of heat exposure (41°C) on ERN1 expression in presumed (A) heat tolerant and (B) heat sensitive mammals. ....	59
Figure 18. The effect of heat stress (41°C) caused an immediate induction of PRKAA2 at 0.5 hours in the rat and dromedary camel.....	60
Figure 19. The effect of heat exposure (41°C) on PRKAA2 expression in squirrels and camel.....	61
Figure 20. The effect of heat exposure (41°C) on PRKAA2 expression in rat, rhino, and human. ....	62
Figure 21. The effect of heat exposure (41°C) on PRKAA2 expression in presumed (A) heat tolerant and (B) heat sensitive mammals. ....	63
Figure 22. The effect of heat stress (41°C) did not cause an immediate induction of CDKN1A at 0.5 hours.....	64

Figure 23. The effect of heat exposure (41°C) on CDKN1A expression in squirrels and camel.....	65
Figure 24. The effect of heat exposure (41°C) on PRKAA2 expression in rat, rhino, and human. ....	66
Figure 25. The effect of heat exposure (41°C) on CDKN1A expression in presumed (A) heat tolerant and (B) heat sensitive mammals. ....	66
Figure 26. The effect of heat exposure (41°C) on HSP expression in presumed heat tolerant and heat sensitive mammals. ....	69
Figure 27. Random forests and box plots depicting relevant and important selected variables from the comparison between all three time points in the 13-lined ground squirrel. ....	70
Figure 28. Random forests and box plots depicting relevant and important selected variables from the comparison between all three time points in the white-tailed antelope squirrel. ....	72
Figure 29. Random forests and box plots depicting relevant and important selected variables from the comparison between all three time points in the rat. ....	72
Figure 30. Random forest and boxplots depicting relevant and important selected variables from the comparison between the three species at 6 hours. ....	73
Figure 31. Random forests and box plots depicting relevant and important selected variables ('LTA4H' and ' PAICS') from the comparison between the three species at 24 hours. ....	75
Figure 32. Box plots depicting relevant and important selected variables ('ANXA6' and ' COASY') from the comparison between the three species at 24 hours. ....	76

Figure 33. DIANA clustering produced 2 gene clusters from 13-lined ground squirrels.	77
Figure 34. DIANA clustering produced 2 gene clusters from white-tailed antelope squirrels. ....	78
Figure 35. DIANA clustering produced 2 gene clusters from rat. (A) Cluster 1 and (B) cluster 2. ....	78

## Chapter 1: Introduction

### Background

#### *Extreme desert environments*

Increasing temperatures across many habitats is one of the hallmarks of global climate change (Hansen et al., 2006; L. G. Thompson, 2010). Heat stress can challenge living organisms to sense and respond to extreme environmental conditions in an effort to prevent cellular damage or death. Adapted phenotypes examined across a range of mammalian diversity inhabiting deserts may offer insights into how organisms have evolved in extreme temperatures, illustrating appropriate physiological and cellular responses to the extreme heat that prevent stresses leading to cellular damage or death. In addition to extreme temperatures, deserts are among the driest environments on the planet, challenging life to both regulate body temperature and preserve water (Rocha et al., 2021). Organisms living in these harsh environments must have mechanisms to deal with environmental extremes, in an effort to maintain homeostasis. Homeostasis is a self-regulating process that works to maintain the internal conditions of an organism as it faces changing external conditions (Billman, 2020). To date, multiomic, genomic, and transcriptomic studies on classic desert dwelling mammals, the kangaroo rat, the Bactrian camel, and the dromedary camel have revealed the broad strokes of their adapted phenotypes (Alvira-Iraizoz et al., 2021; Marra et al., 2014; Wu et al., 2014). For example, these species implement water preservation mechanisms in kidneys that promote survival in arid conditions. Dromedary camels respond to dehydration by downregulating key genes involved in the cholesterol biosynthesis pathway and depleting membrane cholesterol in the kidney (Alvira-Iraizoz et al., 2021). Alvira-Iraizoz et al., suggest that this

suppression of cholesterol biosynthesis may facilitate water retention in the kidney (Alviraz-Iraizoz et al., 2021). A genomic study investigating Bactrian and dromedary camel showed an upregulation of genes in the Bactrian kidney involved in regulating sodium reabsorption e.g.,  $\text{Na}^+/\text{K}^+$ -ATPase and epithelial  $\text{Na}^+$  channel, during water-scarce conditions (Wu et al., 2014). Under conditions of experimentally induced dehydration, Wu et al. (2014) also found aquaporin genes, AQP1-3, were differentially upregulated genes in the renal cortex and medulla of the Bactrian camel kidney. Aquaporin-4 (AQP4) is a key water channel in the mammalian kidney that may play a role in efficient water reabsorption during water-scarce conditions. Additionally, Bactrian camels lacked detectable AQP4 expression (Wu et al., 2014). The physiology of kangaroo rats similarly includes specialization in kidney function, supporting survival in arid environments. Kangaroo rats produce highly concentrated urine as a way to survive for extended periods on a dry diet and without drinking water (Marra et al., 2014). Similar to the Bactrian camel, kangaroo rats lack the expression of AQP4 (Huang et al., 2001; Wu et al., 2014). The lack of AQP4 expression may suggest a unique mechanism for water reabsorption in both the camel and kangaroo rat kidneys (Huang et al., 2001).

Deserts also provide an interesting example in which to study different organisms' capacities to both tolerate and defend against temperature extremes. Temperature is a key determinant of cellular reaction rates. Placental mammals in particular maintain controlled, warm body temperatures to optimize cellular biochemistry. Organismal adaptation to extreme environmental temperature is also reflected in its genomics. As with water conservation, several genomic studies have shown mammalian desert



adaptation and specialized responses to extreme environmental heat (Rocha et al., 2021). Important adaptive responses to heat involve the (1) increased expression of heat shock proteins (HSPs) during the heat shock response (HSR), to protect from cellular cytotoxicity and to improve organismal tolerance to heat stress (Horowitz et al., 1997; Huang et al., 2021) (2) regulation of lipid metabolism by upregulation and activation of the cellular energy sensor, AMP-activated protein kinase (AMPK) (Corton et al., 1994), (3) and blunted endoplasmic (ER) stress via the unfolded protein response (UPR) expressing and activating the three ER master regulators inositol-requiring enzyme 1 (IRE1 $\alpha$  and IRE1 $\beta$ ), RNA-dependent protein kinase-like ER kinase (PERK), and transmembrane activating transcription factor 6 (ATF6) (Zhu et al., 2012). The three ER master regulators are activated to create a robust response of the UPR and reduce ER stress.

#### *Cell physiological changes occur in response to heat stress*

Previous studies have identified cell physiological changes occurring in response to various stresses including mild and severe heat stress. When mammalian cells encounter mild heat stress, they activate stress-response genes. Depending on the severity of the stress (exposure time, amplitude) and the tolerance of the organism or cell, responses can be graded and exposure to severe heat stress can progress from protective/reparative actions to indications of cellular damage (Park et al., 2005).

The heat shock response (HSR) maintains protein homeostasis, also known as proteostasis, in response to stressful conditions e.g., heat stress, that causes protein misfolding or denaturation and is essential for organismal survival (Anckar & Sistonen,

2011; Mahat et al., 2016; McMillan et al., 2002). The HSR pathway represents a cell protective strategy and is managed at the transcriptional level by heat shock factors (HSF). Vertebrates have four types of heat shock factors (HSFs) e.g., HSF1, HSF2, HSF3, and HSF4. HSF1 is a transcription factor responsible for maintaining proteostasis of the HSR and is ubiquitously expressed as an inactive monomer in most cell types and is negatively regulated at several levels (Ankar & Sistonen, 2011; Mahat et al., 2016). Upon heat stress, HSF1 trimerizes and triggers the HSR transcriptionally by binding to the heat shock element (HSE) in the promoter of heat shock proteins (HSPs) and eventually leads to an increased nuclear accumulation of HSF1 (Ankar & Sistonen, 2011; Masser et al., 2020; Su et al., 2019; Vujanac et al., 2005). It has been demonstrated that an excess of HSP70 may negatively regulate HSF activation, creating a feedback loop (Abravaya et al., 1992). However, it has been demonstrated that HSF1-promoter binding does not always induce expression of a gene containing a HSE (Trinklein et al., 2004) and that HSF1 binds to promoters of only a small fraction of heat stress-induced genes (Mahat et al., 2016). Following activation of HSF1, HSF1 elevates protein expression levels of HSPs e.g., HSP27, HSP40, and HSP70, thus preventing protein misfolding and maintaining proteostasis (Tabuchi et al., 2008). HSF2, HSF3, and HSF4 may not counterbalance the physiological response that HSF1 has to heat shock (Mahat et al., 2016; McMillan et al., 1998), meaning HSF2-4 do not play the same specialized role as HSF1 has in inducing the expression of HSP genes in the HSR. Previous functional studies support the role of HSF1 in regulating a heat-induced transcriptional response, as HSF1 knockout mice do not have heat-inducible expression of HSP70, but

not HSF2, HSF2 knockout murine fibroblasts retain this ability (McMillan et al., 1998, 2002).

Environmental factors including heat stress (Zhu et al., 2012) that disrupt ER homeostasis can cause ER stress, a condition characterized by the accumulation of misfolded and unfolded proteins. ER stress activates a protective strategy, the Unfolded Protein Response (UPR), to restore ER homeostasis. Upon initiation of the UPR, the three ER transmembrane proteins, ERN1 (IRE1), ATF6, and PERK, sense ER stress in the lumen (Homma & Fujii, 2016). The three functions of UPR include an adaptive response that reduces ER stress and restores ER homeostasis, a feedback mechanism that turns off UPR signaling pathways if UPR is successful, and regulation of survival and death factors governing cell fate. ERN1 senses unfolded and misfolded proteins during ER stress. Of the two ERN1 isoforms, IRE $\alpha$  and IRE $\beta$ , IRE $\alpha$  is expressed in all cell types and is the most characterized (Oslowski & Urano, 2011). Using an in vitro and in vivo approach, (Homma & Fujii, 2016) ERN1 was shown to downregulate expression in response to heat stress (43°C). Zhu et al., (2012) demonstrated that under heat shock (45°C, 30 minutes), ERN1 has a function in inhibiting the expression of DNA repair proteins e.g., DNA-PKcs, XRCC1, and HSP70.

The AMP-activated protein kinase (AMPK) system detects changes in cellular energy status via the AMP: ATP ratio, and is highly conserved in eukaryotes (Corton et al., 1994; Towler & Hardie, 2007). Three highly conserved genes that encode three subunits of AMPK;  $\alpha$  (isoforms: PRKAA1, PRKAA2),  $\beta$  (isoforms: PRKAB1, PRKAB2), and  $\gamma$

(isoforms: PRKAG1, PRKAG2, and PRKAG3). Two isoforms exist for the  $\alpha$  and  $\beta$  subunits, whereas three exist for the  $\gamma$  subunit. The  $\alpha$  subunit is the catalytic subunit of AMPK and contains the kinase domain, while  $\beta$  and  $\gamma$  subunits are the non-catalytic subunits (Towler & Hardie, 2007). In mammalian cells, elevation of AMP activates a protective response to energy depletion by triggering AMPK which then phosphorylates and inactivates key regulatory enzymes of biosynthetic pathways. Heat shock (42°C and 45°C, 60 minutes) in rat hepatocytes has been shown induce cellular stress responses, including activation and upregulation of AMPK activity, by depletion of ATP levels and concurrent increase in AMP (Corton et al., 1994). Liu and Brooks (2011) also demonstrated upregulation of AMPK activity after mild heat shock of 40°C for 1 hour using C2C12 myotubes. Corton et al., (1994) further demonstrated AMPK's role in regulating lipid metabolism by demonstrating that AMPK phosphorylates and inactivates a key regulatory enzyme, HMG-CoA reductase, which is involved in synthesis of sterols and fatty acids under heat stress. In prolonged exposure to heat, Tang et al., (2018) showed an increase in PRKAA1 and PRKAA2 expression after 4 days and a decrease of PKRAA2 expression at 8 days. Over a similar long-duration experiment, Huang et al., (2021) showed a decrease in AMPK expression in days 2 and 8 at 41.5°C in 3T3-L1 preadipocytes.

Cell cycle progression in eukaryotic organisms is regulated by the activation of cyclin-dependent kinases (CDKs) which phosphorylate key regulatory proteins driving cell cycle progression. Cyclin binding positively regulates CDK activity, whereas CDK inhibitors e.g., INK4 and CIP/KIP family members, can negatively modulate CDK activity (Fuse et

al., 1996; Gorospe et al., n.d.; LaBaer et al., 1997). INK4 family members include p15, p16, p18, and p19, whereas CIP/KIP family members include p21, p27, and p57 (LaBaer et al., 1997). Cell cycle arrest can be triggered by stressful conditions and act as a protective response to facilitate DNA repair prior to cell cycle progression and proliferation. Cyclin dependent kinase inhibitor 1A (CDKN1A/p21) binds to CDKs and can be activated by transcriptional regulator, p53, following exposure to heat shock (Fuse et al., 1996; Gorospe et al., n.d.; Kühl & Rensing, 2000; Woo et al., 2000). Given the ubiquitous ability of CDKN1A (LaBaer et al., 1997), it has been demonstrated that this inhibitor may be involved in inhibiting cell cycle progression. In the presence of heat shock, the regulatory mechanisms of CDK activity result in an increase in the amount of CDK inhibitors (Abe, T. Tamiya, Y. Ono, A. H. Salke, 2001; Fuse et al., 1996; Kühl & Rensing, 2000; Nitta et al., 1997; Ohnishi et al., 1996) and may increase in a temperature- and time- dependent manner (Woo et al., 2000). Abe et al., (2001) investigated and showed that the p53-p21 pathway was activated by heat stress, rather than the p27 pathway in human glioma cells. Nitta et al., (1997) demonstrated that following heat exposure (43°C, 45 minutes) in normal human fibroblasts, the cell cycle arrest at G1/S and G2/M was p53-dependent and that a candidate factor e.g., CDKN1A, may be responsible for this arrest. CDKN1A may be a possible factor responsible for the inhibition of cell cycle arrest given the increased amount of CDKN1A following accumulation of p53, and duration of the increased CDKN1A level nearly coinciding with the duration of cell cycle arrest (Nitta et al., 1997). Ohnishi et al., (1996) have similarly demonstrated an increased amount of CDKN1A accompanying the accumulation of p53 following heat exposure (44°C, 30 minutes) in human glioblastoma cells. Although p53 contributes to

the amount of CDKN1A induced, it has also been demonstrated that CDKN1A induction by heat shock is mediated in p53-deficient cell lines (Fuse et al., 1996). Fuse et al., (1996) demonstrated G1 arrest in p53-deficient glioma cells following heat shock (44°C, 15 minutes), and an increase in CDKN1A expression. Furthermore, demonstrating that p53-independent pathways may be involved in hyperthermia-induced CDKN1A expression and that CKI is an early response gene (Fuse et al., 1996). The mechanism underlying the p53-independent induction was better elucidated by Woo et al., (2000), who demonstrated that the presence of heat shock element (HSE)-like sequences in the promoters of p21 genes in rat fibroblasts, human hepatoblastoma HepG2, and human adenocarcinoma HeLa cells may be responsible for hyperthermia-induced CDKN1A expression and might provide a better explanation of the p53-independent hyperthermia-induced CDKN1A expression. These previous studies indicate that p53-independent and p53-dependent hyperthermia-induced CDKN1A expression can be responsive to heat stress across a broad temperature range (Furusawa et al., 2009).

Past a cell's threshold of viability, cell death occurs. Cell viability and proliferation under heat stress are dependent on different factors including cell type, heat exposure temperature, and heat exposure duration (Huang et al., 2021; Shandilya et al., 2020; Siddiqui et al., 2020; S. M. Thompson et al., 2014). There are different cell death markers that exist to help detect this outcome. A few cell death markers for apoptosis include cleaved caspase 3 and cytochrome c release (Green & Llambi, 2015), while a marker of necrosis may include the release of chromatin protein high-mobility group B1 (HMGB1) and cyclophilin A (CypA) (Christofferson & Yuan, 2010). When a cell's plasma membrane

has ruptured, lactate dehydrogenase, a marker for cell lysis, is released from the cell and can be assayed in the intercellular environment (Stoddart, 2011).

## Research Objectives

Understanding the cell physiological changes that occur under extreme environmental conditions can identify whether an animal is flexible to a changing environment and determine the mechanisms by which an animal is flexible. Cell-level mechanisms of stressor resilience in mammals tolerant to heat stress remain understudied. Specifically, if we can identify the responses of tolerant mammals (those that routinely permit body temperature lability/increases), a comparison with more sensitive species (those that maintain a relatively stable body temperature) may identify links between heat stress responses and negative cellular outcomes. This thesis investigates primary dermal fibroblasts from heat tolerant, compared to heat sensitive species, to determine differences in cellular responses that may be linked to organismal phenotype.

## *Basis for predicting heat tolerant versus heat sensitive mammals*

Cellular mechanisms to maintain homeostasis in the face of heat stress likely differ across species based on naturally tolerated intracellular variability. In some mammals, homeostasis at the cellular level has a narrow range of desired physiological conditions that the organism is required to maintain. Other species tolerate more varied physiological and intracellular conditions, including in temperature. The basis of choosing species include selecting those that are distributed across the mammalian lineage, selecting organisms predicted to be resilient or sensitive to heat stress, and for which cells are

available from San Diego Frozen Zoo or locally. Mammalian species were predicted to be heat tolerant if they are desert dwelling and/or have the ability to fluctuate their body temperature of 5°C or more, based on a literature survey. Conversely, species are predicted to be heat sensitive if they maintain a relatively stable body temperature.

Predicted heat-tolerant mammals include the 13-lined ground squirrel (*Ictidomys tridecemlineatus*), dromedary camel (*Camelus dromedarius*), white-tailed antelope squirrel (*Ammospermophilus leucurus*), and the round-tailed ground squirrel (*Xerospermophilus tereticaudus*). The dromedary camel inhabits the Saharan Desert and exhibits diurnal fluctuation in body temperature, which can range from 34°C-42°C (Bouâouda et al., 2014). Thirteen-lined ground squirrels inhabit North American grasslands and their body temperatures span from 4-8°C during a torpor bout to 37°C during arousals, and when normothermic outside the hibernation season (Bouma et al., 2010). Ground squirrels and camels both have a similar specialization to hot environmental temperatures, each possessing heat-activated ion channel transient receptor potential vanilloid 1 (TRPV1) orthologs with dramatically diminished pain sensitivity to high temperatures (Laursen et al., 2016). The white-tailed antelope squirrels are diurnally active and non-hibernating desert-dwelling mammals that can fluctuate their body temperature with environmental temperature. The fluctuation in body temperatures of antelope squirrels coincides with periods of activity, allowing their body temperature to increase as high as to 43.6°C while the animal is active outside its shaded burrow. Antelope squirrel active body temperature is 38°C and at night and during the winter, this species can drop their body temperature to 31-33°C (Belk & Smith, 1991). Round-tailed



ground squirrels are also diurnally active, desert-dwelling mammals that can fluctuate their body temperature over the range of 36°C-41.4°C depending on environmental temperatures. Round-tailed ground squirrels may use the shade or climb into shrubs and hibernate or estivate to avoid hot environmental temperatures (Ernest and Mares, 1987).

Mammals presumed to be heat-sensitive include the southern white rhinoceros, human, and the Sprague-Dawley rat. While the southern white rhinoceros also inhabits the Savannas and are exposed to hot desert conditions, this species is closely distributed near water. Rhinoceros maintain a more stable diurnal body temperature, especially compared to the dromedary camel, perhaps by behavioral thermoregulation, using a mud coating to protect their skin from the heat load of the sun (Sheil & Kirkby, 2018). As a result, body temperatures recorded from free-ranging rhinoceros are relatively stable at ~37°C (Hiley, 1977). In addition to Sprague Dawley rats preferring cooler ambient temperatures, both the rat and human are found in a variety of habitats and maintain a body temperature of about 37°C (Lillie et al., 1996; Protsiv et al., 2020; Refinetti, 2020). Humans sweat in response to hot conditions to aid in cooling and avoid and reduce heat by changing clothing attire or manipulating their microenvironment through air conditioning (Stolwijk, 1977). Sprague Dawley rats salivate profusely and use this to coat their bodies, which allows for evaporative cooling to occur (Shelton & Alberts, 2018).

For clarification on what is meant by broad and narrow homeostasis, an organism that displays narrow homeostasis has more difficulty in responding to a stressor and exists in a very stable intracellular environment compared to an organism with a broad

homeostatic range. For instance, dromedary camels are heterotherms meaning their body temperatures vary with the environment. On a very hot day, camels can fluctuate their body temperature throughout the day from 34°C to 42°C (Bouâouda et al., 2014; Habte et al., 2021), whereas the rhinoceros maintain a relatively stable body temperature of about 37°C throughout the day (Hiley, 1977). In this case, the dromedary camel can be referred to as displaying broad homeostasis and rhinoceros as displaying narrow homeostasis.

#### *Basis of primary dermal fibroblasts*

Primary dermal fibroblasts are a skin cell type that comes into direct contact with the environment. The basis of using primary dermal fibroblasts for investigating the effects of heat stress is because skin biopsy is a minimally invasive approach that is suitable for many mammals, including protected species, that allow for the use of a skin cell type to study the genome and cellular system of an animal in a laboratory setting. This cell type therefore represents a model for investigating stress outcomes and mechanisms of stress, and organismal outcomes.

#### *Basis of 41°C experimental heat stress*

41°C is considered febrile-range hyperthermia in humans, which is a temperature sufficient to evoke heat shock and enhance inflammatory responses, leading to negative cellular outcomes and ultimately larger scale organ level disruptions. High-grade fever is associated with many health conditions including pneumonia, meningitis, flu, and COVID19. If we can identify the responses of tolerant mammals (those that routinely

permit body temperature lability/increases), a comparison with more sensitive species (including humans) may identify links between heat stress responses and negative cellular outcomes. Further establishing the cellular responses to a high temperature of 41°C of these mammalian species can provide better insight into understanding the cellular mechanisms of stressor resilience and sensitivity of human primary dermal fibroblasts; thus, highlighting advantages that may be used toward aiding humans with health conditions with high grade-fever symptoms.

#### Research questions and hypotheses

Chapter 2 investigates the responses of fibroblasts from these mammals to multi-day heat stress in cell culture, to detect cell proliferation and cell death. Cells from species presumed to be heat tolerant are compared with presumed heat sensitive species to determine whether the stress responses in cells could be predicted based on the known organismal flexibility in body temperature. Chapter 2 strives to understand: Does cell sensitivity match organism sensitivity? It's predicted that mammals that have labile and fluctuating body temperatures, mammals that have broad homeostasis, will display less cell death markers and have more cells proliferating in the heat.

Chapter 3 investigates the mechanisms of fibroblasts from these mammals to short-term heat stress to detect protein abundance and heat-stress gene expression patterns that underlie resilience to heat stress versus patterns reflecting heat sensitivity, thus leaving possible signatures of managing heat stress in tolerant species. The aim for chapter 3 strives to understand the mechanisms of resilience at the cellular level, as well as identify

adaptive and maladaptive responses that can be linked to maintaining cellular homeostasis. It's predicted that the time course or amplitude of heat-stress gene expression is going to differ in tune with the body temperature fluctuations of the organism.

## Chapter 2: Cell sensitivity matches organism sensitivity

### Background

Organism sensitivity may be partly reflected by the behavioral and physiological responses of an organism to a stressful condition. Desert-dwelling squirrels, such as the white-tailed antelope squirrel and round-tailed ground squirrel, evade extremely hot temperatures through behavior and physiological responses (Belk & Smith, 1991; Ernest and Mares, 1987). White-tailed antelope squirrels minimize water loss from pulmonary tissues by exhibiting fewer goblet cells in the lungs, avoiding overheating by salivating in great amounts, and producing highly concentrated urine (Belk & Smith, 1991). On hot days, round-tailed ground squirrels compensate for the physiological water requirement by consuming succulent foods, seeking shade from shrubs, using burrows, and hibernating or estivating (Ernest and Mares, 1987). It's also suggested that round-tailed ground squirrels may reduce thyroid activity during the summer and may be associated with thermoregulation (Ernest and Mares, 1987). The thyroid hormone acts as a major regulator of thermogenesis and may affect susceptibility to environmental temperatures (Vancamp & Demeneix, 2020; Warner et al., 2013). Dromedary camels cannot shelter from heat behaviorally but rather rely on physiological responses to endure extremely hot temperatures (Rocha et al., 2021). Dromedary camels endure environmental temperatures exceeding 42°C and retain water in these arid environments by downregulating genes in the cholesterol biosynthesis pathway and exhibit depleted membrane cholesterol in the kidney (Alvira-Iraizoz et al., 2021). Although only plains-dwelling (but not desert-dwelling), 13-lined ground squirrels fluctuate body temperatures

from normothermic conditions (37°C) to hibernation (4-8°C) (Bouma et al., 2010). During hot days, the body temperature of 13-lined ground squirrels increases when active outside of their burrow. Thirteen-lined ground squirrels will make constant trips to their burrows, and a decrease in body temperature is observed when in the burrow (Vispo & Bakken, 1993).

In comparison, the southern white rhino, human, and rat maintain body temperature by a more restrictive self-regulation not dependent on environmental temperatures. Deviations from the tightly kept body temperature range may lead to hyperthermia or hypothermia and lead to larger-scale organ-level and cellular-level problems (Osilla et al., 2023). Southern white rhinos do not have sweat glands and exhibit behavioral responses including moving toward shaded areas and bathing in mud baths during high temperatures at daytime (Groves, 1972; Sheil & Kirkby, 2018). Humans behaviorally respond to hot environmental temperatures by avoiding or reducing heat stress by changing one's clothing attire or changing their microenvironment through air conditioning. Human physiological responses to heat stress usually entail secretion of sweat in an effort to cool the body (Stolwijk, 1977). Rats respond to hot environmental temperatures by profusely salivating and spreading the saliva throughout the rodent's body, thus allowing for evaporative cooling (Shelton & Alberts, 2018). As a result of behavioral and physiological processes occurring at the organismal level, mammals may tolerate (or avoid) changes in core body temperature under typical environmental conditions.

Exposure to heat stress that impacts the internal, intercellular environment of mammals may therefore occur normally, such as for animals living in desert habitats, or could represent a pathophysiological condition. Responses at the cellular level can elucidate organismal sensitivity to such a stressor. As cells lose viability, cell-death pathways are induced and the type of cell-death pathway that is activated and induced may vary depending on the stressor(s). In the scenarios of apoptotic-induced cell death and necrotic-induced cell death, previous studies have shown a cell recovery phenomenon that rescues cells from cellular death termed anastasis (H. M. Tang & Tang, 2018). Dying cells can exit the activated death pathway (Y.-N. Gong et al., 2017; Sun et al., 2017; H. L. Tang et al., 2012; H. M. Tang & Tang, 2018; Zargarian et al., 2017). Anastasis has been shown to occur in a great proportion of late-stage apoptotic cells of different cell types and has been observed from different apoptotic inducers (H. L. Tang et al., 2012). During necrosis-induced cell death, phosphorylation of the substrate mixed lineage kinase domain-like (MLKL) by receptor-interacting serine/threonine kinase 3 (RIPK3) causes MLKL to oligomerize and translocate to the plasma membrane and execute plasma membrane permeabilization. MLKL is the necrotic executor that directly facilitates necrotic cell death. After phosphorylated MLKL causes plasma membrane permeabilization, an increase of calcium enters the necrotic cells and phosphatidylserine externalizes from the inner to the outer leaflet of the plasma membrane. It was previously considered that the phosphorylation of the MLKL on the plasma membrane is the “point of no return” in necrosis due to this phosphorylation event causing MLKL to permeabilize the plasma membrane, however, it has been demonstrated that at the point of phosphatidylserine externalization, the inactivation of RIPK3 and MLKL can occur and

allow for full cellular recovery (Y. Gong et al., 2019; Sun et al., 2017; Zargarian et al., 2017).

In the scenario of plasma membrane rupture and no rapid repair of the plasma membrane (within ~5-6 seconds) (Klenow et al., 2021), it has been suggested that cellular anastasis may not occur if the cell fails to seal the hole. The collapse of the plasma membrane releases lactate dehydrogenase (LDH). The enzyme is stable for about 36-48 hours after cell death, thus allowing for quantitative cell viability analysis (Stoddart, 2011). Focusing on LDH and not key, activated apoptotic or necrotic machinery, which by itself, may not reflect the occurrence of anastasis, will provide better insight into whether plasma membrane rupture and cell death have occurred. By looking at the cell death marker, LDH, we hope to find cell sensitivity reflecting the organismal sensitivity of both presumed heat tolerant and heat sensitive mammals to extreme environmental temperatures. I hypothesize that more cells will proliferate and LDH (reflecting cell death) levels will be lower in organisms that naturally experience high body temperatures and/or are desert-dwelling, and organisms that maintain a relatively stable body temperature will display less cell proliferation and higher LDH levels.

## Methods

### *Isolation and Culture of Primary Dermal Fibroblasts*

Primary dermal fibroblasts were developed from skin biopsies in all species. Fibroblasts from n=5 dromedary camel and n=5 southern white rhinoceros were obtained from the



San Diego Frozen Zoo under MTA. Fibroblasts from n=5 13-lined ground squirrel and n=4 rats were developed under Massachusetts General Hospital IACUC #2106N000122. N=5 antelope ground squirrel and n=3 round-tailed ground squirrel were developed at UNLV under IACUC #1609973. For all rodent samples, following euthanasia, the biopsy site was shaved of fur, then prepped with depilatory cream for several minutes. A sterile gauze pad was used to remove the fur and product to expose the skin. This area was sterilized with 70% ethanol and a biopsy (~1cm<sup>3</sup>) was collected with a sterile punch or sterile scissors and forceps. The biopsy was placed in a 15mL conical tube containing ice-cold Hanks balanced salt solution (Gibco 14170-112) with 2% penicillin-streptomycin (*Corning; 30-001-CI*).

Working inside a biosafety cabinet, the biopsy was transferred to a petri-dish containing ~5mL of DPBS and minced with a sterile razor blade. The resulting tissue slurry was transferred to a 15mL conical tube for digestion in 2mg/mL collagenase type II (Worthington cat#CLS-2) diluted 1:6 in complete media (Basal medium eagle Gibco 21010-046 + 20% FBS + 1% P/S). The conical tube was incubated horizontally at 37°C for ~24h.

After approximately 24 hours, the 15mL falcon tube containing the minced tissue, BME 1X, and collagenase type II was centrifuged at 16000 rcf for 10 minutes. The supernatant was aspirated and 5mL DPBS added to wash the tissue pellet. This wash was repeated twice. After final removal of the supernatant, 1.5mL of BME 1X was added and the tissue suspension was plated in a T25 cm<sup>2</sup> cell culture flask. The cap of the flask was covered

with aluminum foil to prevent gas exchange for 24 hours, then removed. After 4 days, 2 mL of media was added. Media was exchanged every 2 days until cells reached ~75% confluency.

### *Cell Culture Maintenance*

Primary dermal fibroblasts were maintained in media optimized for each species, and passaged from T25 cm<sup>2</sup> cell culture flasks into T75 cm<sup>2</sup>, then T175 cm<sup>2</sup> cell culture flasks at ~75% confluency. The southern white rhino utilized FGM2 (Fibroblast growth medium-2 + 2% FBS + 0.1% insulin + 0.1% rhFGF-B + 0.1% GA-1000, CAT # CC-3132) medium. Human, rat, white-tailed antelope squirrel utilized DMEM (Dulbecco's Modified Eagle's Medium + 10% FBS + 1% P/S, REF #11965-092). 13-lined ground squirrel, and round-tailed ground squirrel used BME 1X (Basal medium eagle + 20% FBS + 1% P/S, REF # 21010-046), while the dromedary camel used BME 1X (Basal medium eagle + 10% FBS + 1% P/S, REF # 21010-046). Cells were cultured at 37°C in a humidified atmosphere of 5% CO<sub>2</sub>. Cell culture medium was changed every 2-3 days.

Primary dermal fibroblasts were plated in T25 cm<sup>2</sup> cell culture flasks and passaged into T75 cm<sup>2</sup>, and then T175 cm<sup>2</sup> cell culture flasks once reaching ~75% confluency. The southern white rhino utilized FGM2 (Fibroblast growth medium-2 + 2% FBS + 0.1% insulin + 0.1% rhFGF-B + 0.1% GA-1000, CAT # CC-3132) medium. Human, rat, white-tailed antelope squirrel utilized DMEM (Dulbecco's Modified Eagle's Medium + 10% FBS + 1% P/S, REF #11965-092). 13-lined ground squirrel, and round-tailed ground squirrel used BME 1X (Basal medium eagle + 20% FBS + 1% P/S, REF # 21010-046), while the

dromedary camel used BME 1X (Basal medium eagle + 20% FBS + 1% P/S, REF # 21010-046). Cells were cultured at 37°C in a humidified atmosphere of 5% CO<sub>2</sub>. Cell culture medium was changed every 2-3 days.

### *Experimental heat exposure*

Fibroblasts from each species were examined for viability and proliferation over long-term heat stress. The white-tailed antelope squirrels were plated for 2 and 4 days at 41°C, whereas the round-tailed ground squirrel, 13-lined ground squirrel, dromedary camel, human, rat, and southern white rhino were plated for 2-8 days at 41°C. Once cells were grown to ~75% confluency in a T175cm<sup>2</sup> flask, cells were plated into 96 well plates that would be exposed to the multi-day heat exposure to examine cell sensitivity to heat stress. Cell passage numbers are listed under **Table 1** in the **Appendix**. To prevent overcrowding with ongoing cell division and resulting cell death, cells were plated at differing densities corresponding to their eventual harvest day across the experiment. These initial plating densities were optimized for each species prior to the start of experiments using a range of densities. Cells planned to be harvested on days 2 and 3 were optimized using initial plating densities of  $1.0 \times 10^4/100\mu\text{L}$ ,  $2.0 \times 10^4/100\mu\text{L}$ ,  $4.0 \times 10^4/100\mu\text{L}$ ,  $6.0 \times 10^4/100\mu\text{L}$ , and  $8.0 \times 10^4/100\mu\text{L}$  per well. For harvests planned on days 4 and 5, initial plating densities of  $7.5 \times 10^3/100\mu\text{L}$ ,  $1.5 \times 10^4/100\mu\text{L}$ ,  $3.0 \times 10^4/100\mu\text{L}$ ,  $4.5 \times 10^4/100\mu\text{L}$ , and  $6.0 \times 10^4/100\mu\text{L}$  per well were evaluated. For harvests planned for days 6, 7 and 8,  $5.0 \times 10^3/100\mu\text{L}$ ,  $1.0 \times 10^4/100\mu\text{L}$ ,  $2.0 \times 10^4/100\mu\text{L}$ ,  $3.0 \times 10^4/100\mu\text{L}$ , and  $4.0 \times 10^4/100\mu\text{L}$  per well densities were evaluated to ensure that there was appropriate cell material to obtain a result for the LDH assay (see protocol below) in the center range of

the assay's standard curve. Optimal cell numbers for each time point and species are listed in **Table 2** in **Appendix**. Cells were plated at optimal densities into a 96-well plate and given 24 hours to adhere to the bottom of the wells. Cells were then subjected to experimental heat stress at 41°C in a humidified atmosphere with 5% CO<sub>2</sub> over the experimental timecourse of 2 – 8 days. DMEM (Dulbecco's Modified Eagle's Medium + 10% FBS + 1% P/S, REF #11965-092) medium was used at the start of and during each treatment. Cell culture medium was changed every 24 hours, aside from the day of collection.

#### *Crystal violet assay for cell proliferation*

Crystal violet stain was used as a proxy for cell proliferation as it stains DNA. I analyzed changes in crystal violet staining intensity across the experimental time course in cells exposed to 41°C compared to controls held at 37°C over the same time course. A crystal violet assay was performed on two technical replicates. 10µL of methanol and then 50µL crystal violet (0.5% Crystal Violet; 20% ethanol) were added to the two wells exposed to 41°C and two control wells held at 37°C on each experimental day. Wells containing crystal violet were then washed twice with 100µL of MilliQ water. 200µL of 0.1% Acetic Acid (0.1% Acetic Acid; 50% 200 proof EtOH; 49.9% of MilliQ H<sub>2</sub>O) was added to each well, then transferred to a non-culture 96 well plate (1x replicate/well). Crystal violet staining intensity was assayed by absorbance at 585nm using a SpectraMax Plus plate reader. The two technical replicates from each of the control (37°C) and experiment wells (41°C) were averaged and then calculated as a ratio of 41°C/37°C. Ratios of ~1.0 represent minimal to no cell death and cell proliferation occurring, a ratio of less than 1.0

represents more cell death than cell proliferation, and a ratio of more than 1.0 represents more cell proliferation than cell death. Crystal violet absorbance values and cell proliferation ratios are listed in **Table 3** in the **Appendix**.

### *Lactate dehydrogenase assay for cell viability*

Lactate dehydrogenase is an easily detectable intracellular product, and its release into conditioned media as a result of cell lysis can be used as a metric for cytotoxicity or cell viability. For this assay, plates were harvested in tandem with the crystal violet assay on days 2-8 at 41°C, with control plates for each day held at 37°C. Two technical replicates were plated for the ‘low control’ and ‘experimental samples’, and one technical replicate was plated for the ‘high control’ (**Figure 1**). The ‘low control’ technical replicates were plated on the plate designated for 37°C and represented the control group not affected by heat stress. The one ‘high control’ technical replicate was also plated on the plate

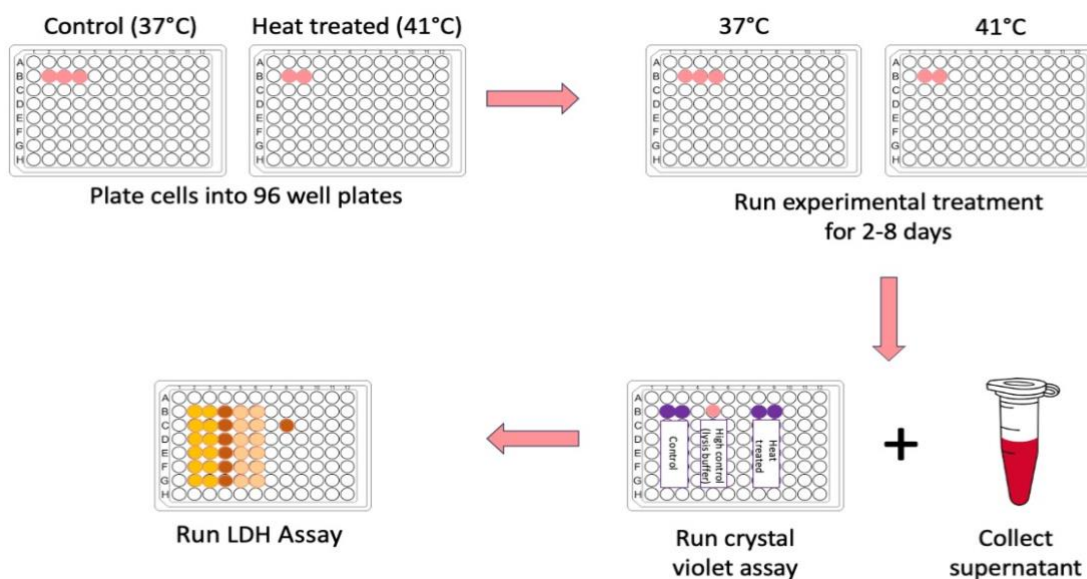


**Figure 1.** Schematic of experimental design for chapter 2.

designated for 37°C and served as a positive control in which LDH is present; a cell lysis buffer was added to this well to lyse the cells and release LDH into the media. The two 'experimental samples' technical replicates were plated on the plate designated for 41°C and represented the replicates that went under heat stress treatment. Plates were first gently shaken to distribute any released lactate dehydrogenase throughout the conditioned media, then supernatant was harvested. Each treatment plate (41°C) was accompanied by a control cultured at 37°C. Then, the supernatants from two technical replicates for each of the low control and experimental samples, from the plate in 37°C and 41°C, respectively, were collected and transferred into separate 0.5mL Eppendorf tubes and stored in -80°C until all time points for an individual were collected. 10µL of a cell lysis buffer (ab65393 LDH-Cytotoxicity Assay Kit II) was added to a third well (intended to serve as a high control) in the 37°C 96 well plate and incubated for 30 minutes in 37°C. The high control serves to ensure the cell lysis buffer lyses the cells, thus causing the release of lactate dehydrogenase into the supernatant. After 30 minutes, the supernatant from the high control well containing the cell lysis buffer was collected and frozen at -80°C.

Once all time points were collected, the supernatants from each time point (days 2-8) were thawed on ice. 10µL of each supernatant was transferred to a new non-culture 96 well plate. In a separate well, 5µL of a LDH positive control was added to the non-culture 96 well plate. 100µL of lactate dehydrogenase (LDH) reaction mix (1.1mL of WST Substrate mix with 10mL of LDH assay buffer (ab65393 LDH-Cytotoxicity Assay Kit II)) was added to each well, gently mixed, and incubated for 30 minutes at room temperature.

The reaction time was increased or decreased depending on the color development. The plate was read until the desired reading was observed in at least one of the cell counts ( $1.0 \times 10^4/100\mu\text{L}$ ,  $2.0 \times 10^4/100\mu\text{L}$ , etc.) for a time point: high control with OD<sub>450nm</sub> of ~2.0, while the low controls (supernatants collected from 37°C without cell lysis buffer) should be OD<sub>450nm</sub> > 0.8. The cell count meeting the desired absorbances was chosen to be the optimal cell count for a time point and species. The absorbance of the 96 well plates was measured using the SpectraMax Plus machine with the 450nm filter. Once the desired readings were reached, a stop solution of 10μL was added to each well to stop the reaction and mixed for 5 minutes, while being protected from light. The non-culture 96 well plate was read again on wavelength 450nm. The LDH assay absorbance values are normalized by the crystal violet absorbance values. Then, a ratio of the normalized experimental sample to the normalized positive control is plotted. Normalized viability data is listed in **Table 4** in the **Appendix**. A schematic of the experimental design for chapter 2 is provided in **Figure 1**.

### Statistical analysis

Statistical analyses were conducted in R or GraphPad Prism (version 9.5.1). A Shapiro Wilks test (Shapiro & Wilk, 1965) was used to ensure normal distribution of cell proliferation and cell viability data and datasets were considered normally distributed when  $P > 0.05$ . To determine whether there were differences across the 8-day time course at 41°C for each species, the cell proliferation data were first analyzed using repeated measures ANOVA (*Mixed-Effects Models in S and S-PLUS*, 2000). To compare cell proliferation between heat sensitive and heat tolerant species, data were compiled

(combining all days of data collection for a given species when there were no significant differences across the time course) and analyzed with the linear mixed-effects model comparing the group of heat tolerant species to the group of heat sensitive species (individual was included in the model as a random factor to account for repeated measures across the days of the experiment). The cell viability data were not normally distributed and could not be transformed to meet normality assumptions for parametric tests. I therefore used simulation (*Mixed-Effects Models in S and S-PLUS*, 2000) to generate a null distribution to test for differences in each species across the time course, to determine whether viability changed by day of heat exposure in any species. After simulation, repeated measures ANOVA and linear mixed effects model (*Mixed-Effects Models in S and S-PLUS*, 2000) were used to analyze the cell viability data. Significant statistical differences were considered when  $P \leq 0.05$ .

## Results

### Cell proliferation

Fibroblast proliferation, assayed at 24h intervals over 2-8 days during experimental heat exposure in cell culture, did not differ in any species (statistical results for repeated measures ANOVA is provided in **Table 5** in the **Appendix**), therefore results across the experimental time course were combined to evaluate differences between species and



phenotypes. Due to sample size limitations, long-term heat exposures were only captured in the white-tailed antelope ground squirrel on days 2 and 4. After 41°C exposure for 2 and 4 days, fibroblast proliferation in this species ranged from 0.9-1.1 (**Figure 2A**), indicating that the total cell population was generally maintained at this incubation temperature. Proliferation (cell DNA content at 41C relative to 37C control) in fibroblasts from the round-tailed ground squirrel ranged from 0.7 - 1.7 with a median ratio of 1.0 (**Figure 2B**). 45% of the ratios in crystal violet staining between 41°C and 37°C were < 1.0 in the round-tailed ground squirrel, while 55% of the samples showed ratios >1.0 (**Figure 2B**), again indicating that the total cell population was generally maintained.

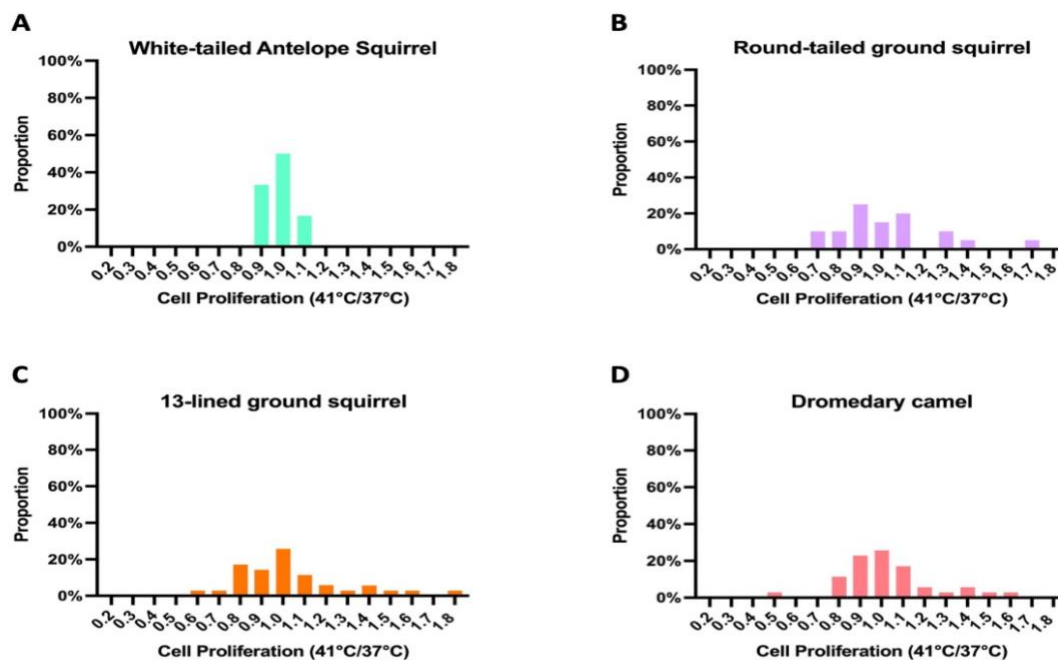


**Figure 2.** Relative frequency (%) distribution exhibiting the effect of chronic heat exposure (41°C) on cell proliferation of presumed heat tolerant mammals. (A) Cell proliferation after heat exposure (41°C) for 2 and 4 days in the white-tailed antelope squirrel. (B) Cell proliferation after heat exposure (41°C) for 2-8 days in the round-tailed ground squirrel (data for biological replicate XT2 for day 7 at 41°C is not included). (C and D) Cell proliferation after heat exposure (41°C) for days 2-8 in the 13-lined ground squirrel and dromedary camel, respectively. X-axis: cell proliferation data are plotted as ratios of cells present for a time point at 41°C by cells present for the same time point at 37°C. Y-axis: relative frequency (%) of the cell proliferation ratio.

During the 2-8 day heat exposure for the 13-lined ground squirrel, ratios denoting cell proliferation ranged from 0.6 - 1.8 with a median ratio of 1.0 (**Figure 2C**). Only 37.12% of ratios for crystal violet intensity were < 1.0 in the 13-lined ground squirrel, whereas 62.88% were >1.0 (**Figure 2C**), indicating fibroblasts resilient to heat stress in this species. Fibroblast proliferation in the dromedary camel cells ranged from 0.5 - 1.6 with a median of 1.0 (**Figure 2D**). 37.11% of the ratios comparing crystal violet staining intensity at 41°C compared to 37°C controls were < 1.0, with 62.89% > 1.0 (**Figure 2D**), also indicating the potential for resilience to heat exposure, but with limited replicates showing lower cell DNA content at 41°C compared to 37°C.

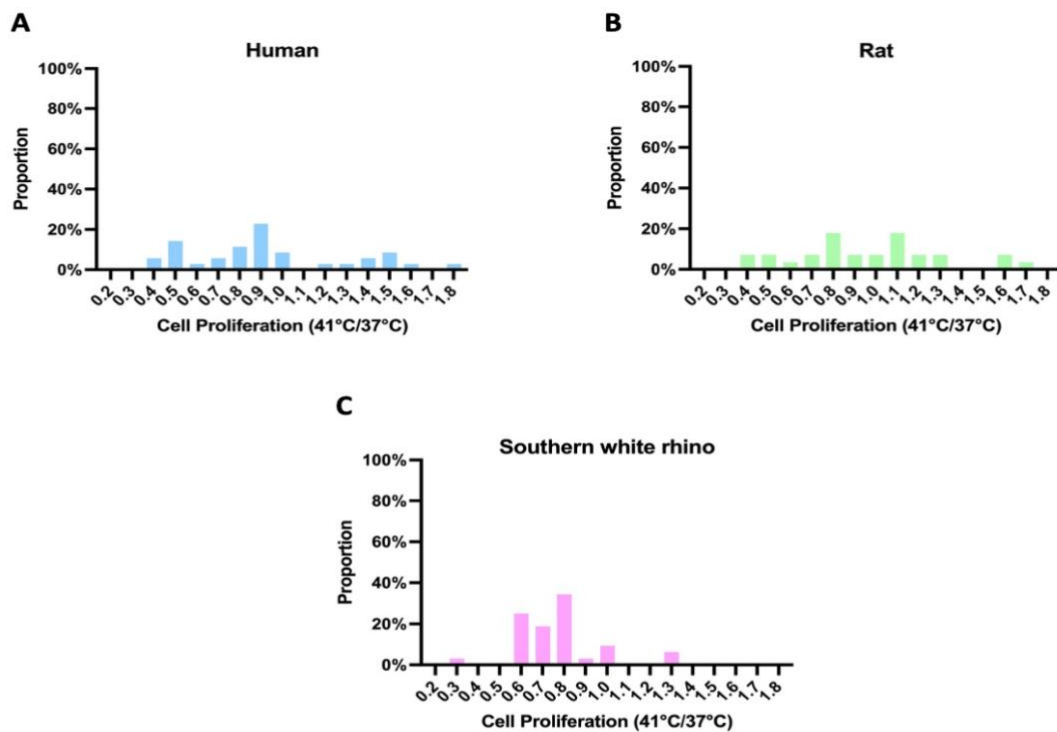


**Figure 3.** Relative frequency (%) distribution exhibiting the effect of chronic heat exposure (41°C) on cell proliferation of presumed heat sensitive mammals. (A and B) Cell proliferation after heat exposure (41°C) for 2-8 days in the white-tailed antelope squirrel and rat, respectively. (C) Cell proliferation after heat exposure (41°C) for 2-8 days in the southern white rhino (data for biological replicates CSO4 and CSO5 for days 4, and days 4 and 6, respectively, at 41°C are not included). X-axis: cell proliferation data are plotted as ratios of cells present for a time point at 41°C by cells present for the same time point at 37°C. Y-axis: relative frequency (%) of the cell proliferation ratio.

Similar analyses were conducted for fibroblasts of three species of presumed heat sensitive mammals (human, southern white rhinoceros and Sprague Dawley rat). Frequency distributions of proliferation ratios in these heat sensitive species tended to demonstrate different patterns compared to the presumed heat tolerant species, with a lower peak of the distribution indicating more variability in proliferation rates (human, rat) or a median for the frequency distribution  $<1.0$  (rhino). Cell proliferation ratios after heat exposure of  $41^{\circ}\text{C}$  (2-8 days) in human fibroblasts had a broad range of 0.2 - 1.8, with a median of 0.9 (**Figure 3A**). The frequency distribution of proliferation ratios for human

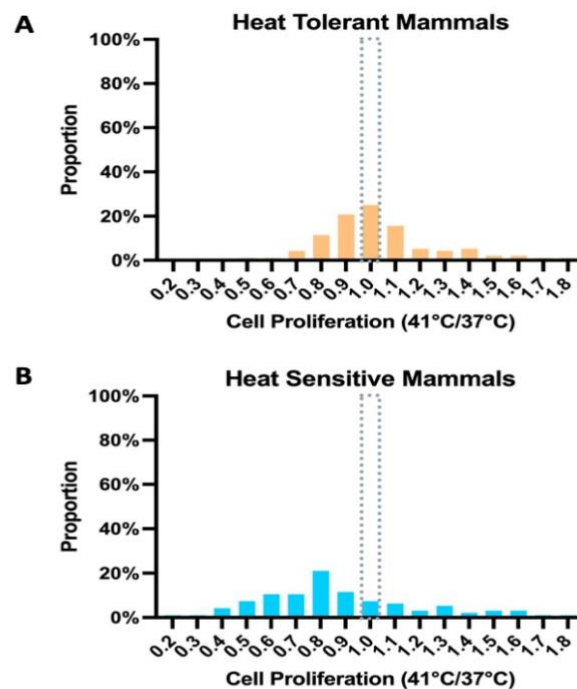


**Figure 4.** Relative frequency (%) distribution exhibiting the effect of chronic heat exposure ( $41^{\circ}\text{C}$ ) for 2-8 days on cell proliferation of all presumed (A) heat tolerant and (B) heat sensitive mammals. Cell proliferation data are plotted as ratios of cells present for a time point at  $41^{\circ}\text{C}$  by cells present for the same time point at  $37^{\circ}\text{C}$ . Biological replicates with missing time points that weren't plotted on the frequency distribution graph for Figures 1 and 2 are also not present in this figure. X-axis: cell proliferation data are plotted as ratios of cells present for a time point at  $41^{\circ}\text{C}$  by cells present for the same time point at  $37^{\circ}\text{C}$ . Y-axis: relative frequency (%) of the cell proliferation ratio.

cells was centered lower than 1.0 (median 0.9), with only 36.16% of replicates over the 2-8 day exposure showing proliferation ratios at 41°C that exceeded those from 37°C controls (**Figure 3A**). Rat fibroblast proliferation ratios ranged from 0.4 - 1.7 and the median of the frequency distribution was 0.9. Replicates of heat exposed rat fibroblasts across the 2-8 day experiment were equally distributed around 1.0 (49.98% < 1.0 and 50.02% > 1.0 ; **Figure 3B**). Compared to human and rat, southern white rhino fibroblasts had a reduced range of proliferation ratios at 41°C compared to 37°C controls (0.3 - 1.3). The median proliferation of southern white rhino cells over the 2-8 day heat exposure was 0.8, with 84.37% of replicates exhibiting ratios < 1.0 and only 15.63% of replicates exhibiting ratios  $\geq$  1.0 (**Figure 3C**).

Overall, 61.46% of data points for fibroblast proliferation ratios in species presumed to be heat tolerant were > 1.0 (**Figure 4A**), whereas 67.36% of proliferation data points in species presumed to be heat sensitive were < 1.0 (**Figure 4B**). Indeed, a linear mixed-effects analysis revealed that cell proliferation ratios were significantly higher in heat tolerant versus heat sensitive species during chronic heat stress ( $F = 7.75_{1,28}$ ,  $P = 0.0095$ ) (**Table 7** in the **Appendix**).

Cell viability

As with fibroblast proliferation, cell viability (measured via cell death/cytotoxicity via LDH release into the conditioned cell media) was assayed at 24h intervals over 2-8 days during experimental heat exposure in cell culture. This metric also did not differ in any species (statistical results for repeated measures ANOVA table is provided in **Table 6** in the

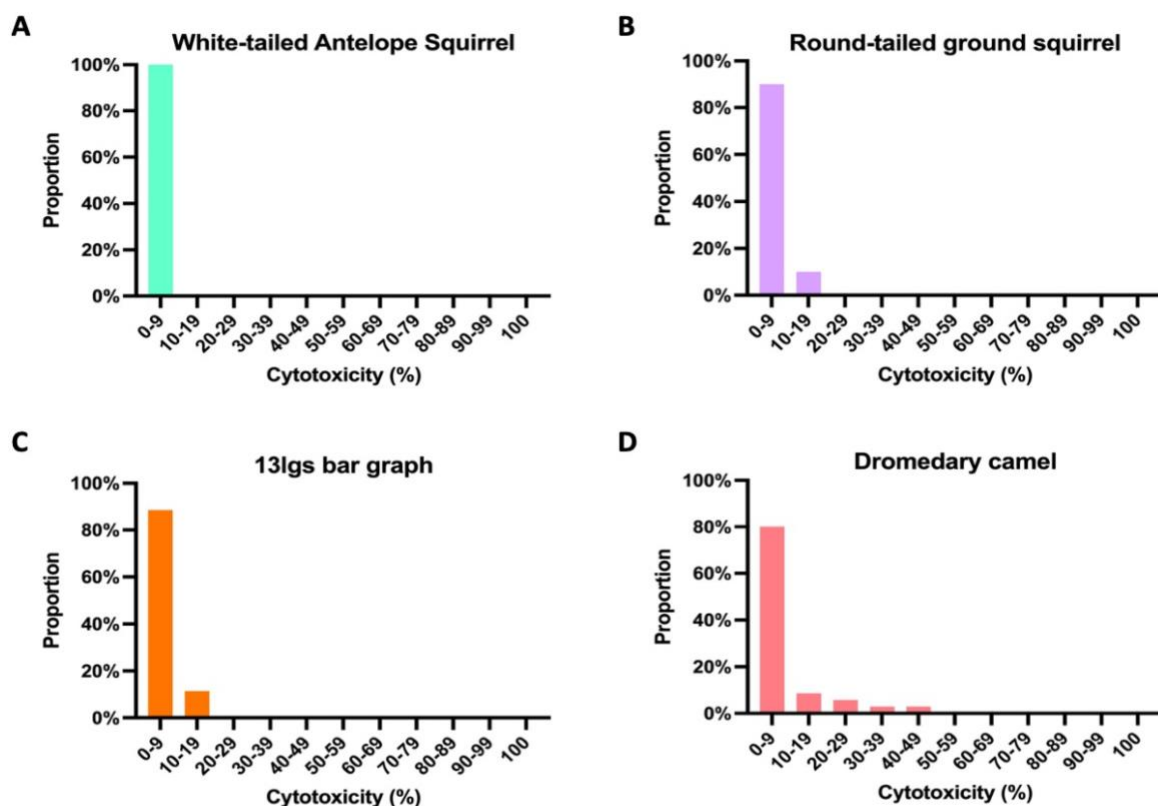


**Figure 5.** Relative frequency (%) distribution exhibiting the effect of chronic heat exposure (41°C) on cell viability of presumed heat tolerant mammals. (A) Cell viability after heat exposure (41°C) for 2 and 4 days in the white-tailed antelope squirrel. (B) Cell viability after heat exposure (41°C) for 2-8 days in the round-tailed ground squirrel (data for biological replicate XT2 for day 7 at 41°C is not included). (C and D) Cell viability after heat exposure (41°C) for days 2-8 in the 13-lined ground squirrel and dromedary camel, respectively. X-axis: cell cytotoxicity (%). Y-axis: relative frequency (%) of the cell cytotoxicity (%).

**Appendix**), therefore results across the experimental time course were combined to evaluate differences between species and phenotypes. Although fibroblasts were only collected from white-tailed antelope squirrels on days 2 and 4 of the experiment, cells displayed 0% cell cytotoxicity at 41°C (**Figure 5A**). Round-tailed ground squirrel cells exhibited a maximum of 16% cytotoxicity throughout the 8-day heat exposure (41°C), with 90% of replicates demonstrating 0% cytotoxicity (**Figure 5B** and **Table 4** in the

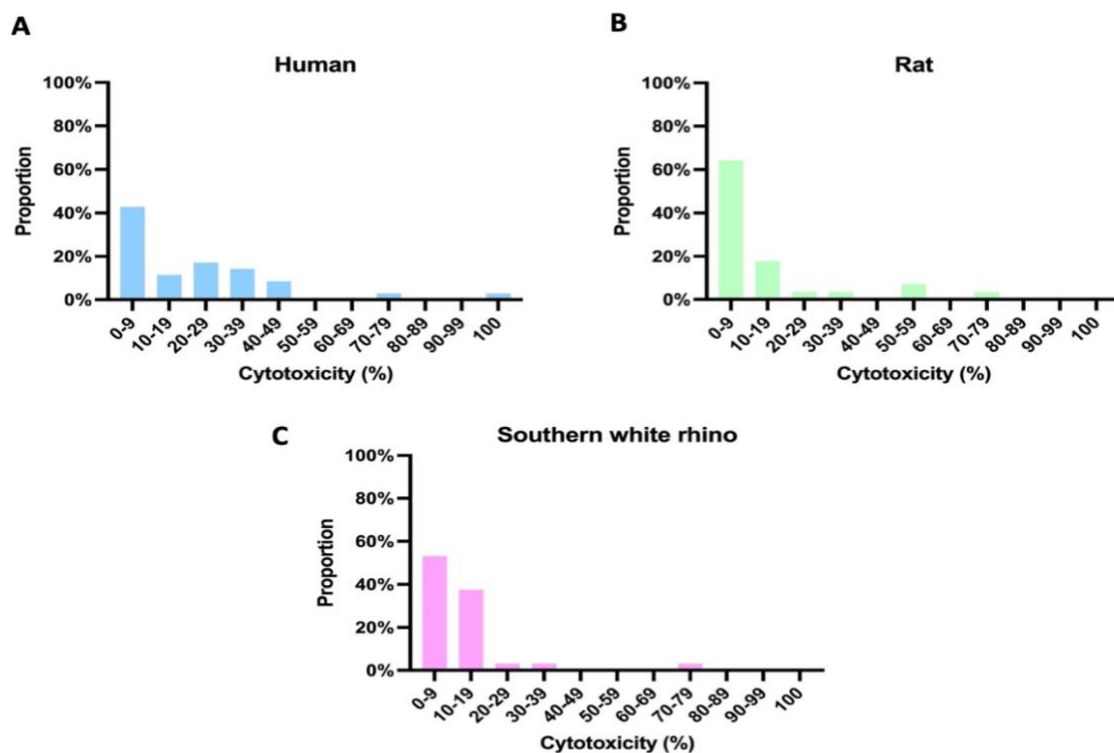


**Figure 6.** Relative frequency (%) distribution exhibiting the effect of chronic heat exposure (41°C) on cell viability of presumed heat sensitive mammals. (A and B) Cell viability after heat exposure (41°C) for 2-8 days in the human and rat, respectively. (C) Cell viability after heat exposure (41°C) for 2-8 days in the southern white rhino (data for biological replicates CSO4 and CSO5 for days 4, and days 4 and 6, respectively, at 41°C are not included). X-axis: cell cytotoxicity (%). Y-axis: relative frequency (%) of the cell cytotoxicity (%).

**Appendix**). Cells from the 13-lined ground squirrel had a cytotoxicity maximum of 14% (**Table 4** in the **Appendix**), with 0% cell death in 88.59% of replicates (**Figure 5C**). The dromedary camel cells had the highest recorded cytotoxicity of any presumed heat tolerant species (40%; **Table 4** in the **Appendix**), however, 80% of cytotoxicity values remained at 0% (**Figure 5D**).

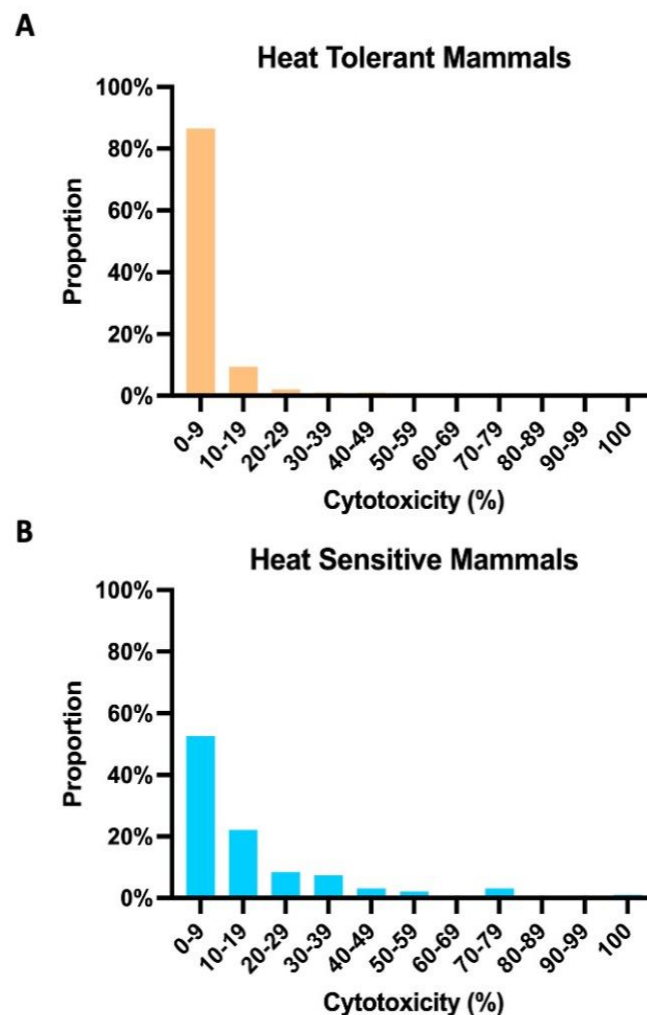


**Figure 7.** Relative frequency (%) distribution exhibiting the effect of chronic heat exposure (41°C) for 2-8 days on cell viability of all presumed (A) heat tolerant and (B) heat sensitive mammals. Biological replicates with missing time points that weren't plotted on the frequency distribution graph for Figures 1 and 2 are also not present in this figure. X-axis: cell cytotoxicity (%). Y-axis: relative frequency (%) of the cell cytotoxicity (%).



Cells from humans displayed the highest proportion as well as amplitude of measured cytotoxicity across the 8-day exposure to heat stress, with one replicate experiencing 100% cytotoxicity (**Figure 6A** and **Table 4** in the **Appendix**). Rat cells had a maximum of 72% cytotoxicity (**Figure 6B** and **Table 4** in the **Appendix**) and southern white rhino cells displayed a maximum of 70% cytotoxicity with the largest frequency occurring for a cytotoxicity (%) of ~10% (**Figure 6C** and **Table 4** in the **Appendix**). The majority of human and southern white rhino cells resulted in cytotoxicity (%) greater than 10% or more.

The frequency distributions for cytotoxicity (%) across all presumed heat tolerant mammals (**Figure 7A**) is left-shifted compared to the frequency distribution for all presumed heat sensitive mammals (**Figure 7B**). 86.46% of replicates for heat tolerant mammals display minimal to no cytotoxicity (0-9%). Presumed heat sensitive mammals display a larger proportion of cytotoxicity (%) equal to or greater than 10% throughout the 8 day exposure to heat stress (41°C). However, a linear mixed effects analysis resulted in no significant differences ( $F_{1,5} = 0.35$ ,  $P = 0.57$ ) (**Table 7** in the **Appendix**) in cell viability between the two phenotypes of presumed heat tolerant versus heat sensitive species during chronic heat stress.

## Discussion

In this evaluation of dermal fibroblasts of white-tailed antelope squirrel, round-tailed ground squirrel, dromedary camel, 13-lined ground squirrel, southern white rhino, human, and rat, lactate dehydrogenase and crystal violet assays were used to describe cell viability and cell proliferation, respectively, due to heat stress of 41°C. I used lactate dehydrogenase and crystal violet assays as a way to understand the sensitivity to



extreme environmental heat over a long (multi-day) duration in mammals that fluctuate or increase body temperatures or are desert-dwelling, versus mammals that maintain body temperatures. Consistent with predictions from organismal phenotypes, fibroblasts derived from heat tolerant mammals were better able to maintain proliferation at high temperature over many days compared to fibroblasts from heat sensitive mammals. Organismal phenotypes were not, however, consistent with measurements of cell death, which did not significantly differ along phenotypic lines.

It was predicted that differences in cell cytotoxicity and proliferation would occur between phenotypes during the multi-day heat exposure reflecting organismal sensitivity to temperature, however, only differences in cell proliferation between phenotypes occurred. The ability of cell machinery from heat tolerant mammals to work well at higher heat thresholds could reflect an adaptive response to this stressor. Proliferation rates at 41°C were higher on average than in 37°C controls primary dermal fibroblasts of white-tailed antelope squirrel, round-tailed ground squirrel, dromedary camel, and 13-lined ground squirrel. It's likely that heat sensitive species may not have had higher proliferation rates due to their cell machinery's inability to work well at higher heat thresholds. In addition, it's also possible that cell death may have obscured the metric for cell proliferation in heat sensitive species. The cytotoxicity (%) increased in primary dermal fibroblasts of both presumed heat tolerant and heat sensitive mammals, however, greater levels of cytotoxicity (%) occurred in presumed heat sensitive mammals. Singh et al., (2020) also reported higher cytotoxicity (LDH) (%) levels in cattle less resilient to harsh environmental extremes, Karan-Fries, versus more resilient cattle, Tarparkar, to heat shock at 44°C for

3 hours, suggesting the higher susceptibility of Karan-Fries cattle to hot environments. In addition, they showed a decrease in cell proliferation in both heat resistant and sensitive cattle, however, the heat resistant cattle remained higher than the heat sensitive cattle (Singh et al., 2020). Therefore, in this present study, decreased cell proliferation in southern white rhino, human, and rat suggests their higher sensitivity to hot environmental weather compared with white-tailed antelope squirrel, round-tailed ground squirrel, dromedary camel, and 13-lined ground squirrel.

Increased levels of LDH are associated with the sensitivity of mammalian dermal fibroblasts to heat stress. Despite the lack of a significant difference, there are observable changes in viability occurring between the two phenotypes. A greater proportion of minimal to no cytotoxicity occurs in presumed heat tolerant mammals compared to presumed heat sensitive mammals. Presumed heat sensitive mammals also show a broader range in LDH levels in comparison to presumed heat tolerant. Significantly lower levels of cytotoxicity (%) in presumed heat tolerant mammals e.g., white-tailed antelope squirrel, round-tailed ground squirrel, dromedary camel, and 13-lined ground squirrel, would have suggested their higher tolerance to the hot environmental temperature (41°C) compared with the presumed heat sensitive mammals e.g., southern white rhino, human and rat. Significantly higher levels of cytotoxicity would have further strengthened the higher sensitivity of heat sensitive species to heat, however, given the lack of significant difference, the occurrence of sublethal changes occurring should not be ruled out.

In addition to LDH, increased levels of cell proliferation ratios greater than, equal to, or less than, may be associated with the sensitivity of mammalian dermal fibroblasts to heat stress. The higher levels of cell proliferation ratios equal to or greater than 1.0 in presumed heat tolerant mammals show more cell proliferation occurring and may suggest a higher tolerance to hot environmental temperatures of 41°C. The higher levels of cell proliferation ratios less than 1.0 in presumed to heat sensitive mammals show less cell proliferation than cell death and may suggest a lower tolerance to hot environmental temperatures of 41°C. Cell proliferation was found to be significantly different between the two phenotypes, heat tolerant versus heat sensitive, thus supporting the hypothesis that the cell machinery of heat-tolerant mammals work well at 41°C compared to heat tolerant mammals.

Viability and cell proliferation during heat stress can vary depending on cell type, heat temperature and duration, time of harvest, and the state of acquired thermotolerance. Acquired thermotolerance is a state that enhances tolerance to a stressor e.g., heat, and is induced by mild heat shock followed by a recovery phase at 37°C, and provides protection from cellular damage by subsequent exposure to heat (Kühl & Rensing, 2000). Several studies have investigated the effects of heat shock and have implemented a recovery time (37°C) after heat exposure in their experimental design, which is a component that was not implemented in this study. Furthermore, it is difficult to compare this study's results to other studies that investigated the effects of this stressor as they also differ in heat temperature and duration used. As such, I was able to find only one study that investigated the effects of heat exposure over a multi-day time course and

specifically focused on viability and proliferation in the dromedary camel (Saadeldin et al., 2019). Dromedary camel fibroblast and granulosa cells exposed to chronic heat stress of 45°C for 20 hours and then exposed to a recovery phase of 38°C for 1-4 days, have been shown to decrease in viability and cell proliferation throughout the 1-4 days, whereas camel granulosa cells increased in viability and cell proliferation (Saadeldin et al., 2019). There seems to be a lack of studies investigating the effects of multi-day heat exposure to white-tailed antelope squirrel, round-tailed ground squirrel, 13-lined ground squirrel, southern white rhino, human, on cell viability or proliferation. It is possible that this study may reflect the mammalian dermal fibroblast response to heat stress in the absence of acquired thermotolerance, a state that likely occurs in these previously mentioned studies. The lack of a recovery period after heat exposure might be a factor in why no differences in viability occurred. It is also possible that 24-hour collections are not the optimal timeframe to collect and observe viability differences.

The difference in proliferation rates between phenotypes may reflect the ability of cell machinery to operate well in presumed heat tolerant mammals to work at higher thresholds of heat. This effect could be due to a Q10 effect by which the increase in temperature from 37°C to 41°C increases the cell proliferation rates. If cell machinery in heat tolerant phenotypes finds this heat temperature within the optimal threshold for normal physiological functioning, an increase in cell reaction rates at high temperatures should be measurable. Proliferation ratios < 1.0 may also indicate high cellular turnover if cell death outpaces high rates of cell division.

Insignificant changes in cell viability between the two phenotypes indicate that there may be no cell death. It's possible that sublethal changes might be occurring and reflect maladaptive responses to environmental extremes. This could be a possible explanation for why the metric in cell proliferation is different between phenotypes and not viability. qPCR and proteomics can provide further insight into identifying adaptive and maladaptive responses between the two phenotypes during heat exposure.

## Chapter 3: Mechanisms of resilience at the cellular level

### Introduction

In addition to behavioral, physiological, and cellular responses reflecting an organism's sensitivity to a stressor, genomics, and transcriptomics can further provide better insight into understanding an organism's mechanistic response to stressful conditions. Previous genomic and transcriptomic studies have investigated traits that may be adaptations to life in hot environments. Heat stress triggers gene expression and genetic adaptive responses (Horowitz et al., 1997; Huang et al., 2021; Liu & Brooks, 2012; Zhu et al., 2012). Measuring the expression of a gene provides insight into the stimulus in response to a stressor. Genome-wide expression analyses showed differentially expressed genes for heat shock response (Sajjanar et al., 2023; Singh et al., 2020), cellular metabolism, and cell cycle between relatively heat tolerant and heat sensitive cattle fibroblasts (Singh et al., 2020) and peripheral blood mononuclear cells (PBMC) (Sajjanar et al., 2023) in response to heat stress. Differentially expressed genes for responding to endoplasmic reticulum stress have also been observed in PBMCs of Holstein dairy cattle (Fang et al., 2021). Given that genes are differentially expressed in relation to the heat shock response, endoplasmic stress, cellular metabolism, and cell cycle, it is worth investigating genes e.g., HSF1, ERN1, PRKAA2, and CDKN1A, involved in these pathways to better understand the heat-stress induced mechanisms occurring between mammals that allow body fluctuations and increases and/or inhabit deserts, and mammals that maintain stable body temperatures.

Heat shock factor 1 regulates heat-shock-induced genes during the HSR and is upregulated in response to heat stress (Sajjanar et al., 2023; Singh et al., 2020; Tabuchi et al., 2008). Out of the four known heat shock factors known to exist in vertebrates, HSF1 seems to be the most characterized and shown to act as the major regulator of the heat shock response (Mahat et al., 2016; McMillan et al., 1998). Previous studies have used HSF1 knockout mouse embryonic fibroblasts (MEFs) and have shown that HSF2 (Mahat et al., 2016), HSF3, and HSF4 (McMillan et al., 1998) is independently regulated from HSF1 and does not compensate for the loss of HSF1 for inducing upregulated expression of genes during the HSR. In addition, HSF2 knockout MEFs were used to show HSF2 has no effect on the HSR (McMillan et al., 2002). Given HSF1's specialized role in the HSR in comparison to HSF2-4, HSF1 expression analysis can provide insight into HSF1 mechanisms of mammals that have the ability to fluctuate body temperatures or that inhabit hot environments versus mammals that don't have this ability nor live in these environmental extremes, in response to heat stress.

ERN1 is one of the three master regulators of the ER that are activated upon initiation of the UPR in response to heat stress (Homma & Fujii, 2016). Of the three UPR master regulators, ERN1 appears to be the most conserved branch given the ERN1 pathway is present in mammals, metazoans, plants, and yeast (Angelos et al., 2017; Hiramatsu et al., 2011; Homma & Fujii, 2016). The three master regulators are present in mammals and metazoans, plants exhibit functional homologs of only ERN1 and ATF6, and only the ERN1 pathway has been identified in yeast (Angelos et al., 2017). As of date, two ERN1 isoforms exist including ERN1 $\alpha$  and ERN1 $\beta$ . Of the two isoforms, ERN1 $\alpha$  is the most

characterized and has been shown to be expressed in all cell types (Homma & Fujii, 2016). Expression analysis on ERN1 in response to heat stress will provide better insight into the mechanisms of the UPR's most conserved pathway in presumed heat tolerant mammals versus presumed heat sensitive mammal fibroblasts.

Metabolic stress caused by heat shock can activate and upregulate AMPK activity, and increase the expression of its catalytic subunit (Corton et al., 1994; Liu & Brooks, 2012; J. Tang et al., 2018). The three genes that encode the  $\alpha$ ,  $\beta$ , and  $\gamma$  subunits of the AMPK are highly conserved in vertebrates and invertebrates (Hardie, 2007). The two isoforms of the gene that encode for the catalytic subunit ( $\alpha$  subunit) of AMPK, PRKAA1, and PRKAA2, are both activated during heat stress and seem to have different tissue distributions (J. Tang et al., 2018; Y. Wang et al., 2016; Yang et al., 2021). AMPK complexes can increase activity when increased AMP levels occur. AMPK complexes that contain PRKAA2 isoform seem to be more sensitive to AMP than AMPK-PRKAA1 complexes. Unlike PRKAA1, PRKAA2 seems to localize in the nucleus, thus raising the possibility that AMPK-PRKAA2 may have a role in regulating gene expression in response to cellular stresses that deplete ATP levels (Salt et al., 1998). Expression analysis on highly conserved PRKAA2 gene may show its sensitivity to changes in AMP: ATP ratios in relation to heat stress across a range of mammalian species.

Heat stress can cause an induction of CDKN1A, which may play a role in inhibiting cell cycle progression (Abe, T. Tamiya, Y. Ono, A. H. Salke, 2001; Fuse et al., 1996; Kühl & Rensing, 2000; Nitta et al., 1997; Ohnishi et al., 1996; Woo et al., 2000). Of the three



inhibitors within the CIP/KIP family, hyperthermia-induced expression of CDKN1A has often been shown to be involved in responding to heat stress rather than the p27 pathway (Abe, T. Tamiya, Y. Ono, A. H. Salke, 2001). To date and to the best of my knowledge, studies have observed p57 and INK4 family proteins playing a role in regulating cell cycle progression, however, the involvement of each of these inhibitors in relation to heat stress remains to be further characterized. (Creff & Besson, 2020; Sherr & Roberts, 1999). Expression analysis on the more characterized response of CDKN1A in relation to heat will provide a better understanding of how the cell cycle is regulated between the two phenotypes of presumed heat tolerant and heat sensitive mammals.

Each of the four genes of interest has been observed to have a response in relation to heat stress. In addition, they are either highly conserved genes and/or part of a conserved pathway, making them good candidates for further investigating their responses in non-model species in relation to heat stress. Using a comparative approach by investigating the timing and amplitude of the heat-stress-related gene expression of HSF1, ERN1, PRKAA2, and CDKN1A and protein abundance patterns between presumed heat tolerant and heat sensitive mammals may provide better insight into the mechanisms that are occurring, which make an animal flexible.

## Methods

### *Samples*

Cells were obtained and proliferated as described in Chapter 2.

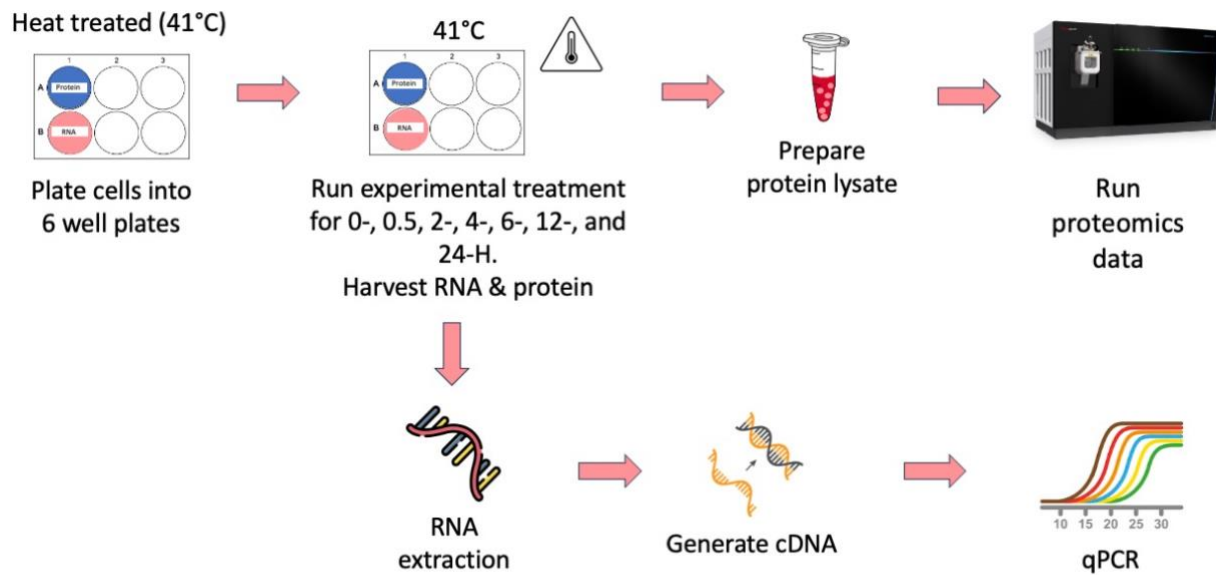


**Figure 8.** Schematic of experimental design for chapter 3.

### *Heat exposure and examination of cell viability and cell proliferation*

Cells were plated into 6 well plates. Cell passage numbers are listed under **Table 1** in the **Appendix**. The seeding density for a 6 well plate is usually around  $0.3 \times 10^6$  cells. Due to the multiple time points and the large number of cells needed for plating, of the entire T175cm<sup>2</sup> flask that was passaged, 75% of the cell stock was used for plating. For one biological replicate, two wells on one plate were plated. One well was to be harvested for protein and the other for RNA. Cells were grown in the 6-well plates until they reached 80-90% confluency. Once cells were confluent, the DMEM Dulbecco's Modified Eagle's Medium + 10% FBS + 1% P/S, REF #11965-092) medium was used at the start of the heat treatment. A schematic of chapter 3's experimental design is shown on **Figure 8**.

### *RNA Extraction and Quantitative PCR (qPCR)*

Cells were treated in 41°C for 0 hours, 0.5 hours, 2 hours, 4 hours, 6 hours, 12 hours, and 24 hours. Cells were washed in PBS twice and collected with TRIzol reagent (Invitrogen™ TRIzol™ Reagent, REF #15596018). 200µL of chloroform per 1mL (1:5) TRIzol was added, vortexed for ~20 seconds, and incubated for 3 minutes at room temperature. The tubes containing RNA samples were spun down for 20 minutes at 12000xg at 4°C. The clear top layer was pipetted and transferred to a new Eppendorf tube. The same amount of isopropanol from the amount of the clear layer that was pipetted into the new Eppendorf tube, to the clear layer. The Eppendorf was inverted to mix, and then incubated for 10 minutes at room temperature. The tubes were spun down for 10 minutes at 12000xg at 4°C. The supernatant was aspirated, and the RNA pellet was washed with 750µL of 75% EtOH. Then the tubes were spun down for 5 minutes at 7500xg at 4°C. EtOH was aspirated, and samples were dried on ice for about 10 minutes, ensuring all ethanol was removed. The RNA was dissolved in 30µL of Invitrogen™ nuclease-free water (not DEPC-treated) and heated for 7 minutes at 60°C. RNA concentration and purity were estimated by NanoDrop® ND-1000 UV-Vis Spectrophotometer. Reverse transcription (RT) was performed using the Applied Biosystems: High Capacity cDNA Reverse Transcription Kit (with RNase Inhibitor) (Thermo Fisher cat #: 4374966). RT reactions consisted of 10µL of 0.5µg of total RNA in a 20µL total reaction volume; with the exception of a few samples that had a lower RNA concentration and instead consisted of 5µL of 0.25µg of total RNA in a 10µL total reaction volume. After running samples through the thermocycler, cDNA samples with a 20µL and 10µL total reaction volume were diluted 1:5 by adding 80µL and 40µL of MilliQ water,

respectively, to freshly made samples. Quantitative PCR (qPCR) was performed using the CFX96 Real-Time PCR. Reactions comprised of a 10 $\mu$ L total volume consisting of 3 $\mu$ L of cDNA, 0.4 $\mu$ L FWD and RVS primers, 1.2 $\mu$ L of MilliQ water, and 5 $\mu$ L of Fast SYBR<sup>™</sup> Green MM (REF #4385612). Housekeeping gene 18S was used for normalization and the fold change of the target transcripts were calculated through the  $2^{-\Delta\Delta C_t}$  method. Negative samples resulted in little (Cq of ~37/38) to no amplification in all assays. Thermal cycling conditions were 10 minutes at 25°C, 120 minutes at 37°C, 5 minutes at 85°C, and then held at 4°C. Details of primers used to amplify target transcripts are listed under **Table 8** in the **Appendix**.

#### *Outlier detection methods*

Technical replicates with a standard deviation of greater than 10% were excluded from the analysis. After normalization and calculating the fold change of target transcripts through the  $2^{-\Delta\Delta C_t}$  method, the z-score and the median absolute deviation (MAD) outlier detection methods were implemented to detect outliers for a given time point (excluded outliers are listed under **Table 9** in the **Appendix**). Cq values of the samples that were detected as outliers through the MAD outlier detection method and not excluded from data analysis were checked to ensure that this was a true response of the biological replicate, and kept for this reason.

#### *qPCR statistical analysis*

Paired t-tests (GraphPad Prism Version 10.0.0.0) were used to analyze if there were significant changes in the immediate induction of a gene at 0- and 0.5-hours for each

species. Wilcoxon tests (GraphPad Prism Version 10.0.0.0) were used to analyze non-parametric datasets and whether there were significant changes in the immediate induction of a gene at 0- and 0.5-hours for each species. The relationship between expression at the 0.5-hour time point and the two phenotypes were analyzed with a nested ANOVA for genes HSF1, ERN1, PRKAA2, and CDKN1A. Furthermore, one-way ANOVA (GraphPad Prism Version 10.0.0.0) analyzed significant differences in the mean expression at the 0.5-hour time point for each species. To investigate patterns across the 24-hour time course at 41°C for each species and gene, repeated measures ANOVA (*Mixed-Effects Models in S and S-PLUS*, 2000) was performed across all time points. Tukey's HSD (*Mixed-Effects Models in S and S-PLUS*, 2000) test was used on data sets with significant statistical differences of  $P \leq 0.05$ . The linear mixed-effects model (*Mixed-Effects Models in S and S-PLUS*, 2000) was used to analyze differences in a gene's expression across all time points between the two phenotypes. Significant statistical differences were considered when  $P \leq 0.05$ .

## **Proteomics analysis**

### *Preparation of cell protein lysate*

Cells were treated in 41°C for 0 hours, 0 hours, 6 hours, and 24 hours. Cells were washed with cold PBS twice and homogenized with a cold cell lysis buffer consisting of RIPA buffer with EDTA #BP-115D, + 1% of protease inhibitor cocktail 100x (Prod #1861278 thermofisher) + 1% of phosphatase inhibitor cocktail (Prod #TG269618 thermofisher). After incubation at 4°C for 10 minutes, the extract was further homogenized with a tuberculin syringe. Homogenized samples were placed in -80°C for at least 2 hours and

then vortexed after thawed. Samples were centrifuged in a microcentrifuge at 14,500rpm for 10 minutes at 4°C. The supernatant was then transferred to a new tube and measured through the BCA method (Pierce™ Bovine Serum Albumin Standard Ampules, 2 mg/mL; REF #23209)

### *Protein digestion*

Protein extracts were reduced, alkylated, and digested with a trypsin/Lys-C protease mixture using Thermo Scientific EasyPep Mini MS Sample prep kit (Cat #A40006).

### *Liquid chromatography and mass spectrometry*

Peptides were trapped prior to separation on a 300 um i.d. x 5 mm C18 PepMap 100 trap (Thermo Scientific, San Jose, CA) and separated on a 50cm uPAC C18 nano-LC column (PharmaFluidics, Ghent, Belgium) with a 15um tip using an UltiMate 3000 RSLCnano system (Thermo Scientific, San Jose, CA).

### *Data-independent acquisition (DIA)*

Mass spectral analysis was performed using an Orbitrap Eclipse mass spectrometer (Thermo Scientific, San Jose, CA) using DIA. Six gas phase fractions (GPF) of the biological sample pool were used to generate a reference library. The GPF acquisition used 4 m/z precursor isolation windows in a staggered pattern (GPF1 398.4-502.5 m/z, GPF2 498.5-602.5 m/z, GPF3 598.5-702.6 m/z, GPF4 698.6-802.6 m/z, GPF5 798.6-902.7 m/z, GPF6 898.7-1002.7 m/z). Biological samples were analyzed on an identical gradient as the GPFs using a staggered 8 m/z window scheme over a mass range of 385-

1015 m/z. Library generation and data analysis were performed using Spectronaut™ software (Biognosys, Schlieren, Switzerland). The white-tailed antelope squirrel was analyzed against the 13-lined ground squirrel database, 13-lined ground squirrel and rat were analyzed against their own database.

#### *Proteomics data analysis*

Data reports (.xsl) were generated from raw files using Spectronaut™ software and included the condition, file name, gene, protein accession number, and quantity. The white-tailed antelope squirrel retained 18,693 protein entries, the 13-lined ground squirrel retained 35,091 protein entries, and the rat retained 34,084 protein entries. Duplicates were removed and resulted in 2,076 proteins in white-tailed antelope squirrels, 3,787 proteins in the 13-lined ground squirrel, and 3,789 proteins in the rat. Protein IDs with no quantity, multiple or no gene names, or are from a different organism than the one being analyzed, were removed from analysis and placed in a separate tab ('filtered out') of the excel sheet. Protein IDs with no gene name and that had a P\*\*\* term was searched in NCBI. Protein IDs with no gene name and that had a I\*\*\* term or A\*\*\* was searched in GenomeNet. Entries that didn't have matching protein accession IDs with gene names and those that listed an unreal gene name were also set aside in the 'filtered out' tab. The mean and standard deviation of the protein quantity of each of the three time points were calculated among the three individuals per species.

#### *Proteomics statistical analysis*

Protein quantity values were analyzed using one-way ANOVA and Tukey test (*Mixed-Effects Models in S and S-PLUS*, 2000). Benjamini-Hochberg method was implemented to correct the false discovery rate. Significant statistical differences were considered when  $P \leq 0.05$ . Random forests (Breiman, 2001) were run 12 times to compare 6 hr. and 24 hr. time points between the three species and used to compare the three time points e.g., 0 hours, 6 hours, and 24 hours, for each of the three species. Lastly, Divisive Analysis Clustering (DIANA) clustering was applied to produce gene clusters (Bolker et al., 2022; Kuhn, 2021; Maechler et al., 2021; Peterson, 2021; Sarkar, 2008; Warnes, 2013; Warnes, Bolker, Bonebakker, et al., 2022; Warnes, Bolker, Lumley, et al., 2022; Warnes et al., 2023; Wickham, 2007; Yan, 2016).

## Results

### *Impact of heat stress on HSF1 transcripts expression*

Paired t-tests and Wilcoxon tests showed no significant change in HSF1 expression from 0- to 0.5-hours at 41°C in any of the mammals (**Figure 9**; **Table 10** and **Table 11** in the **Appendix**). The white-tailed antelope squirrel and southern white rhinoceros were excluded from this paired t-test analysis because only n=2 biological replicates were available for this gene and time collection. Furthermore, one-way ANOVA showed no significant differences in the HSF1 expression mean across all mammals at 0.5 hours at 41°C ( $P = 0.68$ ) (**Figure 10A** and **Table 12** in the **Appendix**). Nested ANOVA analysis resulted in non-significant HSF1 expression differences at 0.5 hours at 41°C for heat tolerant and heat sensitive phenotypes of different mammalian species (**Table 13** in the **Appendix**).



Each of the presumed heat tolerant mammal exhibited a peak of HSF1 expression at different time points into the experimental heat exposure (**Figure 11**). The greatest amplitude of HSF1 gene expression in the white-tailed antelope squirrel occurred at 6 hours at 41°C, and was 1.3-fold higher than baseline on average (**Figure 11A**). For the round-tailed ground, the greatest amplitude of HSF1 expression was at baseline level, which occurred after 24 hours (**Figure 11B**). 13-lined ground squirrel exhibited a peak of 1.5-fold increase above baseline at 2 hours (**Figure 11C**). The dromedary camel showed a 1.1-fold increase in HSF1 expression after 0.5 hours (**Figure 11D**).

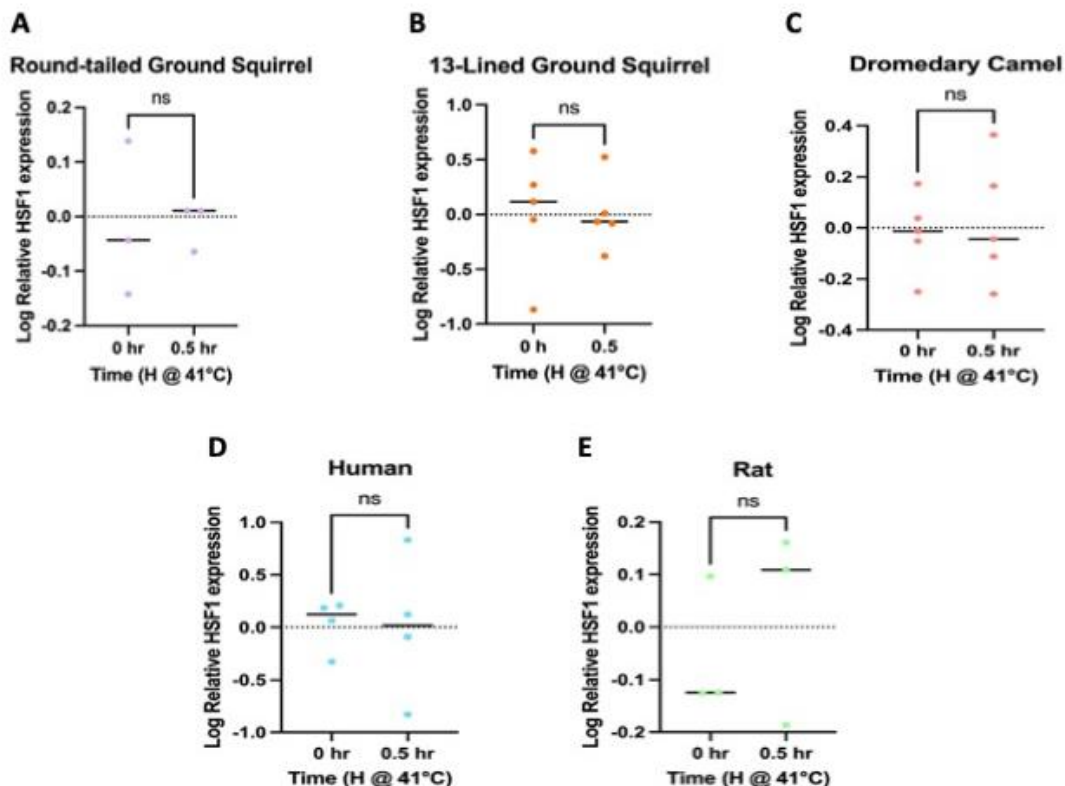


**Figure 9.** The effect of heat stress (41°C) did not cause an immediate induction of HSF1 at 0.5 hours. No significant change in HSF1 expression occurs from 0 to 0.5 hours at 41°C in (A) round-tailed ground squirrel, (B) 13-lined ground squirrel, (C) dromedary camel, (D) human, (E) rat. X-axis: time (H). Y-axis: LOG relative fold change of HSF1 expression.

Likewise, each presumed heat sensitive mammal similarly exhibited a peak in HSF1 expression at different times (**Figure 12**). The rats had a peak of HSF1 expression occur at 24 hours (1.5-fold; **Figure 12A**). Southern white rhinos experienced a 0.84-fold peak in HSF1 expression at 6 hours (**Figure 12B**). Humans had the greatest peak in HSF1 expression (2.2-fold), occurring at 0.5 hours post-heat exposure (**Figure 12C**).

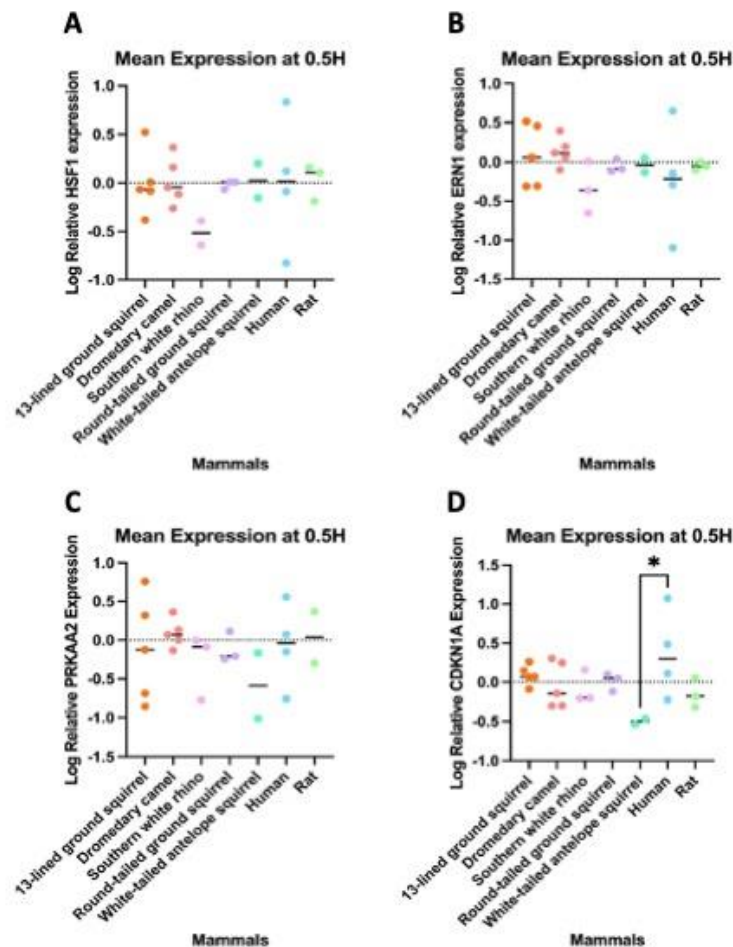


**Figure 10.** The effect of heat stress (41°C) did not cause significant differences in the mean expression of HSF1 (A), ERN1 (B), PRKAA2 (C), and CDKN1A (D) at 0.5 hours. (D) Tukey's multiple comparison tests identified significant differences in the mean expression of CDKN1A between white-tailed antelope squirrels and humans at 0.5 hours. X-axis: time (H). Y-axis: LOG relative fold change of expression. \*P < 0.05

Repeated measures ANOVA did not reveal any differences in HSF1 expression patterns across the 24-hour time course for any of the presumed heat tolerant mammals nor southern white rhino and human (**Table 14** in the **Appendix**). The rat was the only species for which this analysis yielded a significant difference ( $F_{6,18} = 3.44$ ,  $P = 0.01$ ), with Tukey HSD not identifying significant differences between any time points. Linear mixed effects identified no significant differences ( $P = 0.99$ ) in HSF1 expression across all time points between the two phenotypes (**Figure 13**; **Table 15** in the **Appendix**).

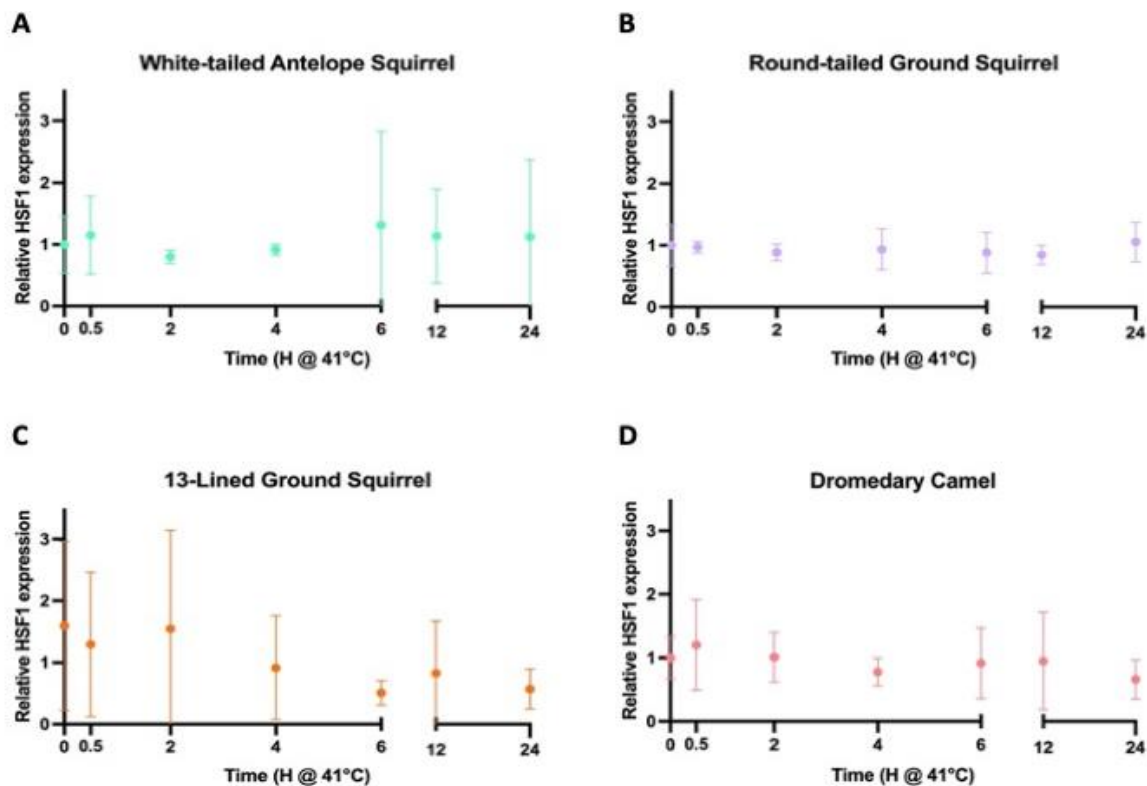


**Figure 11.** The effect of heat exposure (41°C) on HSF1 expression in squirrels and camel. No significant differences in HSF1 gene expression patterns exist across the time course in the (A) white-tailed antelope squirrel ( $P = 0.95$ ), (B) round-tailed ground squirrel ( $P = 0.52$ ), (C) 13-lined ground squirrel ( $P = 0.14$ ), (D) and the dromedary camel ( $P = 0.95$ ). X-axis: time (H). Y-axis: relative fold change of HSF1 expression.

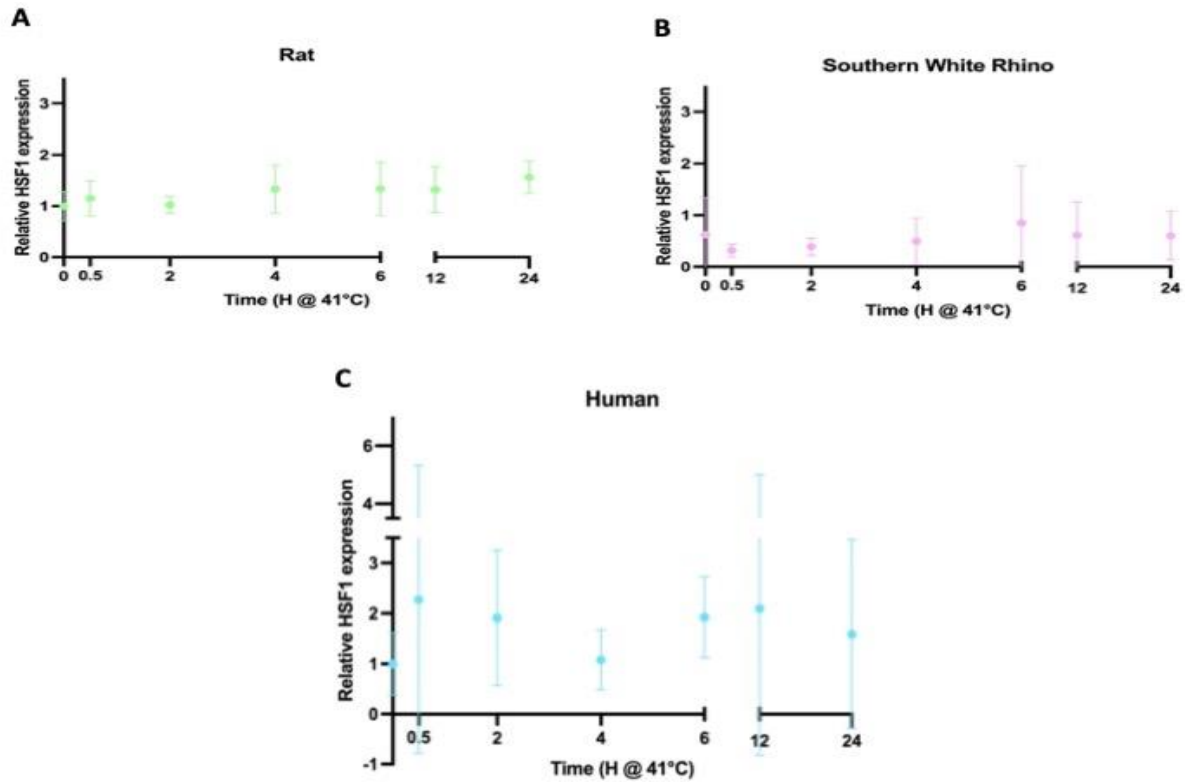


**Figure 12.** The effect of heat exposure (41°C) on HSF1 expression in rat, rhino, and human. Significant differences in HSF1 gene expression patterns exist across the time course in (A) rat ( $P = 0.01$ ). No significant differences in HSF1 gene expression patterns exist across the time course in the (B) southern white rhino ( $P = 0.71$ ) and (C) human ( $P = 0.66$ ). X-axis: time (H). Y-axis: relative fold change of HSF1 expression.

### *Impact of heat stress on ERN1 transcripts expression*

Of the four presumed heat tolerant mammals, paired t-tests revealed a significant increase in ERN1 expression from 0- to 0.5 hours at 41°C in the dromedary camel ( $P = 0.0002$ ) (**Figure 14C**). The white-tailed antelope squirrel was excluded from this paired t-test analysis because only  $n=2$  biological replicates were available for this gene and time collection. ERN1 expression did not change over the first 30 minutes of heat exposure, however, in any of the round-tailed ground squirrel (**Figure 14A**), 13-lined ground squirrel ( $P = 0.31$ ) (**Figure 14B**), human (**Figure 14D**), rat (**Figure 14E**), or southern white rhino (**Figure 14F**) (**Table 10** in the **Appendix**). Furthermore, the one-way ANOVA results

showed no significant differences in the ERN1 expression mean across all mammals at 0.5 hours at 41°C ( $P = 0.63$ ) (**Figure 10B** and **Table 16** in the **Appendix**). Nested ANOVA analysis results showed no significant ERN1 expression differences at 0.5 hours at 41°C for heat tolerant and heat sensitive phenotypes of different mammalian species (**Table 17** in the **Appendix**).

As with HSF1, each presumed heat tolerant mammal exhibited a peak of ERN1 expression at different time points (**Figure 15**). The white-tailed antelope squirrels

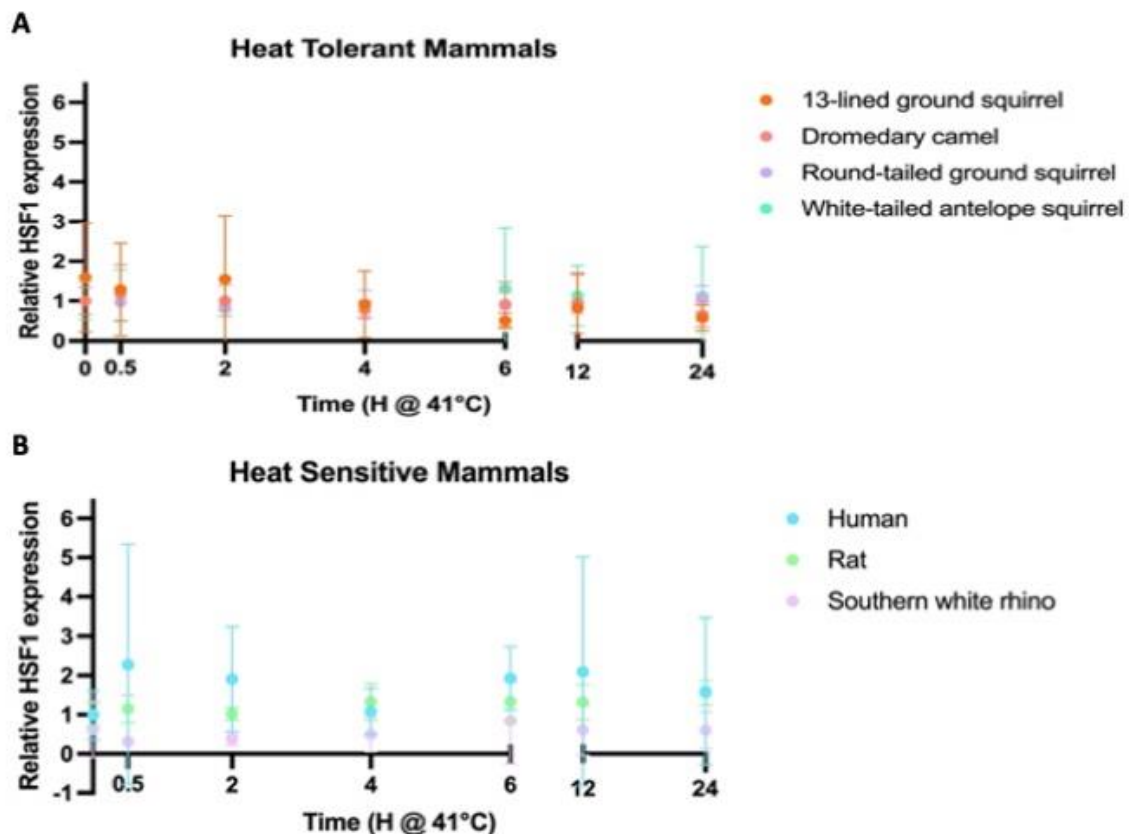


**Figure 13.** The effect of heat exposure (41°C) on HSF1 expression in presumed (A) heat tolerant and (B) heat sensitive mammals. X-axis: time (H). Y-axis: relative fold change of HSF1 expression.

generally had reduced expression of ERN1 across the experimental, with the 6 hour timepoint remaining at slightly below baseline levels (**Figure 15A**). Round-tailed ground squirrels had a peak at 12 hours with an average of 1.2 (**Figure 15B**). 13-lined ground squirrels had the greatest amplitude of ERN1 expression at 2 hours at 1.7-fold baseline levels (**Figure 15C**). Dromedary camels exhibited a peak at 2 hours post-exposure, with ERN1 levels 1.4-fold above baseline (**Figure 15D**).

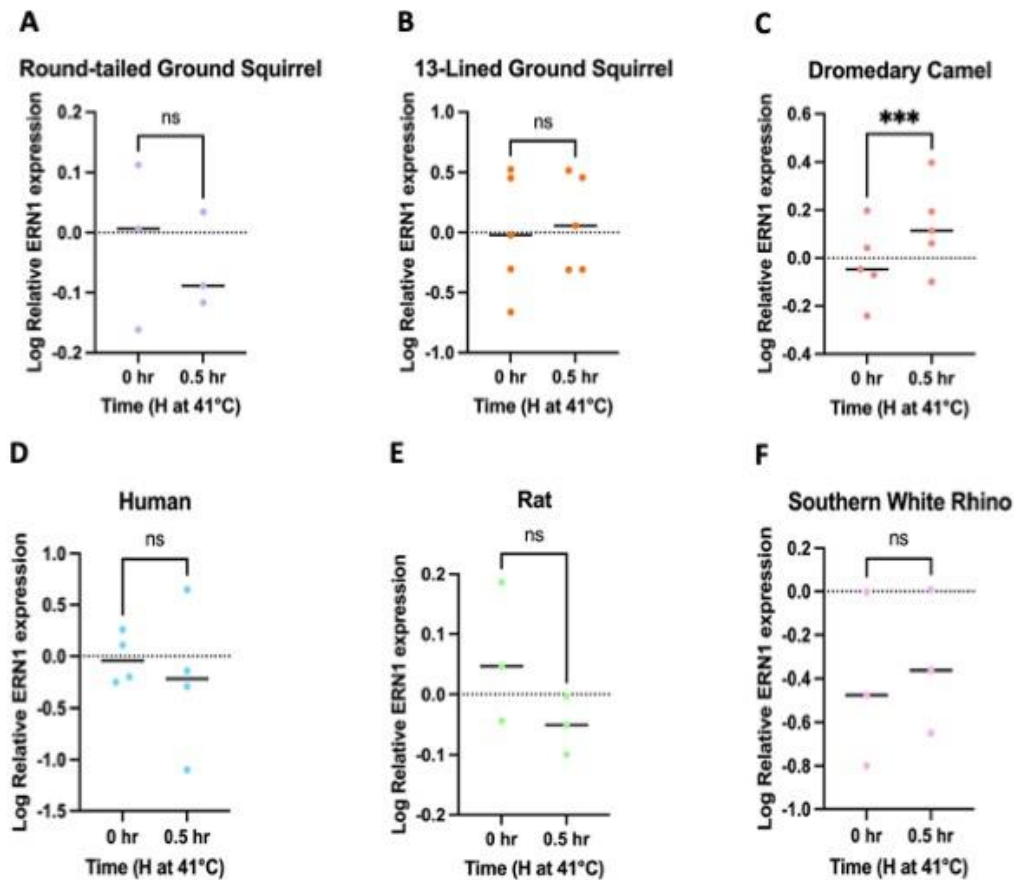


**Figure 14.** The effect of heat stress (41°C) caused an immediate induction of ERN1 at 0.5 hours in the 13-lined ground squirrel and dromedary camel. No significant change in ERN1 expression occurs from 0 to 0.5 hours at 41°C in (A) round-tailed ground squirrel, (B) 13-lined ground squirrel, (D) human, (E) rat, (F) and southern white rhino. However, significant change in ERN1 expression does occur from 0 to 0.5 hours at 41°C in (C) dromedary camel ( $P = 0.0002$ ). X-axis: time (H). Y-axis: LOG relative fold change of ERN1 expression.

\* $P < 0.05$ ; \*\*\* $P < 0.001$



Presumed heat sensitive mammals also exhibited peaks in ERN1 expression at different timepoints (**Figure 16**). The rats had a peak of ERN1 expression at 2 hours (1.2-fold increase) (**Figure 16A**). Southern white rhinos generally had reduced expression of ERN1 across the experimental time course (**Figure 16B**). Of the presumed heat sensitive mammals, humans experienced the greatest peak at 6 hours (2.7-fold increase) (**Figure 16C**).

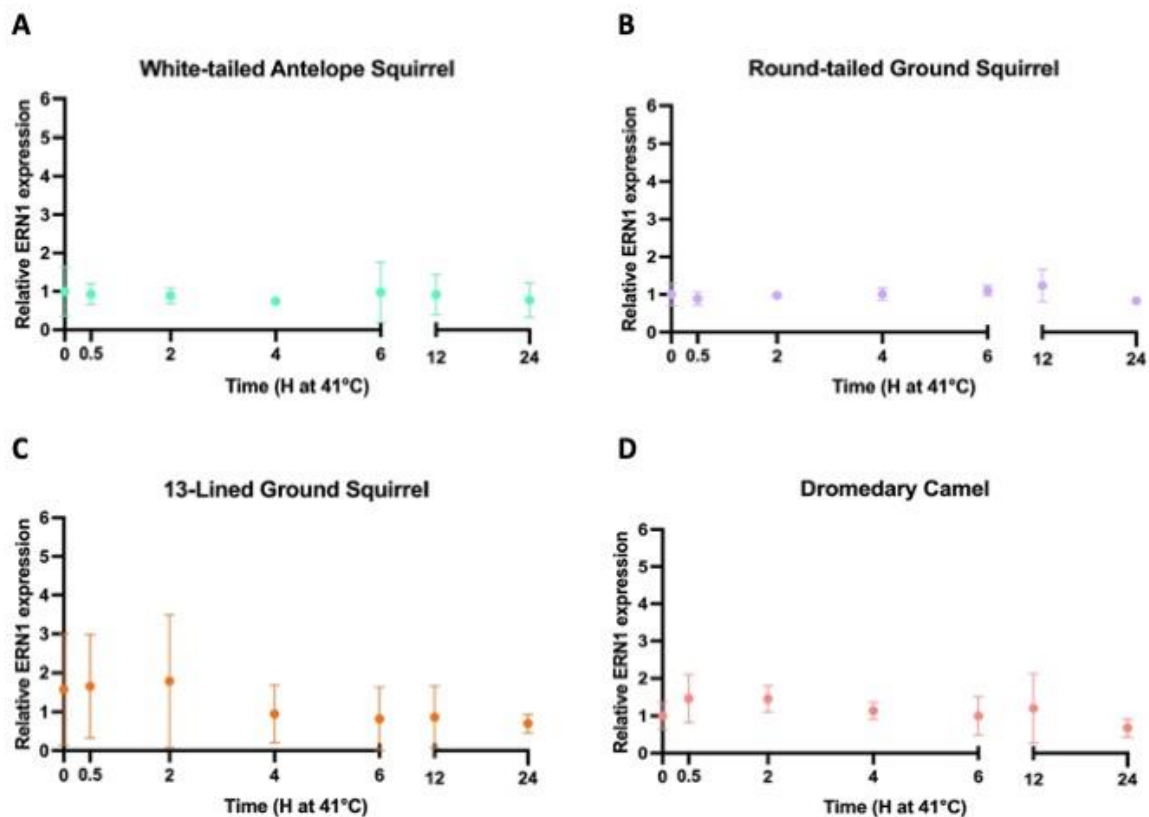


**Figure 15.** The effect of heat exposure (41°C) on ERN1 expression in squirrels and camel. No significant differences in ERN1's gene expression patterns exist across the time course in the (A) white-tailed antelope squirrel ( $P = 0.99$ ), (B) round-tailed ground squirrel ( $P = 0.65$ ), (C) 13-lined ground squirrel ( $P = 0.07$ ), and the (D) dromedary camel ( $P = 0.07$ ). X-axis: time (H). Y-axis: relative fold change of ERN1 expression.

ERN1 expression patterns across the 24 hour time course were analyzed by repeated measures ANOVA. Out of all investigated species, only the southern white rhino ( $F_{6,18}=2.72$ ,  $P = 0.04$ ) showed significant differences in ERN1 expression (**Table 18** in the **Appendix**). Despite a significant difference in ERN1 expression, the southern white rhino showed no significant differences between any time points. Linear mixed effects identified no significant differences ( $F_{1,5} = 0.4$ ,  $P = 0.5$ ) in ERN1 expression across all time points between the two phenotypes (**Figure 17**; **Table 15** in the **Appendix**).

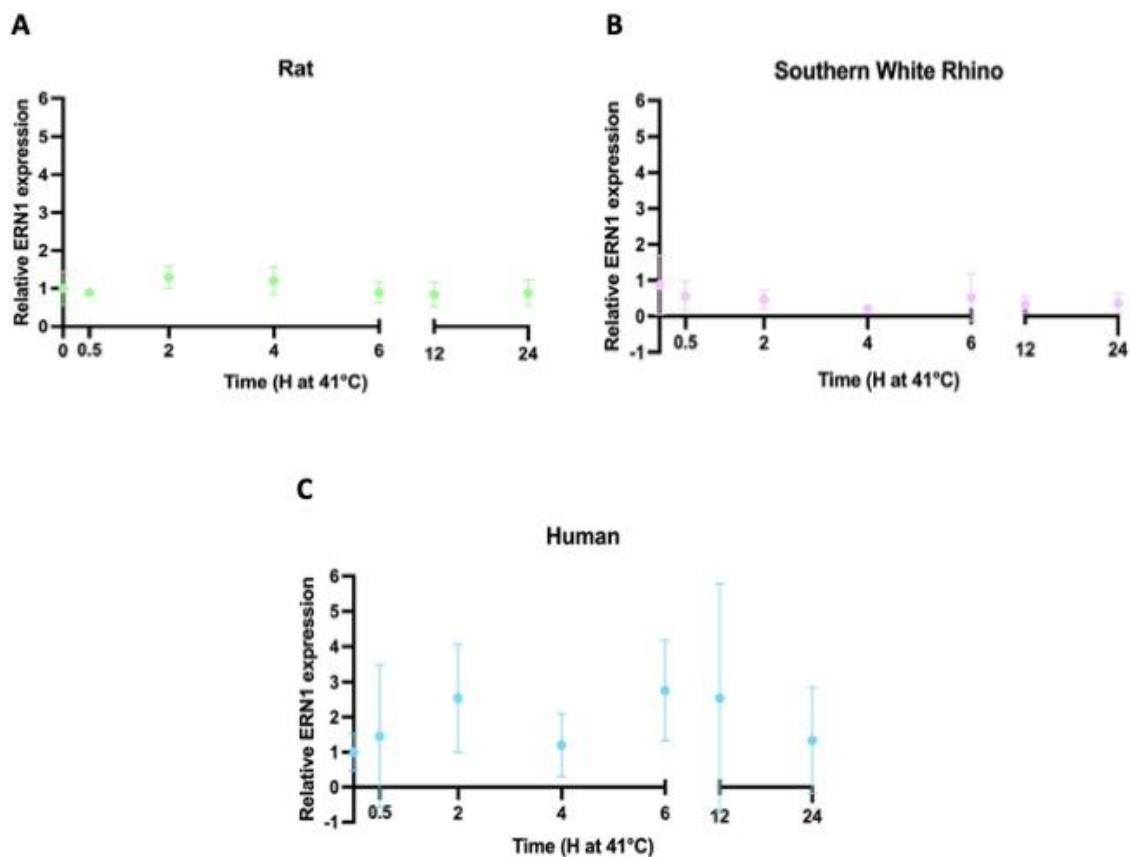


**Figure 16.** The effect of heat exposure (41°C) on ERN1 expression in rat, rhino, and human. Significant differences in ERN1's gene expression patterns exist across the time course in (B) southern white rhino ( $P = 0.04$ ). No significant differences in ERN1 gene expression patterns exist across the time course in the (A) rat ( $P = 0.19$ ) and (C) human ( $P = 0.06$ ). X-axis: time (H). Y-axis: relative fold change of ERN1 expression.



### *Impact of heat stress on PRKAA2 transcripts expression*

Paired T-tests results showed no significant change in PRKAA2 expression from 0- to 0.5 hours at 41°C in any of the mammals (**Figure 18**) (**Table 10** in the **Appendix**). The white-tailed antelope squirrel and rat were excluded from this paired t-test analysis because only n=2 biological replicates were available for this gene and time collection. One-way ANOVA results showed no significant differences in PRKAA2 expression across all mammals at 0.5 hours at 41°C ( $P = 0.73$ ) (**Figure 10C**; **Table 19** in the **Appendix**).

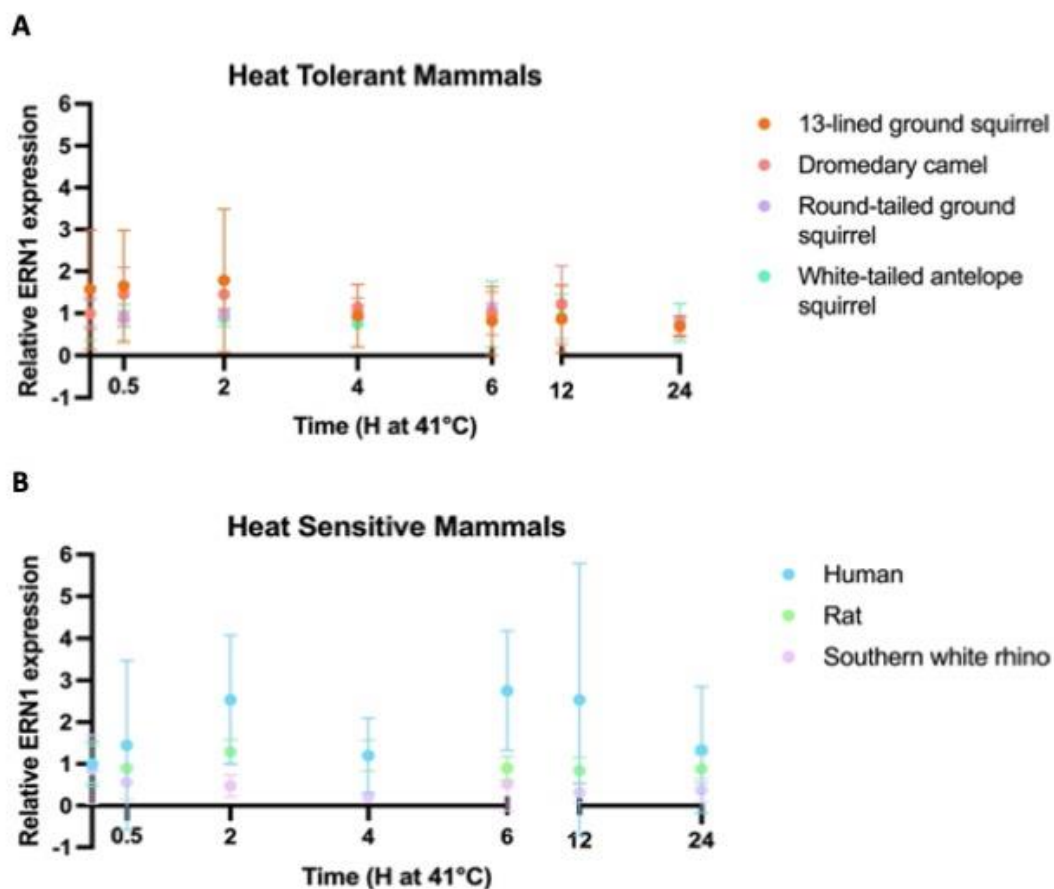


**Figure 17.** The effect of heat exposure (41°C) on ERN1 expression in presumed (A) heat tolerant and (B) heat sensitive mammals. X-axis: time (H). Y-axis: relative fold change of ERN1 expression.

Nested ANOVA results showed no significant differences in PRKAA2 expression mean between phenotypes at 0.5 hours at 41°C ( $P = 0.74$ ) (**Table 20** in the **Appendix**).

The white-tailed antelope squirrel generally had reduced expression of ERN1 across the experimental time course (**Figure 19A**). Round-tailed ground squirrels showed reduced (0.89-fold decline was the peak amplitude at 2h) in PRKAA2 expression over the experimental time course (**Figure 19B**). The 13-lined ground squirrels (**Figure 19C**) and dromedary camels (**Figure 19D**) had a peak at the same time point, 0.5 hours, with fold induction of 1.7 and 1.3, respectively.

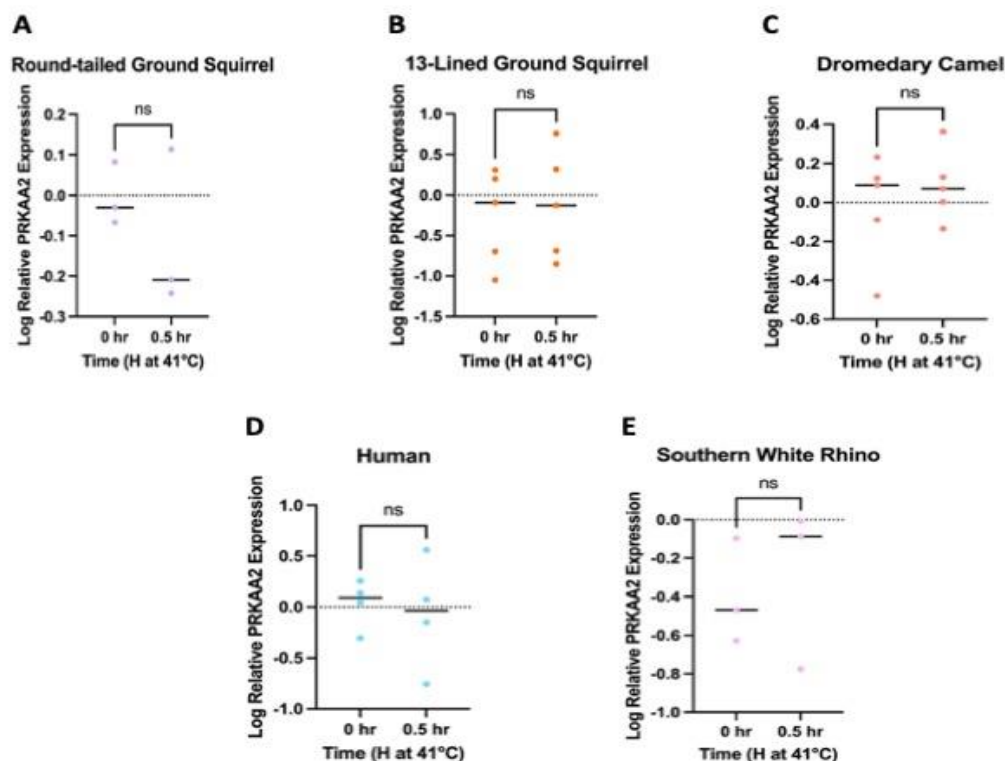


**Figure 18.** The effect of heat stress (41°C) did not cause an immediate induction of PRKAA2 at 0.5 hours. No significant change in PRKAA2 expression occurs from 0 to 0.5 hours at 41°C in (A) round-tailed ground squirrel ( $P = 0.27$ ), (B) 13-lined ground squirrel ( $P = 0.50$ ), (C) dromedary camel ( $P = 0.32$ ), (D) human ( $P = 0.77$ ), (E) and southern white rhino ( $P = 0.61$ ). X-axis: time (H). Y-axis: LOG relative fold change of PRKAA2 expression.

The rat (**Figure 20A**) had its highest amplitude of PRKAA2 expression at 2H post-exposure, which was a 1.3-fold increase for rats. On the other hand, the southern white rhino (**Figure 20B**) generally showed decreased PRKAA2 expression with heat exposure (0.65-fold decline was the peak amplitude at 6h). Human fibroblasts had a peak at 24 hours (1.2-fold increase) (**Figure 20C**).

Repeated measures ANOVA analysis revealed no significant patterns for the dromedary camel, 13-lined ground squirrel, white-tailed antelope nor the human (**Table 21** in the

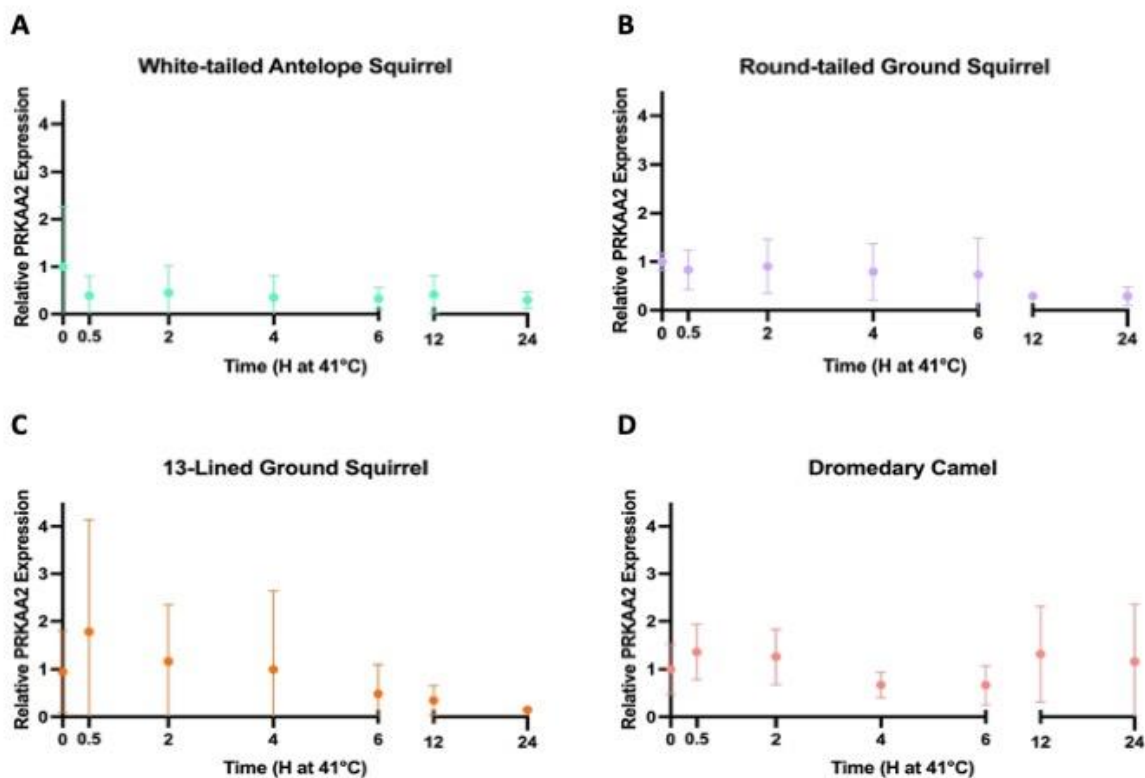


**Figure 19.** The effect of heat exposure (41°C) on PRKAA2 expression in squirrels and camel. Significant differences in PRKAA2's gene expression patterns exist across the time course in (B) round-tailed ground squirrels ( $P = 0.001$ ). No significant differences in PRKAA2's gene expression patterns exist across the time course in the (A) white-tailed antelope squirrel ( $P = 0.74$ ), and (C) 13-lined ground squirrel ( $P = 0.13$ ), (D) and the dromedary camel ( $P = 0.63$ ). X-axis: time (H). Y-axis: relative fold change of PRKAA2 expression.

**Appendix**). However, the round-tailed ground squirrel ( $F_{1,17} = 13.8$ ,  $P = 0.001$ ) rat ( $F_{6,10} = 6.1$ ,  $P = 0.006$ ) and the southern white rhino ( $F_{1,16} = 11.4$ ,  $P = 0.003$ ) with Tukey HSD identifying no significant differences from baseline to any time points (**Table 21** in the **Appendix**). Linear mixed effects identified no significant differences ( $P = 0.59$ ) in PRKAA2 expression across time points between the two phenotypes (**Figure 21**; **Table 15** in the **Appendix**).

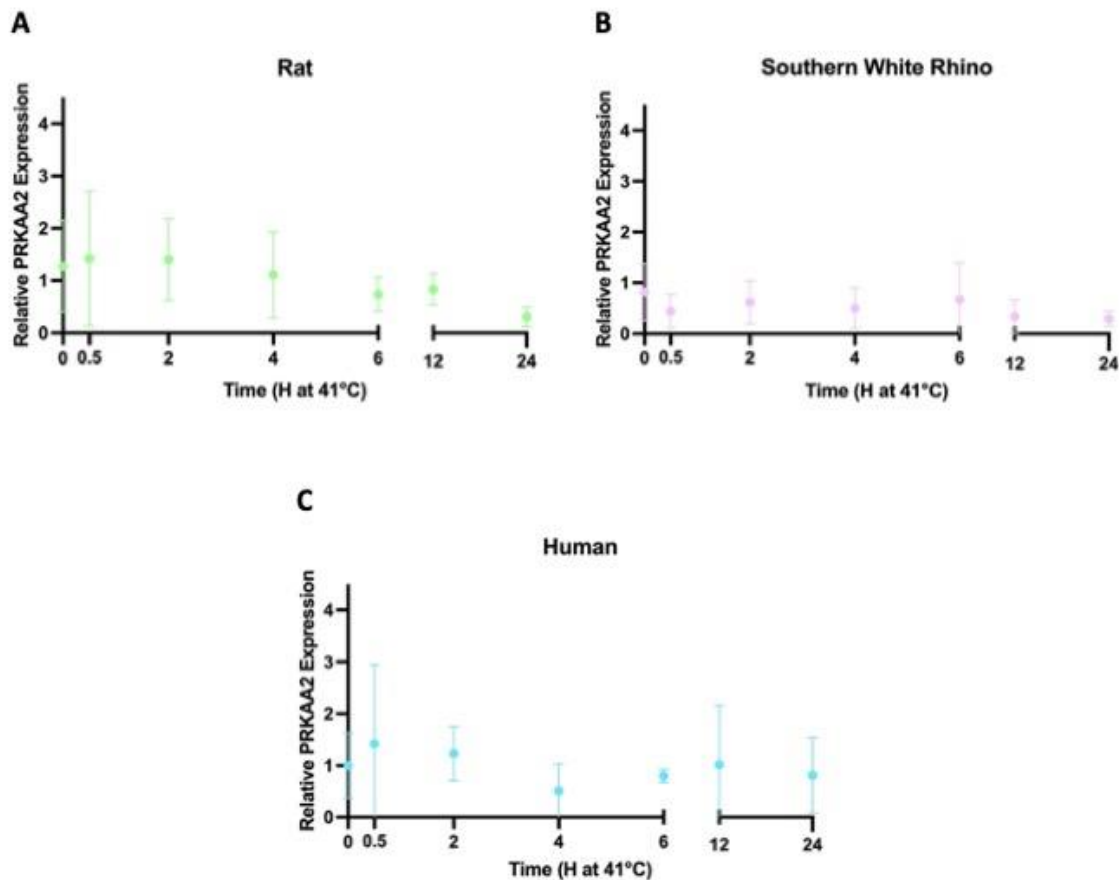


**Figure 20.** The effect of heat exposure (41°C) on PRKAA2 expression in rat, rhino, and human. Significant differences in ERN1's gene expression patterns exist across the time course in (A) rat ( $P = 0.003$ ) and (B) southern white rhino ( $P = 0.01$ ). No significant differences in PRKAA2 expression patterns exist across the time course in (C) human ( $P = 0.57$ ). X-axis: time (H). Y-axis: relative fold change of PRKAA2 expression.

### Impact of heat stress on CDKN1A transcripts expression

Paired T-tests and Wilcoxon test results showed no significant changes in CDKN1A expression from 0- to 0.5 hours at 41°C in any mammalian fibroblasts (**Figure 22; Table 10** and **Table 11** in the **Appendix**). The white-tailed antelope squirrel and rat were excluded from this paired t-test analysis because only n=2 biological replicates were available for this gene and time collection. However, there was a significant difference between white-tailed antelope squirrel and human (Tukey's pairwise posthoc  $P = 0.03$ ), in CDKN1A responses at 30 min post-exposure (one-way ANOVA  $F_{6,18} = 2.28$ ,  $P = 0.08$ )

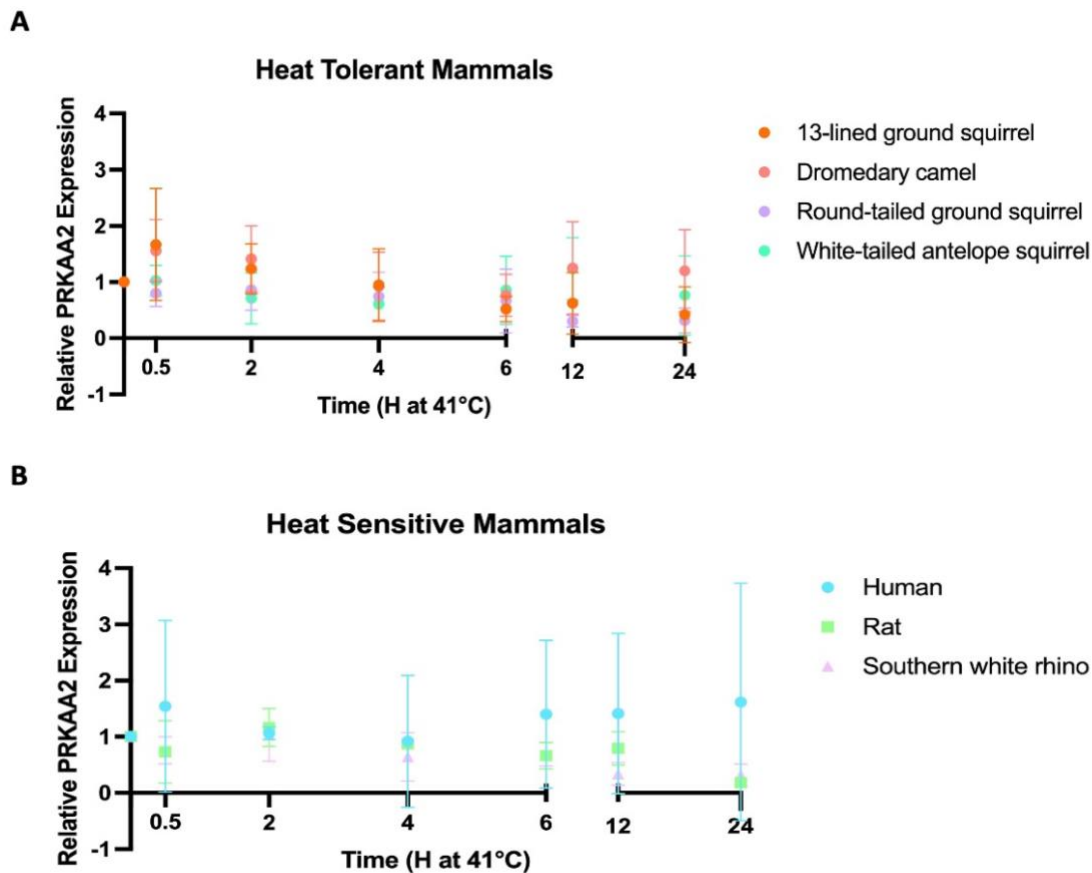


**Figure 21.** The effect of heat exposure (41°C) on PRKAA2 expression in presumed (A) heat tolerant and (B) heat sensitive mammals. X-axis: time (H). Y-axis: relative fold change of PRKAA2 expression.

(Figure 10D; Table 22 in the Appendix). CDKN1A expression differences at 0.5 hours at 41°C for heat tolerant and heat sensitive phenotypes was not significant (Table 23 in the Appendix).

Both the white-tailed antelope squirrel (Figure 23A) and round-tailed ground squirrel (Figure 23B) exhibited a peak of CDKN1A expression at 12 hours at 41°C (1.1-fold and 1.3-fold increase, respectively). The 13-lined ground squirrel (Figure 23C) and the

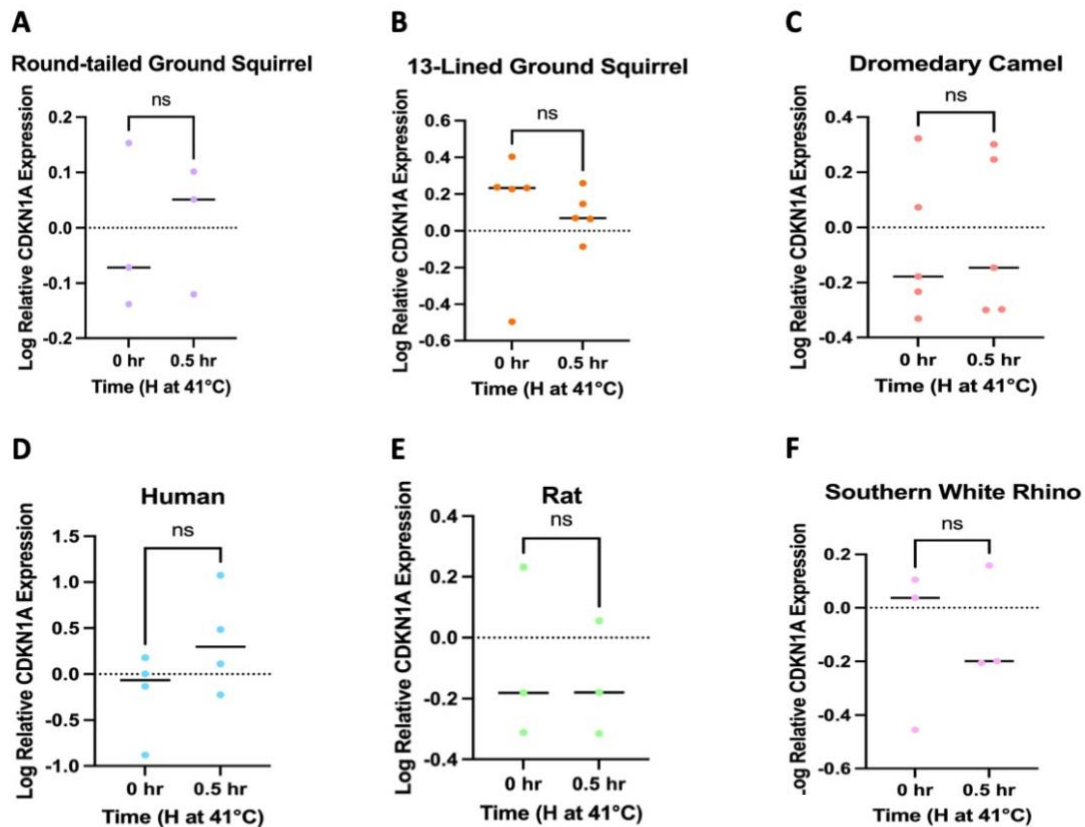


**Figure 22.** The effect of heat stress (41°C) did not cause an immediate induction of CDKN1A at 0.5 hours. No significant change in CDKN1A expression occurs from 0 to 0.5 hours at 41°C in the (A) round-tailed ground squirrel, (B) 13-lined ground squirrel, (C) dromedary camel, (D) human, (E) rat, (F) and southern white rhino. X-axis: time (H). Y-axis: LOG relative fold change of CDKN1A expression.



dromedary camel (**Figure 23D**) also exhibit a peak of CDKN1A expression at the same time of 0.5 hours at 41°C with fold-increases of 1.6 and 1.0, respectively.

The greatest amplitude of CDKN1A gene expression in the rat was 1.35-fold from baseline, which occurred after 4 hours at 41°C (**Figure 24A**). The southern white rhino (**Figure 24B**) exhibited a peak in expression of 1.4-fold beyond baseline after 2 hours at 41°C. Humans also exhibited a peak in CDKN1A expression at 2 hours at 41°C but had a much greater gene expression induction, at 9.1-fold beyond baseline (**Figure 24C**).

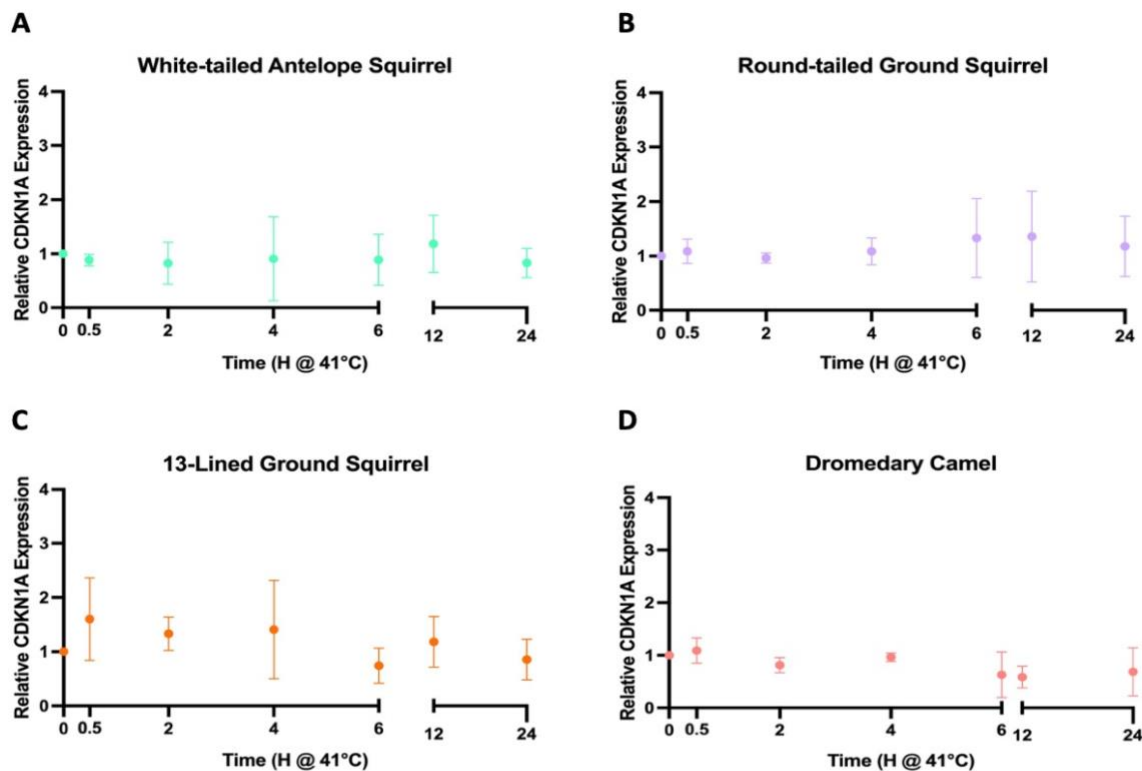


**Figure 23.** The effect of heat exposure (41°C) on CDKN1A expression in squirrels and camel. No significant differences in CDKN1A gene expression patterns exist across the time course in the (A) white-tailed antelope squirrel ( $P = 0.80$ ), (B) round-tailed ground squirrel ( $P = 0.90$ ), and (C) 13-lined ground squirrel ( $P = 0.13$ ). (D) and the dromedary camel ( $P = 0.56$ ). X-axis: time (H). Y-axis: relative fold change of CDKN1A expression.

Repeated measures ANOVA analyzed CDKN1A expression patterns across the 24-hour time course and resulted in no significant patterns for any of the presumed heat tolerant mammals nor human and rat (**Table 24** in the **Appendix**). However, the southern white rhino did exhibit significant changes in CDKN1A gene expression ( $F_{6,18} = 4.4 = P = 0.006$ ), however Tukey pairwise posthoc did not identify significant differences between any time points. Linear mixed effects identified no significant differences ( $P = 0.5$ ) in CDKN1A expression across all time points between the two phenotypes (**Figure 25**; **Table 15** in the **Appendix**).

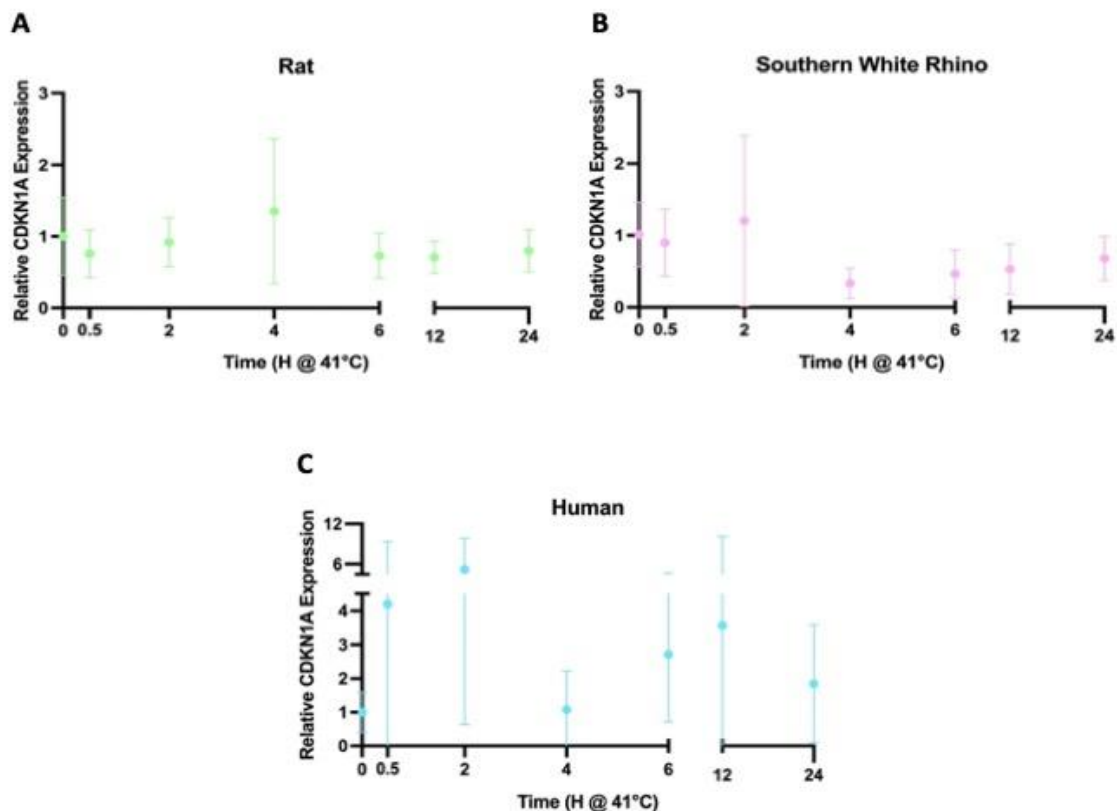


**Figure 24.** The effect of heat exposure (41°C) on PRKAA2 expression in rat, rhino, and human. Significant differences in CDKN1A gene expression patterns exist across the time course in (B) rhino ( $P = 0.006$ ). No significant differences in CDKN1A expression patterns exist across the time course in (A) rat ( $P = 0.49$ ) and (C) human ( $P = 0.15$ ). X-axis: time (H). Y-axis: relative fold change of CDKN1A expression.



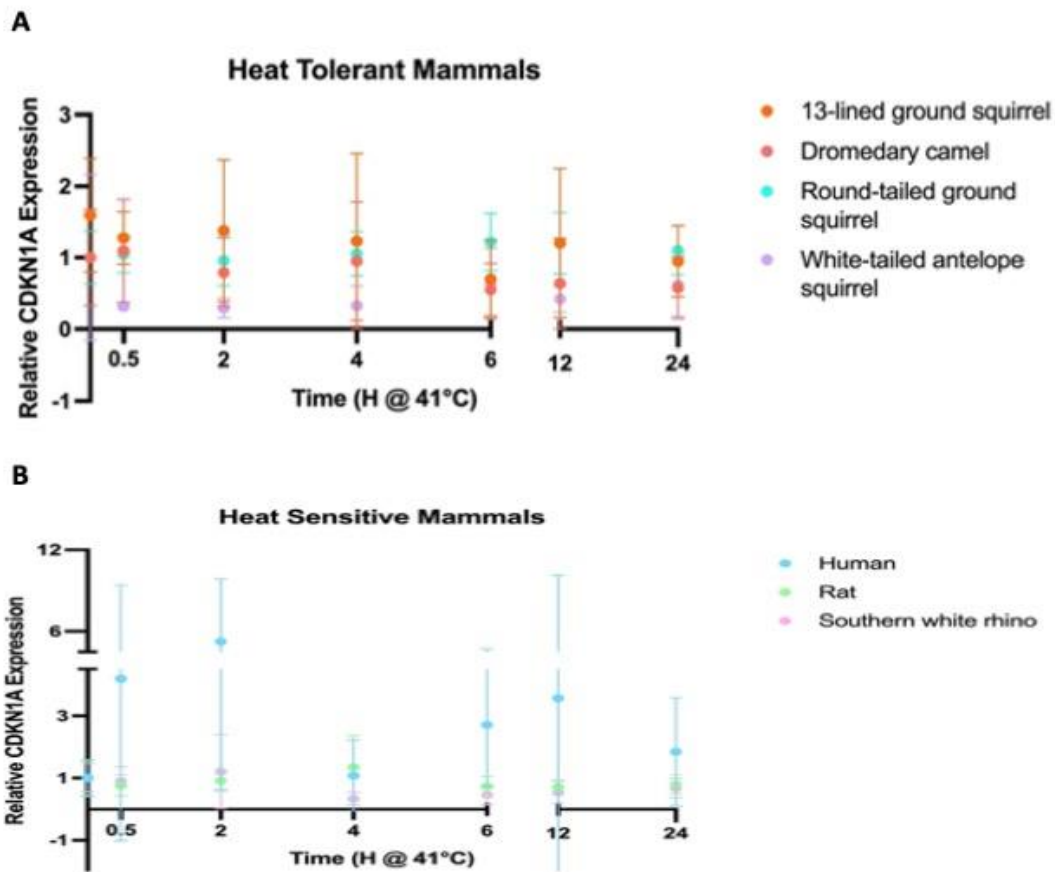


**Figure 25.** The effect of heat exposure (41°C) on CDKN1A expression in presumed (A) heat tolerant and (B) heat sensitive mammals. X-axis: time (H). Y-axis: relative fold change of CDKN1A expression.

### *Proteomics of heat-stressed cells*

#### *Significantly induced HSPs*

489 out of 3,664 detected proteins had abundances that significantly differed following heat stress for 6- and 24-hours in 13-lined ground squirrels, 122 of 2,002 differed in white-tailed antelope squirrels, and 193 out of 3,145 differed significantly in rats. While similar numbers of proteins altered in abundance following heat stress, many responses were species-specific. Significant induction of heat shock proteins such as HSP90AB1 in the

13-lined ground squirrel and white-tailed antelope squirrel identify mechanisms of homeostatic resilience, particularly in desert-dwelling species (**Table 25**). An increased protein abundance of HSP90AB1 occurs at 6- and 24-hours at 41°C in desert-dwelling rodents (**Figure 26A and 26B**). Significant induction of HSP90B1, HSPA1L, HSPA5, and HSPA8 reflect a species-specific response in 13-lined ground squirrel, while significant induction of HSPA1A and HSPD1 reflect a species-specific response in the white-tailed antelope squirrel (**Table 25**). In 13-lined ground squirrel fibroblasts, an increase in abundance occurs at 6- and 24-hours at 41°C for HSP90B1 (**Figure 26C**), HSPA1L (**Figure 26D**), HSPA5 (**Figure 26E**), and HSPA8 (**Figure 26F**). In white-tailed antelope squirrel, an increase in abundance occurs at 6- and 24- hours at 41°C for HSPA1A (**Figure 26G**), whereas a decrease in abundance occurs at 6- and 24- hours at 41°C for HSPD1 (**Figure 26H**).

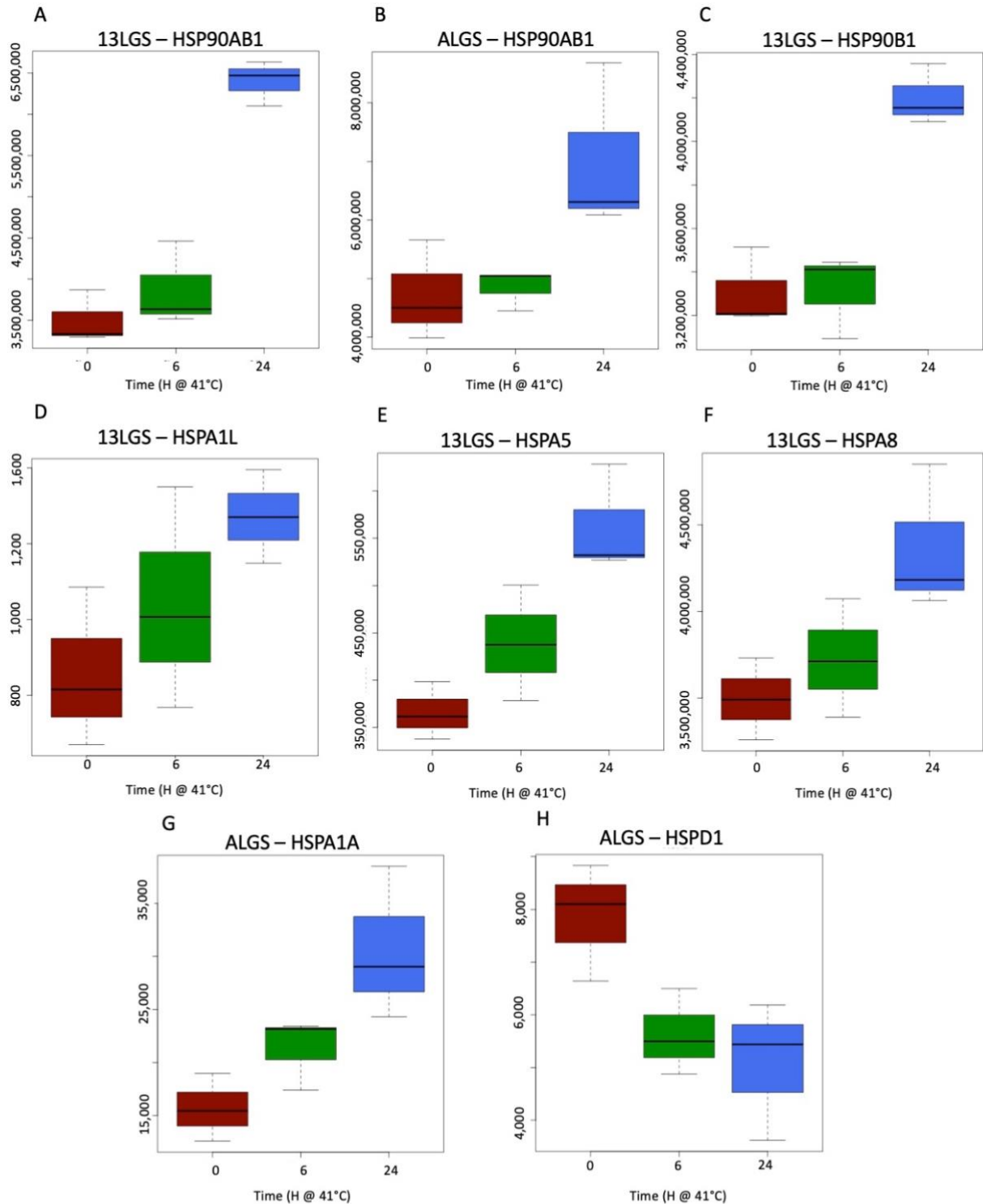


**Figure 26.** The effect of heat exposure (41°C) on HSP expression in presumed heat tolerant and heat sensitive mammals. Heat exposure resulted in significant induction of HSP90AB1 in both (A) 13-lined ground squirrel and (B) white-tailed antelope squirrel, (C) HSP90B1, (D) HSPA1L, (E) HSPA5, and (F) HSPA8 in 13-lined ground squirrel, and (G) HSPA1A and (H) HSPD1 in white-tailed antelope squirrel. X-axis: Time (H) at 41°C. Y-axis: Quantification number. 13LGS = 13-lined ground squirrel, ALGS = White-tailed antelope squirrel.

## Random Forest

After random forest was run 12 times to compare the three time points for each species, 5 different proteins (selected variables) were identified for 13-lined ground squirrel, 2 proteins for white-tailed antelope squirrel, and 1 protein for rat that represent biomarkers whose abundance is capable of defining the time points in each species (**Table 26** in the

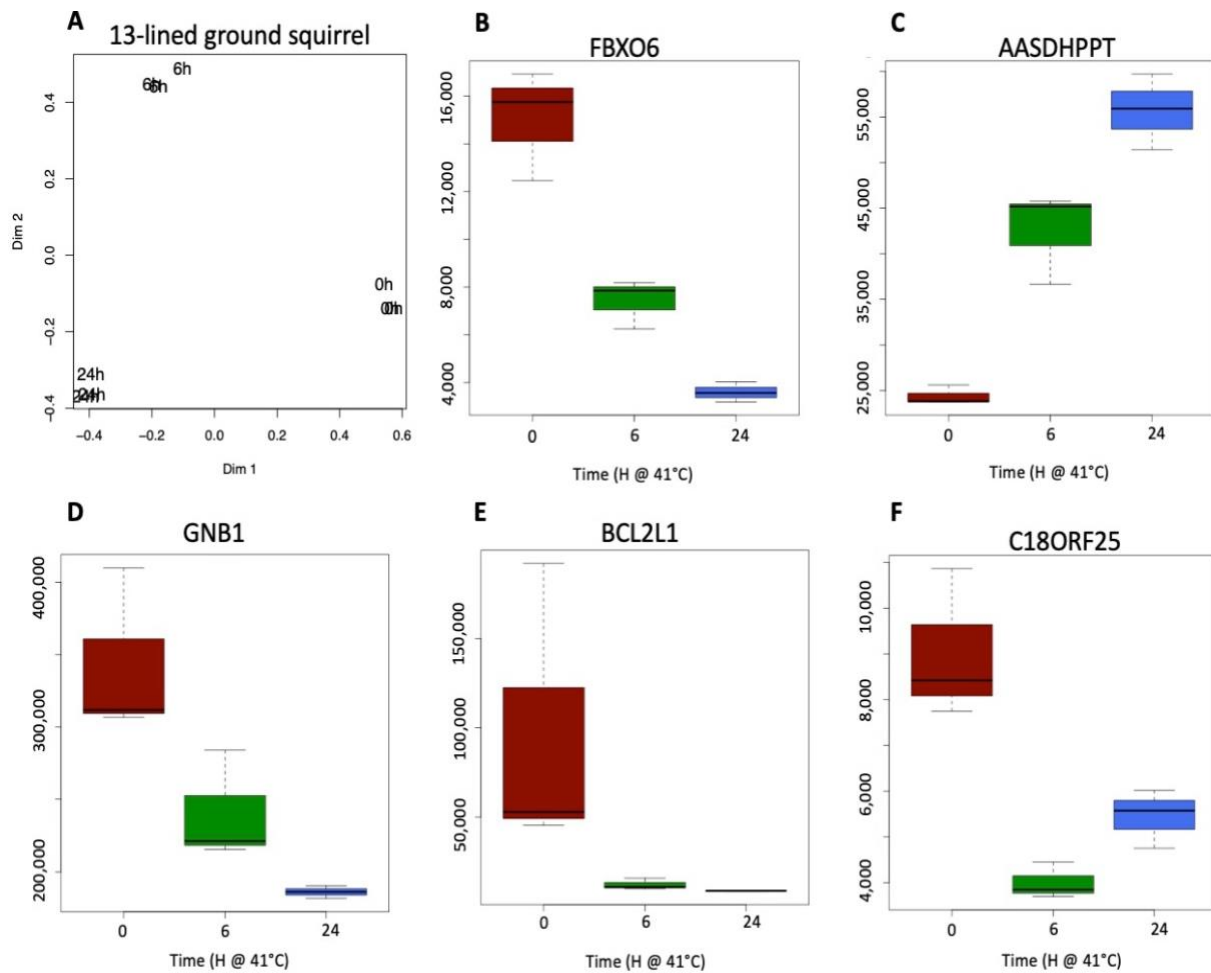


**Figure 27.** Random forests and box plots depicting relevant and important selected variables from the comparison between all three time points in the 13-lined ground squirrel. (A) Random forest plot depicting FBXO6 and AASDHPPT in the 13-lined ground squirrel. Box plots depicting the change in expression in (B) FBXO6, (C) AASDHPPT, (D) GNB1, (E) BCL2L1, and (F) C18ORF25. X-axis: Time (H) at 41°C. Y-axis: Quantification number.

**Appendix**). While random seeding in this machine learning approach can slightly vary the proteins capable of separating the timepoints for each species with 0 error over different runs, the protein listed above were output in at least 75% of runs for each species, and represent likely biomarkers that separate the 0h, 6h, and 24h proteomes from each other (**Table 27** in the **Appendix**). Random Forests generated importance values along with these selected variables that represent the relevance of each variable in the Random Forest model. These selected variables with a high appearance rate are the top 3 importances, representing their relevance in the random forest model.

The five selected variables in 13-lined ground squirrels were FBXO6, AASDHPPT, GNB1, BCL2L1, and C18ORF25 (**Figure 27A-E**). FBXO6 ( $P = 0.00007$ ) (**Figure 27B**), GNB1 ( $P = 0.001$ ) (**Figure 27D**), BCL2L1 ( $P = 0.06$ ) (**Figure 27E**), and C18ORF25 ( $P = 0.06$ ) (**Figure 27F**) decreased in expression from baseline to 6- and 24 hours at 41°C, whereas AASDHPPT ( $P = 0.00002$ ) increases in expression at 6- and 24 hours (**Figure 27C**). The baseline expression for each FBXO6 and AASDHPPT differed in magnitude; AASDHPPT baseline expression was greater than FBXO6. The two selected variables in white-tailed antelope squirrels were MSRB3 and SPTLC2 (**Figure 28A-C**). MSRB3 ( $P = 0.2$ ) increased expression at 6 hours and then decreased at 24 hours at 41°C (**Figure 28B**). SPTLC2 ( $P = 0.003$ ) decreased at 6- and 24 hours (**Figure 28C**). The baseline expression for MSRB3 was greater than SPTLC2. The one selected variable that frequently appeared, with a rate of 91.67%, was MRPL12 (**Figure 29**). MRPL12 ( $P = 0.17$ ) increased at 6 hours at 41°C, and decreased expression at 24 hours.

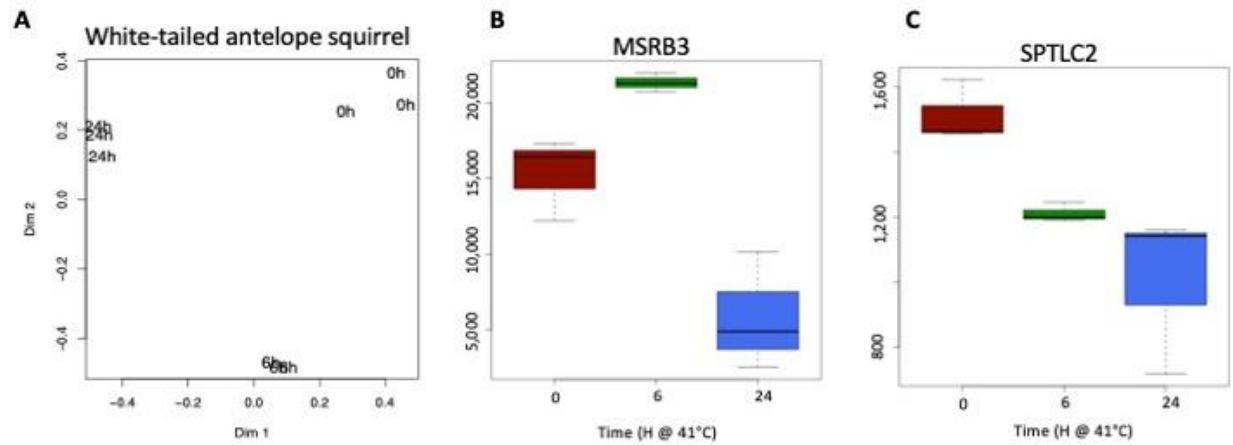


**Figure 28.** Random forests and box plots depicting relevant and important selected variables from the comparison between all three time points in the white-tailed antelope squirrel. (A) Random forest plot depicting MSR3 and SPTLC2 in the white-tailed antelope squirrel. Box plots depicting the change in expression in (B) MSR3 and (C) SPTLC2. X-axis: Time (H) at 41°C. Y-axis: Quantification number.

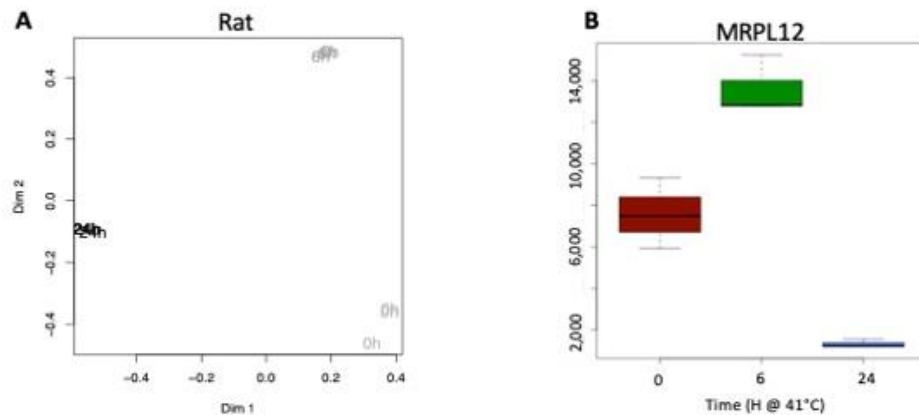


**Figure 29.** Random forests and box plots depicting relevant and important selected variables from the comparison between all three time points in the rat. (A) Random forest plot depicting MRPL12 in the rat. (B) Box plot depicting the change in expression in MRPL12. X-axis: Time (H) at 41°C. Y-axis: Quantification number.

Random Forests was also implemented to compare the three rodent species at each of the 6 h and 24 h time points. After the 75% cutoff, 2 proteins were retained as biomarkers separating the 3 species at 6-h post heat exposure, and 4 proteins were retained as biomarkers for the 24h timepoint (**Table 27**). The two selected proteins with a high at the 6 hour time point between all three species was PPM1A and TRAPPC11 (**Figure 30**).

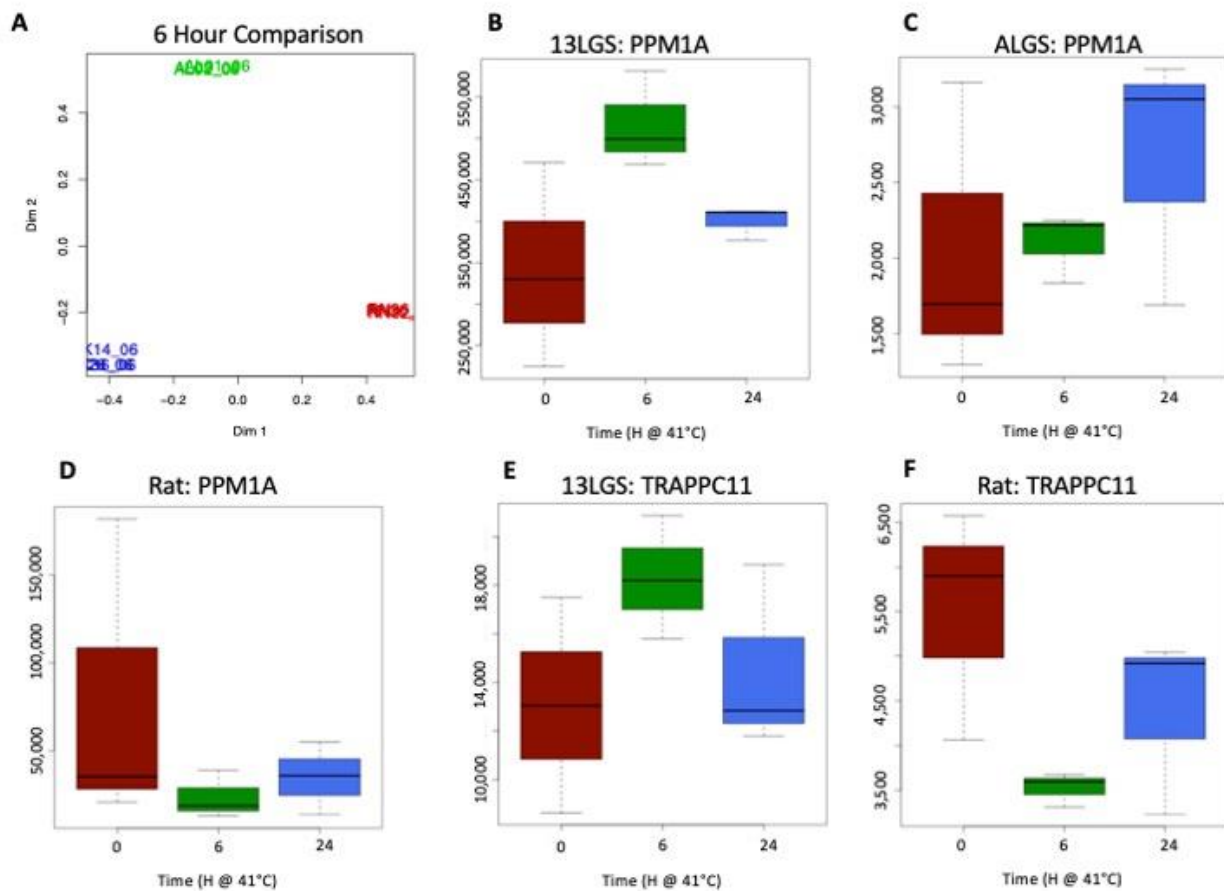


**Figure 30.** Random forest and boxplots depicting relevant and important selected variables from the comparison between the three species at 6 hours. 6-hour time point comparison between all three species: (A) random forest depicting selected variable 'PPM1A' and the (B) box plot depicting 'PPM1A' quantification numbers in 13-lined ground squirrel, (C) white-tailed antelope squirrel, (D) and rat. (E) Box plot depicting 'TRAPPC11' quantification numbers in 13-lined ground squirrel and (F) rat. There is no available box plot for ALGS. X-axis: Time (H) at 41°C. Y-axis: Quantification number. 13LGS = 13-lined ground squirrel, ALGS = White-tailed antelope squirrel.

PPM1A expression increased at 6 hours in both the 13-lined ground squirrel ( $P = 0.5$ ) (**Figure 30B**) and antelope ground squirrel ( $P = 0.3$ ) (**Figure 30C**), whereas PPM1A expression decreased in rat ( $P = 0.5$ ) (**Figure 30D**) at 6 hours at 41°C. The 13-lined ground squirrel exhibited a greater magnitude of PPM1A expression overall throughout each time point, followed by the rat and then the white-tailed antelope squirrel. TRAPPC11 expression showed an increase at 6 hours in the 13-lined ground squirrel ( $P = 0.68$ ) (**Figure 30E**), while there was a decrease in expression in rat ( $P = 0.28$ ) (**Figure 30F**). LTA4H, PAICS, ANXA6, and COASY were the most frequently occurring selected variables when comparing the 24 hour time point between the three species (**Figures 31 and 32**). LTA4H ( $P = 0.09$ ) (**Figure 31B**) and PAICS ( $P = 0.2$ ) (**Figure 31E**) increased expression in 13-lined ground squirrel and decreased expression in white-tailed antelope squirrel (LTA4H:  $P = 0.9$ , PAICS:  $P = 0.03$ ) (**Figure 31C and Figure 31F**) and rat (LTA4H:  $P = 0.2$ , PAICS  $P = 0.05$ ) (**Figure 31D and 31G**) at 24 hours. Overall, there was a greater magnitude of LTA4H expression in 13-lined ground squirrel at each time point, followed by rat and then the white-tailed antelope squirrel. The 13-lined ground squirrel also showed a greater magnitude of PAICS overall throughout each time point, followed by the white-tailed antelope squirrel and then the rat. Similarly, ANXA6 ( $P = 0.02$ ) (**Figure 32A**) and COASY ( $P = 0.68$ ) (**Figure 32D**) increased in expression in 13-lined ground squirrel and decreased in expression in white-tailed antelope squirrel (ANXA6:  $P = 0.77$ ; COASY:  $P = 0.04$ ) (**Figure 32B and Figure 32E**) and rat (ANXA6:  $P = 0.01$ ; COASY:  $P = 0.08$ ) (**Figure 32C and Figure 32F**). Overall, there was a greater magnitude of ANXA6 expression in rat at each time point, followed by the white-tailed antelope squirrel and then the 13-lined ground squirrel. In terms of COASY, there was a greater magnitude of



expression in the 13-lined ground squirrel at each time point, followed by the rat and then the white-tailed antelope squirrel.

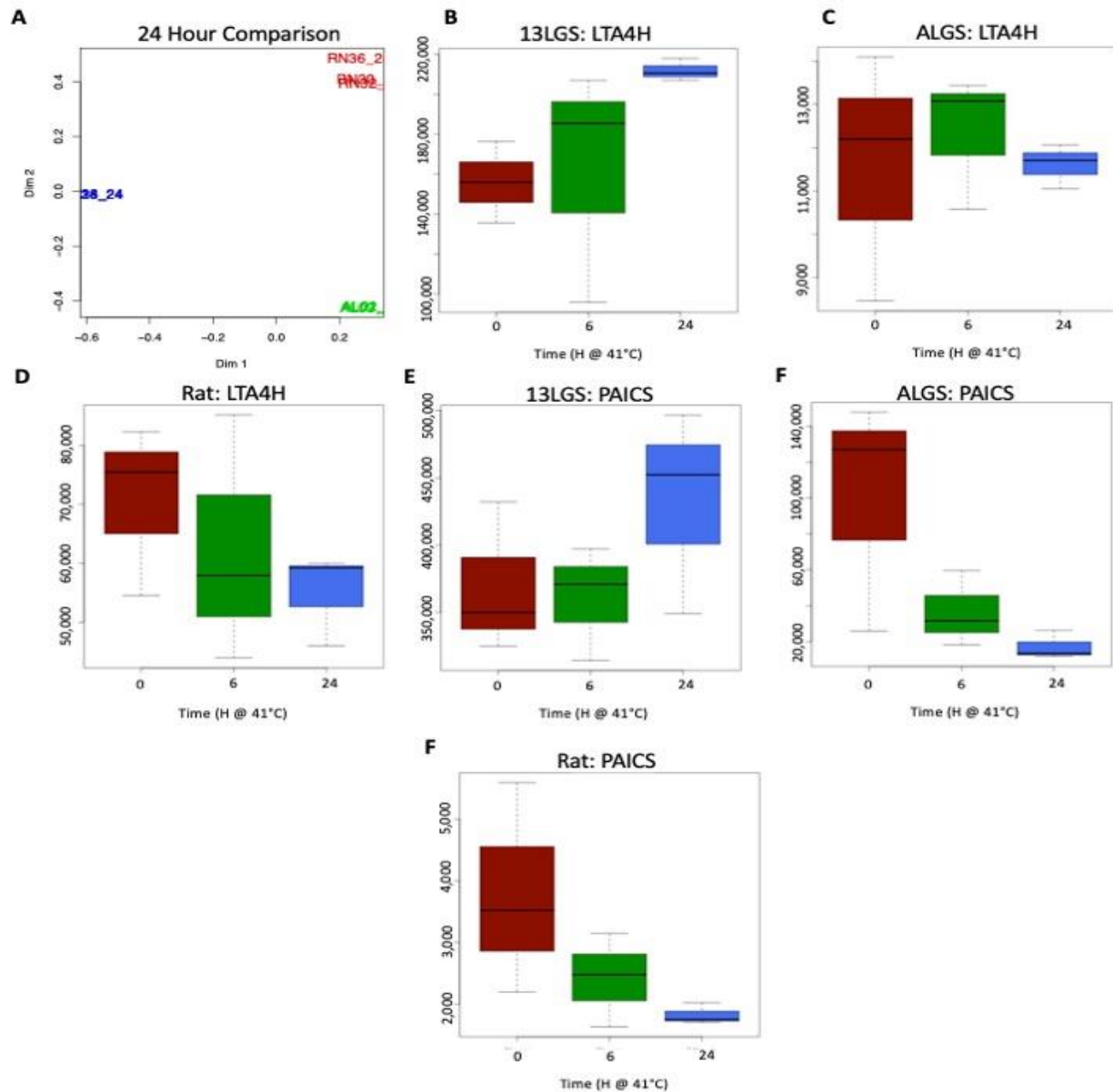


**Figure 31.** Random forests and box plots depicting relevant and important selected variables ('LTA4H' and 'PAICS') from the comparison between the three species at 24 hours. (A) Random forest depicting selected variables 'LTA4H' and 'PAICS' the (B) box plot depicting 'LTA4H' quantification numbers in 13-lined ground squirrel, (C) white-tailed antelope squirrel, (D) and rat. (E) Box plot depicting 'PAICS' quantification numbers in 13-lined ground squirrel, (G) white-tailed antelope squirrel, (H) and rat. X-axis: Time (H) at 41°C. Y-axis: Quantification number.

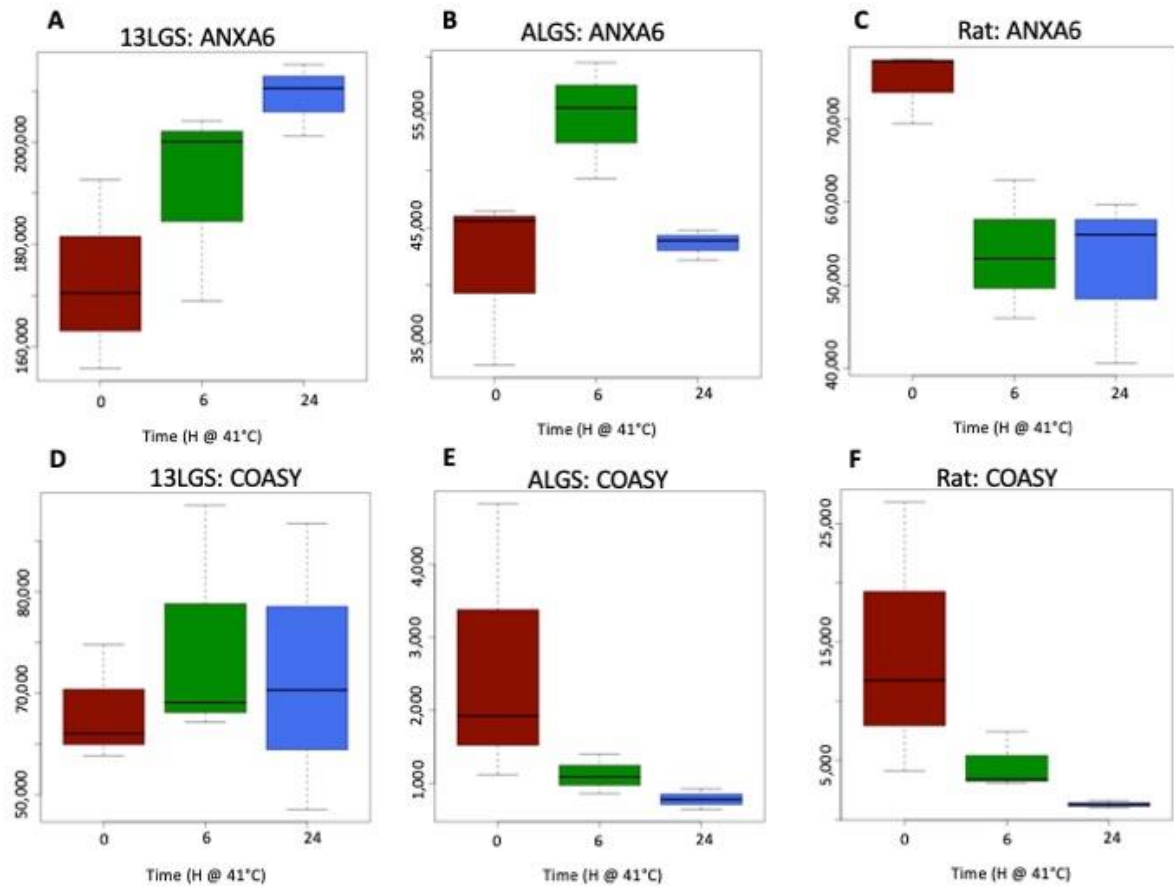


**Figure 32.** Box plots depicting relevant and important selected variables ('ANXA6' and 'COASY') from the comparison between the three species at 24 hours. (A) Box plot depicting 'ANXA6' quantification numbers in 13-lined ground squirrel, (B) white-tailed antelope squirrel, (C) and rat. (D) Box plot depicting 'COASY' quantification numbers in 13-lined ground squirrel, (E) white-tailed antelope squirrel, (F) and rat. X-axis: Time (H) at 41°C. Y-axis: Quantification number.

### *DIANA clustering*

DIANA clustering generated 2 clusters of proteins in each of 13-lined ground squirrels (**Figure 33**), white-tailed antelope squirrel (**Figure 34**), and rat (**Figure 35**). For each species, these clusters represent proteins that are either increasing or decreasing over the two time points of the heat exposure. There is not a pattern of protein abundance changes highlighting a peak in the 6 hours time point for any species. Although there

seems to be a general increase in 13-lined ground squirrel cluster 1 (**Figure 33A**), white-tailed antelope squirrel cluster 2 (**Figure 34B**), and rat cluster 2 (**Figure 35B**), and a general decrease in 13-lined ground squirrel cluster 2 (**Figure 33B**), white-tailed antelope squirrel cluster 1 (**Figure 34A**), and rat cluster 1 (**Figure 35A**), there are no patterns in clustering defining phenotypes. 13-lined ground squirrel had 107 proteins in cluster 1, and an even a greater amount in cluster 2 (381 proteins). Cluster 1 for both the white-tailed antelope and rat had a greater number of proteins, 96 and 187 proteins, respectively, compared to the second cluster which contained 25 and 6, respectively.

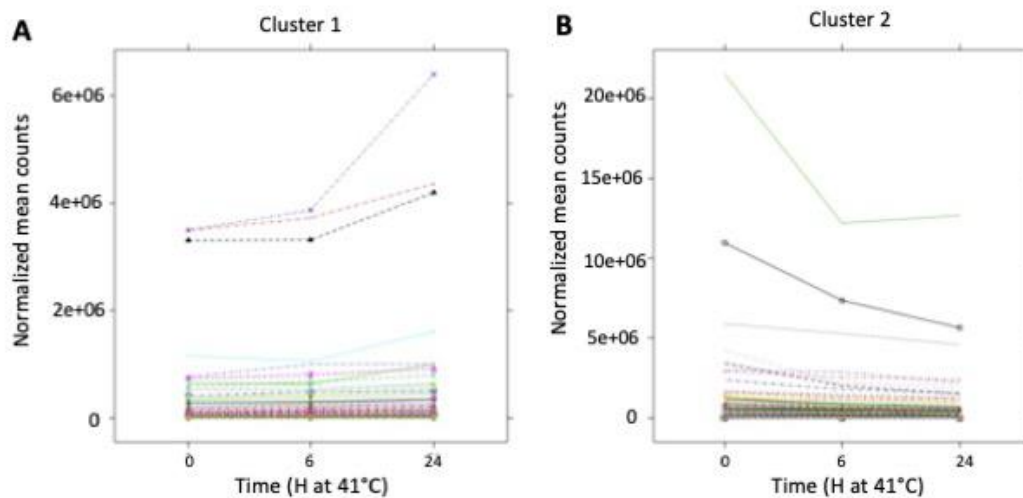


**Figure 33.** DIANA clustering produced 2 gene clusters from 13-lined ground squirrels. (A) Cluster 1 and (B) cluster 2. X-axis: time (H) at 41°C. Y-axis: Normalized quantification mean counts.

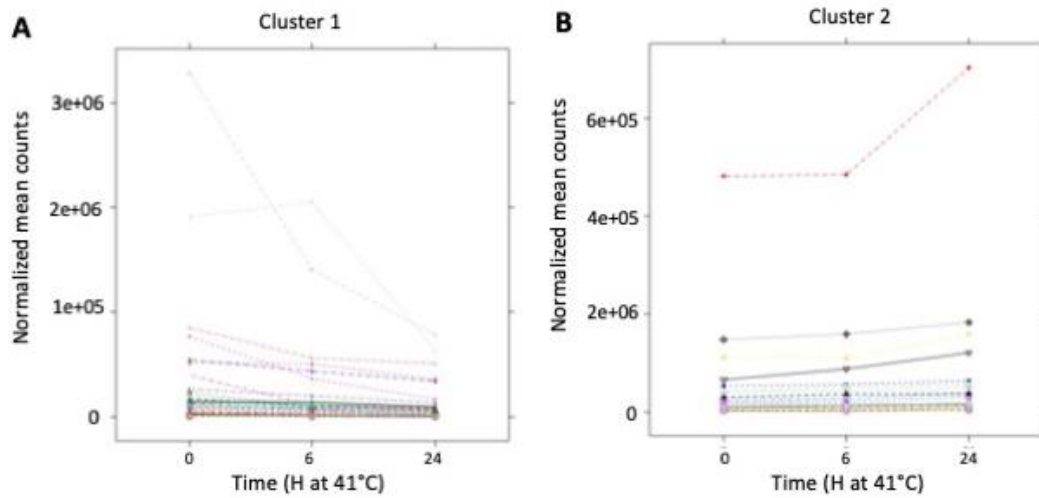


**Figure 34.** DIANA clustering produced 2 gene clusters from white-tailed antelope squirrels. (A) Cluster 1 and (B) cluster 2. X-axis: time (H) at 41°C. Y-axis: Normalized quantification mean counts.

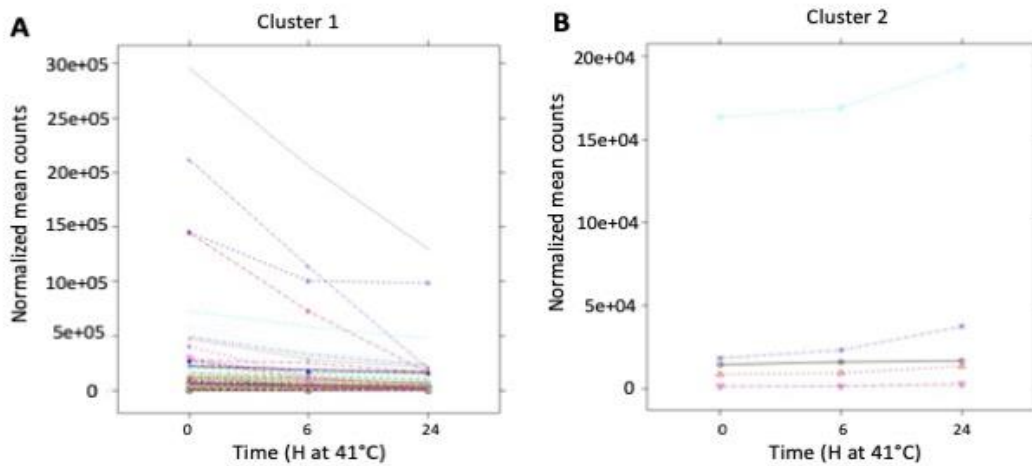


**Figure 35.** DIANA clustering produced 2 gene clusters from rat. (A) Cluster 1 and (B) cluster 2. X-axis: time (H) at 41°C. Y-axis: Normalized quantification mean counts.

## Discussion

In this study on dermal fibroblasts of white-tailed antelope squirrel, round-tailed ground squirrel, dromedary camel, 13-lined ground squirrel, southern white rhino, human, and

rat, qPCR and proteomics were used to describe gene expression and overall protein content arising from heat stress of 41°C. Gene expression and proteomic data analysis were used as a way to understand underlying mechanisms at the cellular level of stressor resilience in mammals that are tolerant to heat stress of 41°C, especially those that occurred over a shorter time course (minutes to hours).

#### *HSF1, ERN1, PRKAA2, and CDKN1A expression*

During mild heat stress, mammalian cells activate response mechanisms associated with the induction and activation of stress-response genes. These cellular responses may initially be associated with cell protection, however severe or long duration heat stress may lead to cells experiencing negative outcomes. Gene expression induction between baseline and the 30min time point were first investigated to identify whether rapid changes in gene expression might occur and might differ between species. No immediate induction was identified in HSF1, PRKAA2, and CDKN1A throughout all investigated species. However, immediate induction of ERN1 was identified for the dromedary camel. Of the four investigated genes, only CDKN1A exhibited differences in gene expression mean between the white-tailed antelope squirrels and human at 0.5 hours at 41°C. Furthermore, there were insignificant differences in gene expression between two phenotypes at 0.5 hours for HSF1, ERN1, PRKAA2, and CDKN1A.

Of all investigated species, only the rat exhibited significant differences in HSF1 gene expression patterns across the shorter time scale of 24 hours at 41°C. Significant differences in ERN1 gene expression patterns across the 24 hour time course did exist

in the southern white rhino. The round-tailed ground squirrel, southern white rhino, and rat also exhibited significant PRKAA2 expression patterns. Whereas, only the southern white rhino exhibited significant CDKN1A expression patterns during heat exposure. Ultimately, there were no significant differences in gene expression between the two presumed phenotypes for all four investigated genes. This project identified immediate induction of ERN1 in the dromedary camel,. Furthermore, this project showed patterns in HSF1 expression in rat, ERN1 expression in the southern white rhino, PRKAA2 expression in the round-tailed ground squirrel, southern white rhino and rat, and CDKN1A expression in the southern white rhino due to heat stress at 41°C.

Overall, the qPCR data showed inconsistent changes across the time course and among species, with no clear differences between the two phenotypes. The majority of gene induction beyond baseline values were small (<2-fold) with the exception of human fibroblasts, suggesting that biological variation was the most important factor in induction of gene expression in this experiment.

#### *Heat shock proteins*

Although gene expression assays were highly variable and showed generally low-amplitude changes, proteomic data revealed several hundred proteins that differed with heat exposure in the three rodent species. Proteomics analysis identified 7 differentially expressed HSPs. Significant induction of HSP90AB1 in the thirteen-lined ground squirrel and white-tailed antelope squirrel may suggest mechanisms of homeostatic resilience in desert-dwelling rodents. HSP90AB1 is known to respond to heat stress and act as a

molecular chaperone by binding to proteins that may be unfolded or denatured (Haase & Fitze, 2016; Prastowo et al., 2021). Significant induction of HSP90B1, HSPA1L, HSPA5, and HSPA8 may reflect a species-specific response in 13-lined ground squirrel, while significant induction of HSPA1A and HSPD1 may reflect a species-specific response in the white-tailed antelope squirrel HSP90B1. Previous proteomic studies have also identified higher abundance of HSP90B1, HSPA5, HSPA8, HSPA1A in response to heat stress (Cui et al., 2016). Although HSPA1L has been shown to have no involvement in the HSR in mice (X. Wang et al., 2020), overexpression of HSPA1L has been shown to play a role in maintaining the function of proximal tubular cells, a cell type that is essential for maintaining renal homeostasis in diabetic kidney disease (Nakatsuka et al., 2021). HSPA1L may play a specialized role in relation to renal homeostasis in 13-lined ground squirrel. Unlike other heat-stress induced HSPs, HSPD1 is constitutively expressed and maintains mitochondrial function by facilitating mitochondrial protein folding in the matrix (Stetler et al., 2010).

#### *Cell cycle regulation*

Random forest identified genes FBXO6, MSRB3, PPM1A, LTA4H as having a high importance to the model and are also known to be involved in regulating cell cycle progression. FBXO6 was significantly downregulated in expression at 6- and 24 hours at 41°C in the 13-lined ground squirrel. FBXO6 regulates cell cycle progression by interacting with spindle assembly checkpoint proteins (Xu et al., 2018). Although identified as a gene with high importance in the random forest model, MSRB3 did not exhibit significant changes in expression during heat stress in white-tailed antelope squirrels.

MSRB3 encodes an oxidoreductase protein in the ER and has also been shown to regulate cell cycle progression through the p53-CDKN1A and p27 pathways (Lee et al., 2014). Lee et al., (2014) demonstrated this by showing MSRB3 knockout cells can inhibit cell proliferation through these pathways. Although PPM1A did not exhibit significant differences across the 6 hour time point between the three species. PPM1A is a gene that encodes for a PP2C family member of the serine/threonine protein phosphatases. PP2C's negatively regulate cell stress response pathways and have been shown to dephosphorylate and inactivate AMPK and regulate the cell cycle by binding to and dephosphorylating CDKs (Li et al., 2022). LTA4H did not exhibit significant differences in expression at 24 hours between the three species. LTA4H encodes a hydrolase that normally generates LTB4, a compound involved in inflammation, and has also been shown to regulate cell cycle progression by negatively regulating p27 (Oi et al., 2017).

### *Biosynthetic pathways*

Proteins AASDHPPT, SPTLC2, and PAICS were identified as important proteins in the random forest model and also exhibited significant induction under heat stress. AASDHPPT encodes 4'-phosphopantetheine transferase (PPTase) which performs a post-translational modification of phosphopantetheinylation on carrier proteins, that is essential to living organisms (Jung et al., 2016). PPTases have essential roles in many biosynthetic pathways, a couple of which include biosynthesis of fatty acids and lysine (Beld et al., 2014). SPTLC2 had a significant decrease in expression at the 6- and 24 hour time points in white-tailed antelope squirrel. SPTLC2 encodes one of the two subunits of serine palmitoyltransferase (SPT) which catalyzes the first step in sphingolipid



biosynthesis, which can usually occur in the ER and is suspected to have a role in apoptosis when upregulated (Axelrod & Kaufmann, 2015; Leipelt & Merrill, 2004). A possible relation to SPTLC2 and apoptosis may be an occurrence of apoptotic cells progressing to necrosis and permeabilization of the plasma membrane. SPTLC2 may play a specialized role in regulating plasma membrane permeabilization during an activated apoptotic state (De Schutter et al., 2022). PAICS is significantly induced at 24 hours at 41°C in the white-tailed antelope squirrel and rat. PAICS encodes a bifunctional enzyme that is involved in the de novo purine biosynthesis pathway (He et al., 2022). Besides the fact that purines act as a building block for nucleic acids, purines can also provide energy and cofactors and thus, boost cell survival and proliferation (Yin et al., 2018).

#### *Mitochondrial translation*

Although MRPL12 did not exhibit significant differences across the three time points in the rat, this protein was identified by Random Forests as the single biomarker necessary to identify the proteomes of rat fibroblasts at each experimental timepoint. Protein encoding MRPL12 may play a role in mitochondrial translation by interacting with the mitochondrial RNA polymerase (Serre et al., 2013; Z. Wang et al., 2007). Translation of mt-mRNA helps maintain cellular energy homeostasis by generating proteins that are involved in oxidative phosphorylation (Aibara et al., 2020).

#### *Summary*

This study identified immediate induction of ERN1 in the dromedary camel,. Furthermore, this aim showed patterns in HSF1 expression in rat, ERN1 expression in the southern white rhino, PRKAA2 expression in the round-tailed ground squirrel, southern white rhino and rat, and CDKN1A expression in the southern white rhino due to heat stress at 41°C. Proteomic analysis identified significantly induced and relevant proteins may reflect species-specific responses in the 13-lined ground squirrel, white-tailed antelope squirrel, and rat during heat stress. Specifically, proteomic data showed important distinctions in heat shock protein induction in the ground squirrels compared with the rat. This gene expression and proteomic data may provide better insight into species-specific response mechanisms to heat stress, however the differences in response mechanisms between the two presumed phenotypes require further investigation.

## Chapter 4

### Summary of findings

This research examined the adapted phenotypes across a range of mammals that inhabit deserts to better understand how organisms respond to these extreme temperatures and gained a better understanding of species-specific cellular responses to this stressor and identified potential links that could prevent stresses that lead to negative cellular outcomes. During the multi-day heat exposure, there were differences in cell proliferation between presumed heat tolerant (white-tailed antelope squirrel, round-tailed ground squirrel, dromedary camel, and 13-lined ground squirrel) and presumed heat sensitive (southern white rhino, human, and rat) phenotypes. There was immediate induction in genes ERN1 in the dromedary camel. Gene expression patterns over 24h at 41°C were identified for HSF1 in rat, ERN1 in the southern white rhino, PRKAA2 in the round-tailed ground squirrel, southern white rhino, and rat, and CDKN1A in the southern white rhino. Proteins that were significantly induced in a proteomic study of three rodents are involved in the heat stress response, renal homeostasis, cell cycle progression, post-translational modifications, apoptosis, and biosynthetic pathways. Identifying cellular mechanisms provides a better understanding of species-specific responses to heat stress using a model of dermal fibroblasts at 41°C. These data also point to potential links between heat stress responses and negative cellular outcomes including decreased cell proliferation and cell death.

## Limitations

It is difficult to compare the results of this study's approach to previous studies that have investigated the effects of heat shock because the effects of this stressor can vary depending on the cell line that is analyzed, the temperature and duration of heat exposure, time of harvest, and the state of acquired thermotolerance. Several studies have investigated the effects of heat shock and have implemented a recovery time (37°C) after mild heat exposure in their experimental design, which is a component that was not implemented in this study. Applying this recovery phase may mock temperature intervals of the mammal's habitats, providing additional insights into recovery following heat stress. Therefore, this study may reflect the mammalian dermal fibroblast response to heat stress in the absence of acquired thermotolerance, a state that likely occurs in real-life settings.

The cell type that was available to run these experiments was primary dermal fibroblasts. Susceptibility to heat stress is known to be cell dependent (Kühl & Rensing, 2000). Despite the multi-day heat exposure, it is possible that 41°C is non-lethal to primary dermal fibroblasts and has a higher threshold to heat stress. Although I expected differences to emerge between species at this temperature and over an 8 day time course, it is possible that stronger differences between species may be observed if the temperature challenge were greater in amplitude (>41°C) or duration. Furthermore, this study represents an in vitro approach that studies this cell type at a 2-dimensional level and does not investigate these responses with an in vivo approach and 3-dimensional point of view. There are increasing studies with 3D cell culture models and organoids, that may capture a more nuanced multi-cellular view of responses to environmental challenge (Berning et al., 2015). It is possible that cellular responses including ER stress

and UPR differ among cell types and can act differently depending on the cell type and ER stress inducer (Osowski & Urano, 2011). Even within a population of 2D fibroblasts, it is possible that variation observed, particularly in the qPCR data, could result from differences between the responses of single cells within culture. An alternative approach such as single cell RNAseq could yield additional insights, and could reveal more detail about differences between species responses to heat stress.

#### Future directions

Previous studies have identified increased gene expression of HSF1, PRKAA2, and CDKN1A in response to heat stress, albeit at different durations and temperatures of heat exposure (Fuse et al., 1996; Nitta et al., 1997; Ohnishi et al., 1996; Sajjanar et al., 2023; Singh et al., 2020; Tabuchi et al., 2008; J. Tang et al., 2018); whereas, ERN1 has been observed to downregulate expression in response to heat stress (Homma & Fujii, 2016). This study differs from these previous studies based on the cell type that was used, heat temperature, heat exposure duration, time of RNA harvest, and/or recovery phase following heat exposure. The differences in mechanisms at the cellular level between the two phenotypes in an experimental design that includes similar time points from this study along with a recovery period of 37°C should be further investigated. This may provide clarification on whether the developed acquired thermotolerance causes significant differences in cell proliferation, cell viability, gene expression, and protein abundance.

In an effort to maintain cellular energy homeostasis, activated AMPK is involved in enhancing mitochondrial biogenesis by phosphorylating components of different

pathways that contribute to nucleosome remodeling and reduction of methylated promoters, thus allowing for promoter activation of PGC-1 $\alpha$  genes, transcription factor A (Tfam), and uncoupling proteins 2 and 3 (UCP2 and UCP3). PGC-1 $\alpha$ , Tfam, and UCP2 and UCP3 are genes that promote mitochondrial biogenesis (Marin et al., 2017). Further investigation of these genes and their responses to heat stress in dermal fibroblasts of the presumed heat tolerant and heat sensitive to better understand the different responses in maintaining cellular homeostasis by an AMPK-mediated pathway.

The three subunits that encode AMPK contain two or more isoforms. Isoforms are a result of alternative splicing. There may be 12 different combinations that form the AMPK (Hardie, 2011). The combinations of the isoforms that form AMPK in response to heat stress remain to be characterized. It may be of interest to investigate how RNA splicing regulates these HSF1, ERN1, and PRKAA2 post-transcriptionally, between the two phenotypes during heat stress.

Morphological changes have been observed in mammalian cells in response to heat stress. The collapse and aggregation of intermediate filaments near the nucleus and denaturation and aggregation of F-actin have been observed (Levitsky et al., 2008; Welch & Suhan, 1985). Future studies should investigate the morphological changes and/or genes essential to maintaining the cellular structure during heat stress between the mammals presumed to be heat tolerant versus heat sensitive.

## Significance

Increasing temperatures across habitats is a hallmark of global climate change and may cause living organisms to be challenged with responding to extreme environmental conditions in an effort to prevent negative cellular outcomes. Further establishment of the cellular responses to a high temperature of 41°C of these mammalian species can provide better insight into understanding the cellular mechanisms of stressor resilience and sensitivity of primary dermal fibroblasts of mammals sensitive to heat stress. This may highlight the advantages of how mammals adapt to these extreme environmental conditions. Furthermore, this may highlight advantages that may be used toward aiding humans with health conditions with high grade-fever symptoms.

## Appendix

Table 1. Passage number of primary dermal fibroblasts used for LDH and crystal violet assays, and qPCR.

Species	Biological replicate	Passage # plated for crystal violet and LDH assays	Time point(s) plated (Days)	Passage # plated for qPCR	Time point(s) plated (H)
<i>Ictidomys tridecemlineatus</i>	OK14	23	2-8	14 8	0-12 24
<i>Ictidomys tridecemlineatus</i>	OK22	13	2-8	10	0-24
<i>Ictidomys tridecemlineatus</i>	OK28	20 22	2-4 5-8	16	0-24
<i>Ictidomys tridecemlineatus</i>	OK29	10 12	4-8 2 & 3	7	0-24
<i>Ictidomys tridecemlineatus</i>	OK36	11 12	4-8 2, 3	7 8	0 0.5-24
<i>Ceratotherium simum</i>	CSO1	19 20	2 & 3 4-8	14	0-24
<i>Ceratotherium simum</i>	CSO2	18 19 20	3 4, 5, 6, 8 2 & 7	14	0-24
<i>Ceratotherium simum</i>	CSO3	12 13	4, 5, 6, 7 2, 3, 8	13	0-24
<i>Ceratotherium simum</i>	CSO4	14 16	2 & 3 4-8	11	0-24
<i>Ceratotherium simum</i>	CSO5	12 14	2, 3, 4, 5, 6 7 & 8	12	0-24



<i>Camelus dromedarius</i>	CDO1	12	2-8	12 13	12 0-6 & 24
<i>Camelus dromedarius</i>	CDO2	21	2-8	17 20 21	0 & 4 0.5, 2 & 6 12 & 2
<i>Camelus dromedarius</i>	CDO3	13	2-8	22 16	0-6, 24 12h
<i>Camelus dromedarius</i>	CDO4	13	2-8	17	0-24
<i>Camelus dromedarius</i>	CDO5	15	2-8	14	0-24
<i>Rattus norvegicus</i>	RN2	16	2-8	9 17	0.5 & 24 0, 2-12
<i>Rattus norvegicus</i>	RN30	17	2-8	13	0-24
<i>Rattus norvegicus</i>	RN32	13	2-8	7 9	0 0.5-24
<i>Rattus norvegicus</i>	RN36	12	2-8	8	0-24
<i>Xerospermophilus tereticaudus</i>	XT1	12 14	2, 3 4-8	6	0-24
<i>Xerospermophilus tereticaudus</i>	XT2	10 11 12 13	8 4, 5 6, 7 2, 3	5 7 13	0-6 12 24
<i>Xerospermophilus tereticaudus</i>	XT3	7	1-8	5	0-24
<i>Ammospermophilus leucurus</i>	AL1	13	1, 2, 4	3	0, 6, 24
<i>Ammospermophilus leucurus</i>	AL2	13	1, 2, 4	3	0-24
<i>Ammospermophilus leucurus</i>	AL3	5 7	4 & 5 1 & 2	4	0-24
<i>Ammospermophilus leucurus</i>	AL4	-	-	3	0, 6, 24

<i>Homo sapiens</i>	HS4057	17	1-8	14	0-24
<i>Homo sapiens</i>	HS3099	15	1-8	17	0-24
<i>Homo sapiens</i>	HS2096	7 10	2-5 6-8	6	0-24
<i>Homo sapiens</i>	HS3869	8	1-8	12	0-24
<i>Homo sapiens</i>	HS967	16	1-8	20	0-24

Table 2. Optimal cell number plated for viability and proliferation assays.

Species	Time point (Days)	Cell # Plated
<i>Ictidomys tridecemlineatus</i>	2 3 4 5 6 7 8	$8 \times 10^4$ $6 \times 10^4$ $4.5 \times 10^4$ $6 \times 10^4$ $2 \times 10^4$ $3 \times 10^4$ $3 \times 10^4$
<i>Camelus dromedarius</i>	2 3 4 5 6 7 8	$6 \times 10^4$ $4 \times 10^4$ $1.5 \times 10^4$ $6 \times 10^4$ $2 \times 10^4$ $4 \times 10^4$ $1 \times 10^4$
<i>Homo sapiens</i>	2 3 4 5 6 7 8	$8 \times 10^4$ $8 \times 10^4$ $4.5 \times 10^4$ $3 \times 10^4$ $5 \times 10^3$ $2 \times 10^4$ $5 \times 10^3$
<i>Rattus norvegicus</i>	2 3 4 5 6 7 8	$8 \times 10^4$ $8 \times 10^4$ $6 \times 10^4$ $6 \times 10^4$ $3 \times 10^4$ $3 \times 10^4$ $3 \times 10^4$

<i>Ceratotherium simum</i>	2	8x10 <sup>4</sup>
	3	8x10 <sup>4</sup>
	4	3x10 <sup>4</sup>
	5	3x10 <sup>4</sup>
	6	7.5x10 <sup>3</sup>
	7	4x10 <sup>4</sup>
	8	3x10 <sup>4</sup>
<i>Xerospermophilus tereticaudus</i>	2	6x10 <sup>4</sup>
	3	8x10 <sup>4</sup>
	4	3x10 <sup>4</sup>
	5	3x10 <sup>4</sup>
	6	5x10 <sup>3</sup>
	7	4x10 <sup>4</sup>
	8	3x10 <sup>4</sup>
<i>Ammospermophilus leucurus</i>	2	1x10 <sup>4</sup>
	4	4.5x10 <sup>4</sup>

Table 3. Crystal violet absorbance values.

Species	Biological replicate	Time point (Days)	Average Crystal violet absorbance for: Low Control	Average Crystal violet absorbance for: Test Sample	Crystal Violet Ratio (41°C/37°C)
<i>Ictidomys tridecemlineatus</i>	OK14	2	2.0534	1.6791	0.817716957
		3	2.0182	1.7561	0.870131801
		4	1.8675	1.8547	0.993145917
		5	1.95145	2.9966	1.53557611
		6	3.3475	3.502	0.813697652
		7	3.5003	2.19545	0.627217667
		8	3.3566	2.85	0.849073467
<i>Ictidomys tridecemlineatus</i>	OK22	2	1.92675	1.8428	0.95642922
		3	1.4641	1.5988	1.092001912
		4	1.8113	1.89715	1.047396897
		5	1.7924	2.0256	1.130104887
		6	0.9803	1.4288	1.457513006
		7	1.275	1.8155	1.423921569
		8	1.2146	1.5588	1.283385477
<i>Ictidomys tridecemlineatus</i>	OK28	2	1.8578	1.69295	0.911266014
		3	1.5517	1.64715	1.061513179
		4	2.2191	1.9488	0.878193862
		5	1.6179	2.15825	1.333982323
		6	3.3177	4	1.20565452
		7	4	4	1

		8	1.25	2.2709	1.809626265
<i>Ictidomys tridecemlineatus</i>	OK29	2	2.52825	2.6801	1.060061307
		3	2.4694	2.49935	1.012128452
		4	1.22125	1.9737	1.616131013
		5	1.8509	2.4043	1.298989681
		6	1.3748	1.5577	1.133037533
		7	1.2808	1.33375	1.041341349
		8	1.34485	1.1579	0.860988214
<i>Ictidomys tridecemlineatus</i>	OK36	2	2.3748	2.2885	0.963660098
		3	2.013	1.7686	0.87858917
		4	2.9185	3.3469	1.146787733
		5	2.36125	2.3454	0.993287454
		6	1.8317	2.1059	1.149697003
		7	1.4914	1.503	1.007777927
		8	1.77025	1.3852	0.782488349
<i>Camelus dromedarius</i>	CDO1	2	3.27965	2.7735	0.845669507
		3	1.0844	1.5755	1.452877167
		4	1.5707	1.662	1.05812695
		5	2.9459	3.25355	1.10443328
		6	2.24685	2.6505	1.179651512
		7	3.3545	3.22235	0.960605157
		8	4.00	3.5289	0.882225
<i>Camelus dromedarius</i>	CDO2	2	1.62815	1.8179	1.116543316
		3	1.4274	2.3399	1.639274205
		4	3.1722	3.278	1.033352248
		5	3.05	3.29515	1.080377049
		6	2.3532	2.9585	1.257224205
		7	3.43555	3.4107	0.992766806
		8	2.275	3.54375	1.557692308
<i>Camelus dromedarius</i>	CDO3	2	1.7538	1.5174	0.865206979
		3	2.38275	2.7935	1.172384849
		4	1.5321	1.7769	1.159780693
		5	2.28635	3.2371	1.41583747
		6	3.3212	3.173	0.955377574
		7	4	4	1
		8	3.74695	4	1.067534928
<i>Camelus dromedarius</i>	CDO4	2	1.5806	1.6185	1.023978236
		3	1.69345	2.147	1.267826036
		4	1.8661	1.9769	1.059375167
		5	4	4	1
		6	2.3143	3.1935	1.37989889
		7	3.2937	3.1197	0.947171874
		8	3.38495	3.10025	0.915892406
<i>Camelus dromedarius</i>	CDO5	2	2.66265	2.4442	0.917957674
		3	1.50255	1.76515	1.174769558
		4	1.64	1.5495	0.944817073

		5	2.5912	2.6422	1.019682001
		6	2.80095	1.49615	0.534158054
		7	2.83665	2.2697	0.800133961
		8	3.18805	3.16275	0.992064114
<i>Homo sapiens</i>	HS967	2	0.85195	0.90945	1.067492224
		3	0.8514	0.78755	0.925005873
		4	3.1231	3.38235	1.08301047
		5	2.1418	3.13525	1.463838827
		6	0.6623	0.8683	1.311037294
		7	1.532	2.8136	1.836553525
		8	0.721	0.92155	1.27815534
<i>Homo sapiens</i>	HS2096	2	1.88425	1.60	0.847445933
		3	3.12	2.6621	0.85
		4	3.04955	2.3251	0.76244036
		5	2.7006	1.60	0.591146412
		6	1.61	0.7387	0.460220547
		7	1.617	1.4553	0.9
		8	1.27685	0.6141	0.480949211
<i>Homo sapiens</i>	HS3099	2	2.416	2.2567	0.93406457
		3	2.7667	2.6731	0.966169082
		4	1.2701	1.2045	0.948350524
		5	0.68555	0.99795	1.45569251
		6	0.94505	0.72715	0.769430189
		7	1.289	1.1934	0.92583398
		8	2.94685	0.8571	0.290852945
<i>Homo sapiens</i>	HS3869	2	1.73285	1.5746	0.908676458
		3	2.2803	3.6573	1.603867912
		4	3.13	1.87345	0.598546326
		5	1.50575	0.86565	0.574896231
		6	0.72065	1.1008	1.527509887
		7	0.9946	1.5105	1.518700985
		8	1.7225	1.0255	0.595355588
<i>Homo sapiens</i>	HS4057	2	1.8078	1.621	0.896669986
		3	1.5837	1.6832	1.062827556
		4	1.3883	1.28175	0.923251459
		5	0.8377	1.2875	1.536946401
		6	1.0237	0.8929	0.872228192
		7	2.04695	1.1674	0.570311928
		8	1.69315	1.1136	0.657709004
<i>Rattus norvegicus</i>	RN2	2	0.89305	1.20565	1.350036392
		3	1.6593	1.52745	0.920538781
		4	1.3812	1.72695	1.250325804
		5	3.4542	1.4962	0.433153842
		6	1.2243	1.0209	0.833864249
		7	1.1059	1.3241	1.197305362
		8	1.9496	1.05315	0.540187731

<i>Rattus norvegicus</i>	RN30	2	1.5289	2.48275	1.623879914
		3	1.65665	0.8821	0.532460085
		4	2.309	4	1.732351667
		5	3.27435	2.6245	0.801533129
		6	1.8151	1.8362	1.011624704
		7	1.3415	2.15225	1.60436079
		8	1.7389	2.2976	1.321295072
<i>Rattus norvegicus</i>	RN32	2	1.4699	1.79625	1.222021906
		3	2.18655	1.55	0.708879285
		4	1.5732	1.33075	0.845887363
		5	1.3104	1.0827	0.826236264
		6	1.43015	1.3484	0.942838164
		7	2.7935	1.2392	0.443601217
		8	1.5858	1.25545	0.791682432
<i>Rattus norvegicus</i>	RN36	2	1.9792	2.3673	1.196089329
		3	2.2861	2.55995	1.119789161
		4	2.2124	1.9313	0.87294341
		5	2.0879	2.12565	1.018080368
		6	1.67945	1.103	0.656762631
		7	1.33225	1.54835	1.162206793
		8	2.072	2.3065	1.113175676
<i>Ceratotherium simum</i>	CSO1	2	1.9506	2.14695	1.100661335
		3	3.26315	2.6621	0.815806812
		4	2.3881	3.2007	1.340270508
		5	3.4189	2.9613	0.866155781
		6	2.88525	1.9589	0.678935967
		7	3.5314	3.1083	0.88018916
		8	3.5360	2.8097	0.794587181
<i>Ceratotherium simum</i>	CSO2	2	3.181	2.8419	0.893398302
		3	3.1913	2.6293	0.823896218
		4	2.26885	2.017	0.888996628
		5	2.0851	1.7768	0.852141384
		6	3.47715	2.3678	0.680959982
		7	2.9222	2.15525	0.737543632
		8	3.2994	2.2366	0.677880827
<i>Ceratotherium simum</i>	CSO3	2	1.9837	1.7147	0.864394818
		3	2.8358	2.2819	0.804675929
		4	2.4623	1.90495	0.773646591
		5	2.55175	2.2769	0.892289605
		6	3.0435	2.95135	0.969722359
		7	4	3.2074	0.80185
		8	3.491	2.14575	0.614651962
<i>Ceratotherium simum</i>	CSO4	2	4	2.6198	0.65495
		3	2.2825	2.47965	1.086374589
		4	0.6895	1.2219	1.772153735
		5	1.3229	1.8177	1.374026759

		6	1.31625	0.91265	0.69337132
		7	2.10225	1.5168	0.721512665
		8	2.1821	1.5227	0.697814032
<i>Ceratotherium simum</i>	CSO5	2	4	4	1
		3	4	1.53385	0.3834625
		4	0.7227	2.49465	3.45184724
		5	3.523	2.49215	0.707394266
		6	1.0087	2.1336	2.115197779
		7	2.5135	1.9933	0.793037597
		8	2.6925	1.7215	0.639368617
<i>Xerospermophilus tereticaudus</i>	XT1	2	2.0536	1.76	0.85600896
		3	2.7771	2.0588	0.741348889
		4	0.7852	1.3419	1.70899134
		5	1.1943	1.19375	0.999539479
		6	0.8087	1.2027	1.487201682
		7	2.0793	2.2275	1.071273986
		8	1.7927	1.9676	1.097562336
<i>Xerospermophilus tereticaudus</i>	XT2	2	1.75135	2.36815	1.352185457
		3	2.5251	1.9256	0.76258366
		4	1.39525	1.5391	1.103099803
		5	1.5529	1.6192	1.042694314
		6	0.99835	0.81795	0.819301848
		7			
		8	1.61235	1.5269	0.947002822
<i>Xerospermophilus tereticaudus</i>	XT3	2	1.7688	1.7499	0.98931479
		3	2.2385	2.1847	0.975966049
		4	1.1968	1.5724	1.313836898
		5	1.5748	1.74685	1.109251969
		6	0.94805	1.118	1.179262697
		7	1.76225	2.0601	1.169016882
		8	1.87255	1.68795	0.901417853
<i>Ammospermophilus leucurus</i>	AL1	2	0.9597	1.04955	1.093623007
		4	1.1156	1.28065	1.147947293
<i>Ammospermophilus leucurus</i>	AL2	2	1.0166	1.0191	1.002459178
		4	1.3541	1.3306	0.982645299
<i>Ammospermophilus leucurus</i>	AL3	2	0.93335	0.8551	0.916162211
		4	1.6884	1.8121	1.073264629

Table 4. Normalized viability data.

Species	Biological replicate	Time point (Days)	Normalized Low Control	Normalized High Control	Normalized Test Sample	Cytotoxicity (%)
---------	----------------------	-------------------	------------------------	-------------------------	------------------------	------------------

			LDH Value	LDH Value	LDH Value	
<i>Ictidomys tridecemlineatus</i>	OK14	2	0.4641	1.3832	0.5671	11.22
		3	0.3545	1.3254	0.3159	0
		4	0.3631	1.5217	0.2648	0
		5	0.4009	1.5067	0.2184	0
		6	0.1687	0.6228	0.3288	0
		7	0.2519	0.8004	0.3109	10.76
		8	0.2228	0.6564	0.2592	8.41
<i>Ictidomys tridecemlineatus</i>	OK22	2	0.4793	1.4746	0.4811	0.17
		3	0.5733	1.9643	0.5366	0
		4	0.4395	1.6289	0.4533	1.16
		5	0.3803	1.6409	0.3436	0
		6	0.7542	2.8393	0.5046	0
		7	0.5989	2.2620	0.4481	0
		8	0.6398	1.8147	0.4482	0
<i>Ictidomys tridecemlineatus</i>	OK28	2	0.5502	1.5293	0.5880	3.86
		3	0.6078	1.4989	0.5628	0
		4	0.4109	1.2808	0.5257	13.19
		5	0.5389	1.8173	0.4430	0
		6	0.2205	0.8390	0.1710	0
		7	0.185225	0.70065	0.171912	0
		8	0.6063	1.7561	5 0.3117	0
<i>Ictidomys tridecemlineatus</i>	OK29	2	0.2716	1.2100	0.2725	0.09
		3	0.2944	1.2257	0.2810	0
		4	0.6736	2.4158	0.3980	0
		5	0.4444	1.5940	0.3267	0
		6	0.6010	1.7072	0.4417	0
		7	0.6266	2.2516	0.5663	0
		8	0.5169	2.1342	0.5435	0
<i>Ictidomys tridecemlineatus</i>	OK36	2	0.3916	1.1961	0.4257	4.23
		3	0.3958	1.4283	0.4558	5.81
		4	0.2832	1.0107	0.2584	0
		5	0.3433	1.2452	0.3629	2.17
		6	0.3995	1.5191	0.3555	0
		7	0.5146	1.9333	0.4847	0
		8	0.4299	1.2446	0.5453	14.17
<i>Camelus dromedarius</i>	CDO1	2	0.3653	1.0462	0.4060	5.97
		3	0.8391	2.0195	0.5323	0
		4	0.6039	1.8827	0.5630	0
		5	0.3072	0.9569	0.2694	0
		6	0.3930	1.5163	0.3543	0
		7	0.3020	0.9234	0.3627	9.78



		8	0.2109	0.4954	0.3031	32.4
<i>Camelus dromedarius</i>	CDO2	2	0.1361	1.7838	0.1182	0
		3	0.7015	2.1911	0.3210	0
		4	0.2418	0.6806	0.1448	0
		5	0.2850	1.1018	0.2141	0
		6	0.3452	1.4474	0.1672	0
		7	0.2101	0.9843	0.2488	5.01
		8	0.5964	1.4226	0.1650	0
<i>Camelus dromedarius</i>	CDO3	2	0.5165	1.7727	0.6515	10.75
		3	0.3261	1.3458	0.3068	0
		4	0.5073	1.4243	0.4481	0
		5	0.4067	1.1456	0.2465	0
		6	0.2678	1.0315	0.3222	7.13
		7	0.2527	0.5522	0.2131	0
		8	0.2831	0.7106	0.2837	0.15
<i>Camelus dromedarius</i>	CDO4	2	0.6778	1.9551	0.6462	0
		3	0.4682	1.8822	0.4205	0
		4	0.5097	1.6875	0.4638	0
		5	0.2249	0.7838	0.2476	4.06
		6	0.4308	1.3572	0.3155	0
		7	0.3044	1.0271	0.3854	11.21
		8	0.2660	0.8574	0.4028	23.13
<i>Camelus dromedarius</i>	CDO5	2	0.3077	1.1570	0.3808	8.61
		3	0.5279	1.4196	0.4574	0
		4	0.4503	1.7309	0.5153	5.08
		5	0.2996	0.9171	0.4021	16.61
		6	0.3242	1.2163	0.6901	41.01
		7	0.3911	1.0557	0.5383	22.15
		8	0.2335	0.6216	0.2035	0
<i>Homo sapiens</i>	HS967	2	0.8913	3.2348	0.9318	1.73
		3	0.9041	2.8548	1.0976	9.92
		4	0.2290	0.9462	0.4276	27.69
		5	0.3841	1.3791	0.3573	0
		6	1.1067	4.1495	1.0129	0
		7	0.5488	1.7837	0.4202	0
		8	0.9614	2.7151	1.0352	4.21
<i>Homo sapiens</i>	HS2096	2	0.1265	1.2229	0.3754	22.7
		3	0.2088	0.6258	0.3217	27.07
		4	0.2223	1.0600	0.2302	19.64
		5	0.3041	1.0937	0.5581	32.16
		6	0.5101	2.1796	1.2864	46.5
		7	0.5712	1.9681	0.7935	15.92
		8	0.7211	2.4829	2.1190	79.34
<i>Homo sapiens</i>	HS3099	2	0.3561	1.2029	0.6499	34.7
		3	0.3391	1.0731	0.5048	22.58

		4	0.5281	2.3269	0.6770	8.27
		5	0.9328	3.7646	0.8098	0
		6	0.6638	2.1423	0.9219	17.45
		7	0.4453	2.2248	0.5493	5.85
		8	0.2317	0.6643	0.7095	100
<i>Homo sapiens</i>	HS3869	2	0.5393	1.6446	0.9738	39.31
		3	0.4546	1.2452	0.3599	0
		4	0.2851	0.8999	0.5493	42.98
		5	0.5747	1.8888	0.9493	28.51
		6	1.0547	3.8135	0.8712	0
		7	0.7721	2.7474	0.5182	0
		8	0.3479	1.5702	0.8689	42.63
<i>Homo sapiens</i>	HS4057	2	0.3965	1.3980	0.6633	26.63
		3	0.5093	1.5348	0.6027	9.11
		4	0.4848	1.7423	0.6253	11.17
		5	0.7347	2.1084	0.5929	0
		6	0.6458	2.0071	0.7584	8.27
		7	0.3193	1.0883	0.6145	39.39
		8	0.3771	1.1562	0.6250	31.82
<i>Rattus norvegicus</i>	RN2	2	1.0924	3.4356	0.7253	0
		3	0.4147	1.7519	0.4574	3.19
		4	0.5348	1.5204	0.3049	0
		5	0.1659	0.8151	0.2914	19.34
		6	0.6927	2.3609	1.5737	52.81
		7	0.6244	2.6215	0.5246	0
		8	0.4163	1.4825	0.5845	15.78
<i>Rattus norvegicus</i>	RN30	2	0.4996	1.5531	0.3448	0
		3	0.3873	2.3846	1.1404	37.7
		4	0.3300	0.9097	0.1911	0
		5	0.2088	0.6635	0.2494	8.92
		6	0.4631	1.6416	0.4564	0
		7	0.5654	2.1771	0.3918	0
		8	0.4565	1.6622	0.3651	0
<i>Rattus norvegicus</i>	RN32	2	0.6602	2.0873	0.5336	0
		3	0.3905	1.3297	0.4833	9.88
		4	0.4891	1.3338	0.6417	18.06
		5	0.6235	2.1483	0.7290	6.92
		6	0.5626	1.4643	0.6362	8.16
		7	0.2783	1.0015	0.6653	53.51
		8	0.5107	1.3304	0.6183	13.13
<i>Rattus norvegicus</i>	RN36	2	0.3850	1.1999	0.2997	0
		3	0.3547	1.0332	0.2909	0
		4	0.1222	0.3655	0.2991	72.72
		5	0.4076	1.3486	0.3995	0
		6	0.4288	1.2473	0.6088	21.99

		7	0.5506	2.1924	0.4482	0
		8	0.3775	0.1618	0.3357	19.39
<i>Ceratotherium simum</i>	CSO1	2	0.4687	1.8241	0.3274	0
		3	0.2232	0.7315	0.3019	15.48
		4	0.2841	1.1271	0.2046	0
		5	0.2003	0.7341	0.2239	4.43
		6	0.2660	0.8643	0.3493	13.93
		7	0.1928	0.8826	0.2402	6.88
		8	0.2199	0.8814	0.2440	3.64
<i>Ceratotherium simum</i>	CSO2	2	0.2396	0.9157	0.2699	4.47
		3	0.2419	0.7683	0.3303	16.8
		4	0.2821	1.1865	0.3417	6.59
		5	0.3069	1.2039	0.3589	5.8
		6	0.2474	0.7825	0.3054	10.84
		7	0.2572	1.0667	0.3556	12.15
		8	0.2289	0.9447	0.3131	11.75
<i>Ceratotherium simum</i>	CSO3	2	0.3600	1.2036	0.4040	5.22
		3	0.2262	0.5815	0.3343	30.42
		4	0.3147	1.0929	0.3533	4.96
		5	0.3211	0.9836	0.3273	0.94
		6	0.2547	0.8938	0.2947	6.25
		7	0.1931	0.7791	0.2308	6.45
		8	0.2212	0.8929	0.3521	19.48
<i>Ceratotherium simum</i>	CSO4	2	0.1927	0.7283	0.3366	26.88
		3	0.3162	1.0457	0.3352	2.61
		4	0.7566	3.9046	0.4492	0
		5	0.5173	1.8977	0.3496	0
		6	0.5466	2.0673	0.7949	16.33
		7	0.3422	1.4829	0.4783	11.93
		8	0.3481	1.4286	0.4694	11.23
<i>Ceratotherium simum</i>	CSO5	2	0.2030	0.5968	0.2039	0.21
		3	0.2143	0.6128	0.4967	70.87
		4	1.1934	3.7240	0.2588	0
		5	0.2247	0.7123	0.2760	10.51
		6	0.7917	2.6967	0.2789	0
		7	0.2553	1.2399	0.3326	7.85
		8	0.2362	1.1575	0.3332	10.52
<i>Xerospermophilus tereticaudus</i>	XT1	2	0.4143	1.3498	0.4269	1.35
		3	0.3312	1.0032	0.3814	7.46
		4	0.8264	3.7283	0.4072	0
		5	0.6310	2.4255	0.5399	0
		6	0.9858	2.6475	0.5040	0
		7	0.3268	1.0965	0.2233	0
		8	0.4101	1.2199	0.3111	0

<i>Xerospermophilus tereticaudus</i>	XT2	2	0.5695	1.5819	0.4260	0
		3	0.3985	1.1027	0.5151	16.55
		4	0.5246	2.0970	0.4647	0
		5	0.5042	1.8643	0.5080	0.28
		6	0.7027	2.1436	0.7925	6.23
		7	-	-	-	-
		8	0.4335	1.3552	0.4674	3.67
<i>Xerospermophilus tereticaudus</i>	XT3	2	0.5171	1.6605	0.5339	1.47
		3	0.4105	1.3215	0.4363	2.84
		4	0.5062	2.4457	0.4033	0
		5	0.4418	1.8392	0.4221	0
		6	0.7577	2.2587	0.5866	0
		7	0.4123	1.2940	0.3538	0
		8	0.3844	1.1675	0.4679	10.66
<i>Ammospermophilus leucurus</i>	AL1	2	0.7496	2.0659	0.5990	0
		4	0.7133	2.6948	0.5954	0
<i>Ammospermophilus leucurus</i>	AL2	2	0.8293	1.9502	0.6841	0
		4	0.6276	2.2201	0.5925	0
<i>Ammospermophilus leucurus</i>	AL3	2	0.8253	2.0712	0.6396	0
		4	0.3536	1.3410	0.2664	0

Table 5. Repeated measures ANOVA table for cell proliferation data.

Parameter (cell proliferation)	Species	Transformation or simulation	df1	df2	F	P
Min.: 0.6272 1st Qu.: 0.9338 Median: 1.0462 Mean: 1.0936 3 <sup>rd</sup> Qu.: 1.1777 Max.: 1.8096	<i>Ictidomys tridecemlineatus</i>	No	1	29	1.3099	0.2618
Min.: 0.9162 1st Qu.: 0.9876 Median: 1.0379 Mean: 1.0360 3 <sup>rd</sup> Qu.: 1.0885 Max.: 1.1479	<i>Ammospermophilus leucurus</i>	No	1	2	1.5505	0.3392
Min.: 0.5342 1st Qu.: 0.9513 Median: 1.0334 Mean: 1.0793 3 <sup>rd</sup> Qu.: 1.1736 Max.: 1.6393	<i>Camelus dromedarius</i>	No	1	29	0.6780	0.417

Min.: 0.2909 1st Qu.: 0.7101 Median: 0.9233 Mean: 0.9714 3 <sup>rd</sup> Qu.: 1.1806 Max.: 1.8366	<i>Homo sapiens</i>	No	1	29	0.457 3	0.5043
Min.: 0.4332 1st Qu.: 0.7991 Median: 1.0149 Mean: 1.0181 3 <sup>rd</sup> Qu.: 1.2291 Max.: 1.7324	<i>Rattus norvegicus</i>	No	1	23	1.557 1	0.2246
Min.: 0.3835 1st Qu.: 0.7026 Median: 0.8158 Mean: 0.9669 3 <sup>rd</sup> Qu.: 0.9316 Max.: 3.4518	<i>Ceratotherium simum</i>	No	1	29	0.970 2	0.3328
Min.: 0.7413 1st Qu.: 0.9356 Median: 1.0570 Mean: 1.0813 3 <sup>rd</sup> Qu.: 1.1716 Max.: 1.7090	<i>Xerospermophilus tereticaudus</i>	No	1	16	0.016 8	0.8985

Table 6. Repeated measures ANOVA table for cell viability data.

Parameter (cell viability)	Species	Transformation or simulation	df1	df2	F	P
Min.: -7.1847 1st Qu.: 0.1357 Median: 1.8879 Mean: 2.4907 3 <sup>rd</sup> Qu.: 5.1963 Max.: 11.8058	<i>Ictidomys tridecemlineatus</i>	Simulate	1	29	0.858 2	0.3619
Min.: - 1st Qu.: - Median: - Mean: - 3 <sup>rd</sup> Qu.: - Max.: -	<i>Ammospermophilus leucurus</i>	Overfitted model – due to the presence all values being 0.	-	-	-	-
Min.: -10.972 1st Qu.: 1.125	<i>Camelus dromedarius</i>	Simulate	1	29	3.318 5	0.0788

Median: 7.835 Mean: 7.963 3 <sup>rd</sup> Qu.: 13.924 Max.: 26.322						
Min.: -39.17 1st Qu.: 6.70 Median: 17.10 Mean: 17.42 3 <sup>rd</sup> Qu.: 33.48 Max.: 54.18	<i>Homo sapiens</i>	Simulate	1	29	2.578 4	0.1192
Min.: -26.392 1st Qu.: -2.557 Median: 6.333 Mean: 6.133 3 <sup>rd</sup> Qu.: 15.281 Max.: 34.054	<i>Rattus norvegicus</i>	Simulate	1	23	0.027 5	0.8696
Min.: -22.027 1st Qu.: 4.549 Median: 13.705 Mean: 12.444 3 <sup>rd</sup> Qu.: 21.472 Max.: 38.930	<i>Ceratotherium simum</i>	Simulate	1	26	0.595 9	0.4471
Min.: -7.355 1st Qu.: -2.077 Median: 1.674 Mean: 1.640 3 <sup>rd</sup> Qu.: 4.789 Max.: 9.582	<i>Xerospermophilus tereticaudus</i>	Simulate	1	14	0.008 3	0.9287

Table 7. Linear mixed effects analysis on cell proliferation and cell viability data.

Data set	Parameter	Transformation or simulation	df1	df2	F	P
Cell Proliferation	Min.: 0.2909 1st Qu.: 0.8398 Median: 0.9921 Mean: 1.0099 3 <sup>rd</sup> Qu.: 1.1547 Max.: 1.8366	No	1	28	7.7507	0.0095
Cell viability	Min.: -34.722 1st Qu.: -1.277 Median: 10.268 Mean: 8.935 3 <sup>rd</sup> Qu.: 20.106	Simulate	1	5	0.3518	0.5789

	Max.: 44.082				
--	--------------	--	--	--	--

Table 8. SYBR Green primers developed for qPCR gene expression assays.

Gene	Species that utilized this primer	Primer Name	Primer Sequence (5' - 3')	Working primer concentration
CDKN1A	<i>Ceratotherium simum</i>	CS-Cdkn1a-03-FWD	CCACCCAGGGATGCTCAG	100µM
CDKN1A	<i>Ceratotherium simum</i>	CS-Cdkn1a-03-RVS	ACAGGTAGATCTTGGGCA GG	100µM
CDKN1A	<i>Camelus dromedarius</i>	CD-Cdkn1a-01-FWD	TGTGGGTGAGGAGCAGAT TT	100µM
CDKN1A	<i>Camelus dromedarius</i>	CD-Cdkn1a-01-RVS	CTCACA ACTCCCAGGTCC AT	100µM
CDKN1A	<i>Ictidomys tridecemlineatus</i> , <i>Xerospermophilus tereticaudus</i> , <i>Ammospermophilus leucurus</i> , <i>Rattus norvegicus</i>	IT-Cdkn1a-01-FWD	CAGCTGAACAAGGAGATG GC	100µM
CDKN1A	<i>Ictidomys tridecemlineatus</i> , <i>Xerospermophilus tereticaudus</i> , <i>Ammospermophilus leucurus</i> , <i>Rattus</i>	IT-Cdkn1a-01-RVS	CAGGCCAGGATGTAACAG GA	100µM

	<i>norvegicus</i>			
CDKN1 A	<i>Homo sapiens</i>	HS- Cdkn1a- 02-FWD	GGGCTGGGAGTAGTTGTC TT	100µM
CDKN1 A	<i>Homo sapiens</i>	HS- Cdkn1a- 02-RVS	ATTGTGGGAGGAGCTGTG AA	100µM
ERN1	<i>Ceratotherium simum, Camelus dromedarius</i>	CD-Ern1- 03-FWD	AGCTCCAGTTCTTCCAGG AC	100µM
ERN1	<i>Ceratotherium simum, Camelus dromedarius</i>	CD-Ern1- 03-RVS	CCCGGTAGTGGTGCTTCT TA	100µM
ERN1	<i>Ictidomys tridecemlineatu s, Xerospermophil us tereticaudus, Ammospermop hilus leucurus, Rattus norvegicus</i>	IT-Ern1- 01-FWD	GCGACAGTTAGAAAGAGG CG	100µM
ERN1	<i>Ictidomys tridecemlineatu s, Xerospermophil us tereticaudus, Ammospermop hilus leucurus, Rattus norvegicus</i>	IT-Ern1- 01-RVS	CTCCCGGTAGTGGTGTTT CT	100µM
ERN1	<i>Homo sapiens</i>	HS-Ern1- 02-FWD	AGATGCACCAAGTACAGC CT	100µM
ERN1	<i>Homo sapiens</i>	HS-Ern1- 02-RVS	CCTAATGCCACACCTCATG C	100µM



HSF1	<i>Ceratotherium simum</i>	CS-Hsf1-01-FWD	AAGATTCGCCAGGACAGTGT	10μM
HSF1	<i>Ceratotherium simum</i>	CS-Hsf1-01-RVS	TGTTGACGACTTTCTGCTGC	10μM
HSF1	<i>Camelus dromedarius</i>	CD-Hsf1-01-FWD	TGAAGATTCGCCAGGACAGT	100μM
HSF1	<i>Camelus dromedarius</i>	CD-Hsf1-01-RVS	GGATGAGCTTGTTGACGACC	100μM
HSF1	<i>Ictidomys tridecemlineatus</i> , <i>Xerospermophilus tereticaudus</i> , <i>Ammospermophilus leucurus</i>	IT-Hsf1-02-FWD	AAGTGACCAGCGTATCCACA	100μM
HSF1	<i>Ictidomys tridecemlineatus</i> , <i>Xerospermophilus tereticaudus</i> , <i>Ammospermophilus leucurus</i>	IT-Hsf1-02-RVS	TGTTGACGACTTTCTGCTGC	100μM
HSF1	<i>Rattus norvegicus</i>	RN-Hsf1-03-FWD	GATGTGCAGCTGATGAAGGG	100μM
HSF1	<i>Rattus norvegicus</i>	RN-Hsf1-03-RVS	CTGCACCAGTGAGATCAGGA	100μM
HSF1	<i>Homo sapiens</i>	HS-Hsf1-01-FWD	CCCAGCAACAGAAAGTCGTC	100μM
HSF1	<i>Homo sapiens</i>	HS-Hsf1-01-RVS	GGAGAACTGCCGGCTATAC	100μM
PRKAA2	<i>Ceratotherium simum</i>	CS-Prkaa2-01-FWD	TCTACCTCGCCTCTAGTCC	100μM
PRKAA2	<i>Ceratotherium simum</i>	CS-Prkaa2-	TCGGATTCCAAGATGCCACT	100μM

		01-RVS		
PRKAA2	<i>Camelus dromedarius</i>	CD-Prkaa2-01-FWD	GGTCACAGTTTTGGCTCCTG	100µM
PRKAA2	<i>Camelus dromedarius</i>	CD-Prkaa2-01-RVS	CCCTCTCCCTGCCTATTAGC	100µM
PRKAA2	<i>Ictidomys tridecemlineatus</i>	IT-Prkaa2-06-FWD	ACACAGACCAAGATCCAGCT	100µM
PRKAA2	<i>Ictidomys tridecemlineatus</i>	IT-Prkaa2-06-RVS	GGGAGATCATCAACGGGCTA	100µM
PRKAA2	<i>Xerospermophilus tereticaudus</i> , <i>Ammospermophilus leucurus</i>	IT-Prkaa2-01-FWD	CTGTCTGGCGGTGGATTATTG	10µM
PRKAA2	<i>Xerospermophilus tereticaudus</i> , <i>Ammospermophilus leucurus</i>	IT-Prkaa2-01-RVS	AGATGACTTCAGGTGCTGCA	10µM
PRKAA2	<i>Rattus norvegicus</i>	RN-Prkaa2-04-FWD	GGTCATCTCAGGAAGGCTGT	10µM
PRKAA2	<i>Rattus norvegicus</i>	RN-Prkaa2-04-RVS	GCAGAGTGGCAATAGAACGG	10µM
PRKAA2	<i>Homo sapiens</i>	HS-Prkaa2-05-FWD	GAAGACACGGGAGAAGAGCT	10µM
PRKAA2	<i>Homo sapiens</i>	HS-Prkaa2-05-RVS	GAGGGGAAGAGTAGCATGCA	10µM

Table 9. Outliers excluded from qPCR analysis.

Species	Biological replicate	Time point (H)	Gene(s)
<i>Ictidomys tridecemlineatus</i>	OK14	24	CDKN1A, ERN1
<i>Ceratotherium simum</i>	CSO2	2	HSF1
<i>Rattus norvegicus</i>	RN36	24	PRKAA2
<i>Rattus norvegicus</i>	RN32	0-24	PRKAA2
<i>Rattus norvegicus</i>	RN2	0.5	HSF1, ERN1, CDKN1A, PRKAA2
<i>Homo sapiens</i>	HS2096	2	HSF1, ERN1, CDKN1A, PRKAA2

Table 10. T-test results comparing relative fold change of expression between 0- and 0.5 hours.

Species	Gene	Transform	Mean of Difference	SD of Difference	t	Df	p
<i>Ictidomys tridecemlineatus</i>	HSF1	Log	-0.008	0.31	0.0	4	0.95
	ERN1	Log	0.08	0.16	6	4	0.31
	PRKAA2	Log	0.14	0.45	0.7	4	0.50
<i>Camelus dromedarius</i>	ERN1	Log	0.15	0.02	13	4	0.0002
	CDKN1A	Log	0.03	0.09	0.7	4	0.49
	PRKAA2	Log	0.11	0.22	1.1	4	0.32
<i>Ceratotherium simum</i>	HSF1	Log	0.09	0.11	1.1	1	0.44
	ERN1	Log	0.09	0.42	0.3	2	0.74
	CDKN1A	Log	0.02	0.28	0.1	2	0.90
	PRKAA2	Log	0.10	0.31	0.5	2	0.61
<i>Xerospermophilus tereticaudus</i>	HSF1	Log	0.001	0.11	0.0	2	0.98
	ERN1	Log	-0.04	0.16	0.4	2	0.69
	CDKN1A	Log	0.02	0.08	0.5	2	0.62
	PRKAA2	Log	-0.10	0.12	1.4	2	0.27
<i>Homo sapiens</i>	HSF1	Log	-0.02	0.70	0.0	3	0.95
	ERN1	Log	-0.20	0.57	0.7	3	0.53
	CDKN1A	Log	0.56	0.49	2.3	3	0.10
	PRKAA2	Log	-0.10	0.66	0.3	3	0.77
<i>Rattus norvegicus</i>	HSF1	Log	0.07	0.14	0.9	2	0.45
	ERN1	Log	-0.11	0.16	1.2	2	0.35

Table 11. Wilcoxon test results comparing relative fold change of expression between 0- and 0.5 hours.

Species	Gene	Transformed	p
<i>Ictidomys tridecemlineatus</i>	CDKN1A	Log	0.79
<i>Camelus dromedarius</i>	HSF1	Log	0.81
<i>Rattus norvegicus</i>	CDKN1A	Log	0.5

Table 12. One-way ANOVA test results comparing the mean expression at 0.5 hours at 41°C for HSF1.

	Transformed	Sum of Squares	Df	Mean square	F	P
Treatment (between columns)	Log	0.51	6	0.08	0.65	0.68
Residual (within columns)	Log	2.24	17	0.13	-	-
Total	-	2.75	23	-	-	-

Table 13. Three-level nested ANOVA analyzing HSF1 expression differences at 0.5 hours at 41°C for heat tolerant and heat sensitive phenotypes of different species.

	Transformed or Simulated	Sum of Squares	Df	Mean Square	F	P
Phenotype	Log	0.25	1	0.25	0.41	0.52
Residuals	Log	14.43	23	0.62		

Table 14. Repeated measures ANOVA results for HSF1 gene expression patterns.

Parameter	Species	Transformation or simulation	df1	df2	F	P
Min.: -1.81 1st Qu.: -0.65 Median: 0.06	<i>Ictidomys tridecemlineatus</i>	Log	6	24	1.78	0.14

Mean: - 3 <sup>rd</sup> Qu.: 0.52 Max.: 1.60						
Min.: -1.42 1st Qu.: -0.53 Median: -0.01 Mean: - 3 <sup>rd</sup> Qu.: 0.50 Max.: 1.46	<i>Ammospermophilus leucurus</i>	Log	6	10	0.2	0.95
Min.: -1.42 1st Qu.: -0.53 Median: -0.01 Mean: - 3 <sup>rd</sup> Qu.: 0.50 Max.: 1.46	<i>Camelus dromedarius</i>	Log	6	10	0.23	0.95
Min.: -1.90 1st Qu.: -0.67 Median: 0.01 Mean: - 3 <sup>rd</sup> Qu.: 0.72 Max.: 1.43	<i>Homo sapiens</i>	Log	6	22	0.68	0.66
Min.: -1.38 1st Qu.: -0.65 Median: -0.01 Mean: - 3 <sup>rd</sup> Qu.: 0.54 Max.: 1.57	<i>Rattus norvegicus</i>	Log	6	18	3.44	0.01
Min.: -2.41 1st Qu.: -1.15 Median: -0.78 Mean: -0.75 3 <sup>rd</sup> Qu.: -0.24 Max.: 0.70	<i>Ceratotherium simum</i>	Log and Simulate	1	21	0.13	0.71
Min.: -0.65 1st Qu.: -0.32 Median: -0.10 Mean: -0.10 3 <sup>rd</sup> Qu.: 0.31 Max.: 0.48	<i>Xerospermophilus tereticaudus</i>	Log and Simulate	1	17	0.41	0.52

Table 15. Linear mixed effects analysis on HSF1, ERN1, PRKAA2, and CDKN1A gene expression.

Gene	Parameter	Transformation or simulation	df1	df2	F	P
HSF1	Min.: 0.65 1st Qu.: -0.32 Median: -0.10 Mean: -0.10 3 <sup>rd</sup> Qu.: 0.13 Max.: 0.48	Log	1	5	0.0	0.99
ERN1	Min.: -2.0 1st Qu.: -0.62 Mean: -0.16 Median: -0.11 3 <sup>rd</sup> Qu.: 0.40 Max.: 2.57	Log and Simulated	1	5	0.4	0.53
PRKAA2	Min.: - 1st Qu.: - Median: - Mean: - 3 <sup>rd</sup> Qu.: - Max.: -	Log	1	5	0.32	0.59
CDKN1A	Min.: -2.0 1st Qu.: -0.64 Median: -0.18 Mean: -0.13 3 <sup>rd</sup> Qu.: -0.38 Max.: 2.58	Log	1	5	0.4	0.53

Table 16. One-way ANOVA test results comparing the mean expression at 0.5 hours at 41°C for ERN1.

	Transformed	Sum of Squares	Df	Mean square	F	P
Treatment (between columns)	Log	0.61	6	0.10	0.71	0.63
Residual (within columns)	Log	2.56	18	0.14	-	-
Total	-	3.17	24	-	-	-

Table 17. Three-level nested ANOVA analyzing ERN1 expression differences at 0.5 hours at 41°C for heat tolerant and heat sensitive phenotypes of different species.

	Transformed or Simulated	Sum of Squares	Df	Mean Square	F	P
Phenotype	-	2.13	1	2.13	3.3	0.08
Residuals	-	14.70	23	0.63		

Table 18. Repeated measures ANOVA results for ERN1 gene expression patterns.

Parameter	Species	Transformation or simulation	df1	df2	F	P
Min.: -1.48 1st Qu.: -0.58 Median: -0.10 Mean: - 3 <sup>rd</sup> Qu.: 0.73 Max.: 1.65	<i>Ictidomys tridecemlineatus</i>	Log	6	23	2.2	0.07
Min.: -0.96 1st Qu.: -0.62 Median: -0.01 Mean: - 3 <sup>rd</sup> Qu.: 0.65 Max.: 1.40	<i>Ammospermophilus leucurus</i>	Log	6	10	0.09	0.99
Min.: -2.5 1st Qu.: -0.30 Median: 0.12 Mean: - 3 <sup>rd</sup> Qu.: 0.44 Max.: 1.93	<i>Camelus dromedarius</i>	Log	6	23	2.2	0.07
Min.: -1.96 1st Qu.: -0.455 Median: -0.09 Mean: - 3 <sup>rd</sup> Qu.: 0.62 Max.: 1.63	<i>Homo sapiens</i>	Log	6	22	2.3	0.06
Min.: -1.53 1st Qu.: -0.49 Median: -0.08 Mean: - 3 <sup>rd</sup> Qu.: 0.43 Max.: 1.89	<i>Rattus norvegicus</i>	Log	6	17	1.63	0.19

Min.: -1.9 1st Qu.: -0.62 Median: -0.10 Mean: - 3 <sup>rd</sup> Qu.: 0.43 Max.: 1.47	<i>Ceratotherium simum</i>	Log	6	18	2.72	0.04
Min.: -1.90 1st Qu.: -0.62 Median: -0.10 Mean: - 3 <sup>rd</sup> Qu.: 0.43 Max.: 1.47	<i>Xerospermophilus tereticaudus</i>	Log	1	17	0.20	0.65

Table 19. One-way ANOVA test results comparing the mean expression at 0.5 hours at 41°C for PRKAA2.

	<b>Transformed</b>	<b>Sum of Squares</b>	<b>Df</b>	<b>Mean square</b>	<b>F</b>	<b>P</b>
Treatment (between columns)	Log	0.61	6	0.10	0.71	0.63
Residual (within columns)	Log	2.56	18	0.14	-	-
Total	-	3.17	24	-	-	-

Table 20. Nested ANOVA analyzing PRKAA2 expression differences at 0.5 hours at 41°C for heat tolerant and heat sensitive phenotypes of different species.

	<b>Transformed or Simulated</b>	<b>Sum of Squares</b>	<b>Df</b>	<b>Mean Square</b>	<b>F</b>	<b>P</b>
Phenotype	-	0.12	1	0.12	0.10	0.74
Residuals	-	25.31	22	1.15		

Table 21. Repeated measures ANOVA results for PRKAA2 gene expression patterns.

<b>Parameter</b>	<b>Species</b>	<b>Transformation or simulation</b>	<b>df1</b>	<b>df2</b>	<b>F</b>	<b>P</b>
------------------	----------------	-------------------------------------	------------	------------	----------	----------



Min.: -1.24 1st Qu.: 0.25 Median: 1.09 Mean: 1.10 3 <sup>rd</sup> Qu.: 1.84 Max.: 3.38	<i>Ictidomys tridecemlineatus</i>	Log and simulated	6	24	1.85	0.13
Min.: -0.94 1st Qu.: -0.60 Median: -0.10 Mean: - 3 <sup>rd</sup> Qu.: 0.35 Max.: 1.90	<i>Ammospermophilu s leucurus</i>	Log	6	10	0.56	0.74
Min.: -0.13 1st Qu.: -0.72 Median: 1.17 Mean: 1.14 3 <sup>rd</sup> Qu.: 1.38 Max.: 2.59	<i>Camelus dromedarius</i>	Log and Simulated	6	23	0.72	0.85
Min.: -1.65 1st Qu.: -0.55 Median: -0.03 Mean: - 3 <sup>rd</sup> Qu.: 0.39 Max.: 1.79	<i>Homo sapiens</i>	Log	6	22	0.80	0.57
Min.: -1.80 1st Qu.: -0.71 Median: 0.09 Mean: - 3 <sup>rd</sup> Qu.: 2.30 Max.: 1.76	<i>Rattus norvegicus</i>	Log	1	16	11.41	0.003
Min.: -2.23 1st Qu.: -0.35 Median: -0.05 Mean: - 3 <sup>rd</sup> Qu.: 0.46 Max.: 1.49	<i>Ceratotherium simum</i>	Log	6	17	3.74	0.01
Min.: -2.23 1st Qu.: -0.35 Median: -0.05 Mean: - 3 <sup>rd</sup> Qu.: 0.46 Max.: 1.49	<i>Xerospermophilus tereticaudus</i>	Log	1	17	13.83	0.001

Table 22. One-way ANOVA test results comparing the mean expression at 0.5 hours at 41°C for CDKN1A.

Gene	Transformed	Sum of Squares	Df	Mean square	F	P
Treatment (between columns)	Log	1.156	6	0.192	2.28	0.08
Residual (within columns)	Log	1.520	18	0.084	-	-
Total	-	2.675	24	-	-	-

Table 23. Nested ANOVA analyzing CDKN1A expression differences at 0.5 hours at 41°C for heat tolerant and heat sensitive phenotypes of different species.

Gene	Transformed	Sum of Squares	Df	Mean square	F	P
Phenotype	Log and simulated	51.32	1	51.31	3.21	0.08
Residuals	Log and simulated	366.79	23	15.94	-	-

Table 24. Repeated measures ANOVA results for CDKN1A gene expression patterns.

Parameter	Species	Transformation or simulation	df1	df2	F	P
Min.: -1.6 1st Qu.: -0.60 Median: -0.03 Mean: - 3 <sup>rd</sup> Qu.: 0.69 Max.: 1.35	<i>Ictidomys tridecemlineatus</i>	Log	6	23	1.83	0.13
Min.: -1.25 1st Qu.: -0.35 Median: -0.03 Mean: - 3 <sup>rd</sup> Qu.: 0.50 Max.: 1.29	<i>Ammospermophilus leucurus</i>	Log	6	10	0.62	0.70

Min.: -2.84 1st Qu.: -0.35 Median: 0.01 Mean: - 3 <sup>rd</sup> Qu.: 0.38 Max.: 1.35	<i>Camelus dromedarius</i>	Log	6	23	2.15	0.08
Min.: -1.49 1st Qu.: -0.51 Median: -0.008 Mean: - 3 <sup>rd</sup> Qu.: 0.42 Max.: 1.98	<i>Homo sapiens</i>	Log	6	22	1.74	0.15
Min.: -1.32 1st Qu.: -0.61 Median: -0.10 Mean: - 3 <sup>rd</sup> Qu.: 0.52 Max.: 1.93	<i>Rattus norvegicus</i>	-	6	17	0.93	0.49
Min.: -1.59 1st Qu.: -0.45 Median: 0.04 Mean: - 3 <sup>rd</sup> Qu.: 0.62 Max.: 1.83	<i>Ceratotherium simum</i>	Log	6	18	4.46	0.60
Min.: -1.41 1st Qu.: -0.22 Median: 0.02 Mean: 0.02 3 <sup>rd</sup> Qu.: 0.29 Max.: 0.70	<i>Xerospermophilus tereticaudus</i>	Log and simulated	1	17	0.41	0.52

Table 25. Significant induction of HSPs demonstrating desert-dwelling and species-specific mechanisms.

Protein	Mammal	P-value
HSP90AB1	13-lined ground squirrel White-tailed antelope squirrel Rat	0.001 0.03  No induction identified
HSP90B1	13-lined ground squirrel White-tailed antelope squirrel Rat	0.006 0.067  0.896

HSPA1A	13-lined ground squirrel White-tailed antelope squirrel Rat	0.148 0.005  0.356
HSPA1L	13-lined ground squirrel White-tailed antelope squirrel Rat	0.041 No induction identified  No induction identified
HSPA5	13-lined ground squirrel White-tailed antelope squirrel Rat	0.001 0.813  0.302
HSPA8	13-lined ground squirrel White-tailed antelope squirrel Rat	0.015 0.298  No induction identified
HSPD1	13-lined ground squirrel White-tailed antelope squirrel Rat	No induction identified 0.018  0.941

Table 26. Selected variables generated by Random Forest.

<b>Comparison</b>	<b>Protein (Selected Variable)</b>	<b># of Appearances</b>
By species: 13-lined ground squirrel	FBXO6	5
	GNB1	3
	LMF1	1
	SELENOO	1
	TM4SF1	1
	BCL2L1	4
	INT55	2
	AASDHPPT	3
	BSDC1	1
	IGF2R	1
	LRRC58	1
	RABGEF1	2
	C18ORF25	5
	WDR61	1
	KIAA1191	1
By species: Rat	PPP3CA	1
	MRPL12	11
	SRSF9	7
	STX5	3

	TARS2	4
By species: White-tailed antelope squirrel	MFSD10	2
	PSMB4	4
	RNMT	3
	MSRB3	9
	SPTLC2	8
	LAMTOR3	3
By time: 6 hours	COPS6	3
	CCT6A	1
	PPM1A	5
	TRAPPC11	7
	GSTP1	1
	RHOT1	2
	MFN1	2
	LNPB	1
By time: 24 hours	ANXA6	3
	LTA4H	5
	COASY	4
	CACYBP	1
	TMP1	1
	HADHA	2
	SEPTIN11	1
	TTLL12	2
	PAICS	5

Table 27. Selected variables with 75% or higher appearance rate.

<b>Comparison</b>	<b>Protein (Selected Variable)</b>	<b># of Appearances (out of the 12 runs)</b>
By species: 13-lined ground squirrel	FBXO6	5
	GNB1	3
	BCL2L1	4
	AASDHPPT	3
	C18ORF25	5
By species: White-tailed antelope squirrel	MSRB3	9
	SPTLC2	8
By species: Rat	MRPL12	11
By time: 6hr	PPM1A	5
	TRAPPC11	7
By time: 24hr	ANXA6	3
	LTA4H	5
	COASY	4
	PAICS	5

## References

- Abe, T. Tamiya, Y. Ono, A. H. Salke, T. (2001). Accumulation of cell cycle regulatory proteins, p21 and p27, induced after hyperthermia in human glioma cells. *International Journal of Hyperthermia*, 17(6), 499–507. <https://doi.org/10.1080/02656730110070219>
- Abravaya, K., Myers, M. P., Murphy, S. P., & Morimoto, R. I. (1992). The human heat shock protein hsp70 interacts with HSF, the transcription factor that regulates heat shock gene expression. *Genes & Development*, 6(7), 1153–1164. <https://doi.org/10.1101/gad.6.7.1153>
- Aibara, S., Singh, V., Modelska, A., & Amunts, A. (2020). Structural basis of mitochondrial translation. *ELife*, 9, e58362. <https://doi.org/10.7554/eLife.58362>
- Alvira-Iraizoz, F., Gillard, B. T., Lin, P., Paterson, A., Pauža, A. G., Ali, M. A., Alabsi, A. H., Burger, P. A., Hamadi, N., Adem, A., Murphy, D., & Greenwood, M. P. (2021). Multiomic analysis of the Arabian camel (*Camelus dromedarius*) kidney reveals a role for cholesterol in water conservation. *Communications Biology*, 4(1), 779. <https://doi.org/10.1038/s42003-021-02327-3>
- Anckar, J., & Sistonen, L. (2011). Regulation of HSF 1 Function in the Heat Stress Response: Implications in Aging and Disease. *Annual Review of Biochemistry*, 80(1), 1089–1115. <https://doi.org/10.1146/annurev-biochem-060809-095203>
- Angelos, E., Ruberti, C., Kim, S., & Brandizzi, F. (2017). Maintaining the factory: The roles of the unfolded protein response in cellular homeostasis in plants. *The Plant Journal*, 90(4), 671–682. <https://doi.org/10.1111/tpj.13449>
- Axelrod, F. B., & Kaufmann, H. (2015). Hereditary Sensory and Autonomic Neuropathies. In *Neuromuscular Disorders of Infancy, Childhood, and Adolescence* (pp. 340–352). Elsevier. <https://doi.org/10.1016/B978-0-12-417044-5.00018-4>
- Bates, D., Mächler, M., Bolker, B., & Walker, S. (2015). Fitting Linear Mixed-Effects Models Using **lme4**. *Journal of Statistical Software*, 67(1). <https://doi.org/10.18637/jss.v067.i01>

- Beld, J., Sonnenschein, E. C., Vickery, C. R., Noel, J. P., & Burkart, M. D. (2014). The phosphopantetheinyl transferases: Catalysis of a post-translational modification crucial for life. *Nat. Prod. Rep.*, 31(1), 61–108. <https://doi.org/10.1039/C3NP70054B>
- Belk, M. C., & Smith, H. D. (1991). *Ammospermophilus leucurus*. *Mammalian Species*, 368, 1. <https://doi.org/10.2307/3504191>
- Berning, M., Prätzel-Wunder, S., Bickenbach, J. R., & Boukamp, P. (2015). Three-Dimensional *In Vitro* Skin and Skin Cancer Models Based on Human Fibroblast-Derived Matrix. *Tissue Engineering Part C: Methods*, 21(9), 958–970. <https://doi.org/10.1089/ten.tec.2014.0698>
- Billman, G. E. (2020). Homeostasis: The Underappreciated and Far Too Often Ignored Central Organizing Principle of Physiology. *Frontiers in Physiology*, 11, 200. <https://doi.org/10.3389/fphys.2020.00200>
- Bolker, B., Warnes, G. R., & Lumley, T. (2022). *gtools: Various R Programming Tools* (R package version 3.9.4). <https://CRAN.R-project.org/package=gtools>
- Bouâouda, H., Achâaban, M. R., Ouassat, M., Oukassou, M., Piro, M., Challet, E., El Allali, K., & Pévet, P. (2014). Daily regulation of body temperature rhythm in the camel ( *Camelus dromedarius* ) exposed to experimental desert conditions. *Physiological Reports*, 2(9), e12151. <https://doi.org/10.14814/phy2.12151>
- Bouma, H. R., Carey, H. V., & Kroese, F. G. M. (2010). Hibernation: The immune system at rest? *Journal of Leukocyte Biology*, 88(4), 619–624. <https://doi.org/10.1189/jlb.0310174>
- Breiman, L. (2001). Breiman and Cutler's Random Forests for Classification and Regression. *Machine Learning*, 45(1), 5–32. <https://doi.org/10.1023/A:1010933404324>
- Christofferson, D. E., & Yuan, J. (2010). Cyclophilin A release as a biomarker of necrotic cell death. *Cell Death & Differentiation*, 17(12), 1942–1943. <https://doi.org/10.1038/cdd.2010.123>

- Corton, J. M., Gillespie, J. G., & Hardie, D. G. (1994). Role of the AMP-activated protein kinase in the cellular stress response. *Current Biology*, 4(4), 315–324.  
[https://doi.org/10.1016/S0960-9822\(00\)00070-1](https://doi.org/10.1016/S0960-9822(00)00070-1)
- Creff, J., & Besson, A. (2020). Functional Versatility of the CDK Inhibitor p57Kip2. *Frontiers in Cell and Developmental Biology*, 8, 584590. <https://doi.org/10.3389/fcell.2020.584590>
- Cui, Y., Hao, Y., Li, J., Bao, W., Li, G., Gao, Y., & Gu, X. (2016). Chronic Heat Stress Induces Immune Response, Oxidative Stress Response, and Apoptosis of Finishing Pig Liver: A Proteomic Approach. *International Journal of Molecular Sciences*, 17(5), 393.  
<https://doi.org/10.3390/ijms17050393>
- De Schutter, E., Ramon, J., Pfeuty, B., De Tender, C., Stremersch, S., Raemdonck, K., De Beeck, K. O., Declercq, W., Riquet, F. B., Braeckmans, K., & Vandenabeele, P. (2022). Plasma membrane perforation by GSDME during apoptosis-driven secondary necrosis. *Cellular and Molecular Life Sciences*, 79(1), 19. <https://doi.org/10.1007/s00018-021-04078-0>
- Fang, H., Kang, L., Abbas, Z., Hu, L., Chen, Y., Tan, X., Wang, Y., & Xu, Q. (2021). Identification of key Genes and Pathways Associated With Thermal Stress in Peripheral Blood Mononuclear Cells of Holstein Dairy Cattle. *Frontiers in Genetics*, 12, 662080.  
<https://doi.org/10.3389/fgene.2021.662080>
- Furusawa, Y., Tabuchi, Y., Takasaki, I., Wada, S., Ohtsuka, K., & Kondo, T. (2009). Gene networks involved in apoptosis induced by hyperthermia in human lymphoma U937 cells. *Cell Biology International*, 33(12), 1253–1262.  
<https://doi.org/10.1016/j.cellbi.2009.08.009>
- Fuse, T., Yamada, K., Asai, K., Kato, T., & Nakanishi, M. (1996). Heat Shock-Mediated Cell Cycle Arrest Is Accompanied by Induction of p21 CKI. *Biochemical and Biophysical Research Communications*, 225(3), 759–763. <https://doi.org/10.1006/bbrc.1996.1247>



- Gong, Y., Crawford, J. C., Heckmann, B. L., & Green, D. R. (2019). To the edge of cell death and back. *The FEBS Journal*, 286(3), 430–440. <https://doi.org/10.1111/febs.14714>
- Gong, Y.-N., Guy, C., Olauson, H., Becker, J. U., Yang, M., Fitzgerald, P., Linkermann, A., & Green, D. R. (2017). ESCRT-III Acts Downstream of MLKL to Regulate Necroptotic Cell Death and Its Consequences. *Cell*, 169(2), 286-300.e16. <https://doi.org/10.1016/j.cell.2017.03.020>
- Gorospe, M., Wang, X., & Holbrook, N. J. (1999). *Functional Role of p21 During the Cellular Response to Stress*.
- Green, D. R., & Llambi, F. (2015). Cell Death Signaling. *Cold Spring Harbor Perspectives in Biology*, 7(12), a006080. <https://doi.org/10.1101/cshperspect.a006080>
- Groves, C. P. (1972). *Ceratotherium simum*. *Mammalian Species*, 8, 1. <https://doi.org/10.2307/3503966>
- Haase, M., & Fitze, G. (2016). HSP90AB1: Helping the good and the bad. *Gene*, 575(2), 171–186. <https://doi.org/10.1016/j.gene.2015.08.063>
- Habte, M., Eshetu, M., Maryo, M., Andualem, D., Legesse, A., & Admassu, B. (2021). The influence of weather conditions on body temperature, milk composition and yields of the free-ranging dromedary camels in Southeastern rangelands of Ethiopia. *Cogent Food & Agriculture*, 7(1), 1930932. <https://doi.org/10.1080/23311932.2021.1930932>
- Hansen, J., Sato, M., Ruedy, R., Lo, K., Lea, D. W., & Medina-Elizade, M. (2006). Global temperature change. *Proceedings of the National Academy of Sciences*, 103(39), 14288–14293. <https://doi.org/10.1073/pnas.0606291103>
- Hardie, D. G. (2007). AMP-activated/SNF1 protein kinases: Conserved guardians of cellular energy. *Nature Reviews Molecular Cell Biology*, 8(10), 774–785. <https://doi.org/10.1038/nrm2249>

- Hardie, D. G. (2011). AMP-activated protein kinase—An energy sensor that regulates all aspects of cell function. *Genes & Development*, 25(18), 1895–1908.  
<https://doi.org/10.1101/gad.17420111>
- He, J., Zou, L.-N., Pareek, V., & Benkovic, S. J. (2022). Multienzyme interactions of the de novo purine biosynthetic protein PAICS facilitate purinosome formation and metabolic channeling. *Journal of Biological Chemistry*, 298(5), 101853.  
<https://doi.org/10.1016/j.jbc.2022.101853>
- Hiley, P. G. (1977). The thermoregulatory response of the rhinoceros (*Diceros bicornis* and *Ceratotherium simum*) and the zebra (*Equus burchelli*) to diurnal temperature change. *African Journal of Ecology*, 15(4), 337–337. <https://doi.org/10.1111/j.1365-2028.1977.tb00417.x>
- Hiramatsu, N., Joseph, V. T., & Lin, J. H. (2011). Monitoring and Manipulating Mammalian Unfolded Protein Response. In *Methods in Enzymology* (Vol. 491, pp. 183–198). Elsevier. <https://doi.org/10.1016/B978-0-12-385928-0.00011-0>
- Homma, T., & Fujii, J. (2016). Heat stress promotes the down-regulation of IRE1 $\alpha$  in cells: An atypical modulation of the UPR pathway. *Experimental Cell Research*, 349(1), 128–138.  
<https://doi.org/10.1016/j.yexcr.2016.10.006>
- Horowitz, M., Maloyan, A., & Shlaier, J. (1997). HSP 70 kDa Dynamics in Animals Undergoing Heat Stress Superimposed on Heat Acclimation. *Annals of the New York Academy of Sciences*, 813(1 Thermoregulation), 617–619. <https://doi.org/10.1111/j.1749-6632.1997.tb51755.x>
- Huang, Y., Tracy, R., Walsberg, G. E., Makkinje, A., Fang, P., Brown, D., & Van Hoek, A. N. (2001). Absence of aquaporin-4 water channels from kidneys of the desert rodent *Dipodomys merriami merriami*. *American Journal of Physiology-Renal Physiology*, 280(5), F794–F802. <https://doi.org/10.1152/ajprenal.2001.280.5.F794>

- Huang, Y., Xie, H., Pan, P., Qu, Q., Xia, Q., Gao, X., Zhang, S., & Jiang, Q. (2021). Heat stress promotes lipid accumulation by inhibiting the AMPK-PGC-1 $\alpha$  signaling pathway in 3T3-L1 preadipocytes. *Cell Stress and Chaperones*, 26(3), 563–574.  
<https://doi.org/10.1007/s12192-021-01201-9>
- Jung, J., Bashiri, G., Johnston, J. M., & Baker, E. N. (2016). Mass spectral determination of phosphopantetheinylation specificity for carrier proteins in *Mycobacterium tuberculosis*. *FEBS Open Bio*, 6(12), 1220–1226. <https://doi.org/10.1002/2211-5463.12140>
- Klenow, M. B., Heitmann, A. S. B., Nylandsted, J., & Simonsen, A. C. (2021). Timescale of hole closure during plasma membrane repair estimated by calcium imaging and numerical modeling. *Scientific Reports*, 11(1), 4226. <https://doi.org/10.1038/s41598-021-82926-6>
- Kühl, N. M., & Rensing, L. (2000). Heat shock effects on cell cycle progression: *Cellular and Molecular Life Sciences*, 57(3), 450–463. <https://doi.org/10.1007/PL00000707>
- Kuhn, M. (2021). *caret: Classification and Regression Training* (R package version 6.0-90).  
<https://CRAN.R-project.org/package=caret>
- LaBaer, J., Garrett, M. D., Stevenson, L. F., Slingerland, J. M., Sandhu, C., Chou, H. S., Fattaey, A., & Harlow, E. (1997). New functional activities for the p21 family of CDK inhibitors. *Genes & Development*, 11(7), 847–862. <https://doi.org/10.1101/gad.11.7.847>
- Laursen, W. J., Schneider, E. R., Merriman, D. K., Bagriantsev, S. N., & Gracheva, E. O. (2016). Low-cost functional plasticity of TRPV1 supports heat tolerance in squirrels and camels. *Proceedings of the National Academy of Sciences*, 113(40), 11342–11347.  
<https://doi.org/10.1073/pnas.1604269113>
- Lee, E., Kwak, G.-H., Kamble, K., & Kim, H.-Y. (2014). Methionine sulfoxide reductase B3 deficiency inhibits cell growth through the activation of p53–p21 and p27 pathways. *Archives of Biochemistry and Biophysics*, 547, 1–5.  
<https://doi.org/10.1016/j.abb.2014.02.008>
- Leipelt, M., & Merrill, A. H. (2004). *Sphingolipid Biosynthesis*.

- Levitsky, D. I., Pivovarova, A. V., Mikhailova, V. V., & Nikolaeva, O. P. (2008). Thermal unfolding and aggregation of actin: Stabilization and destabilization of actin filaments. *FEBS Journal*, 275(17), 4280–4295. <https://doi.org/10.1111/j.1742-4658.2008.06569.x>
- Li, M., Xu, X., Su, Y., Shao, X., Zhou, Y., & Yan, J. (2022). A comprehensive overview of PPM1A: From structure to disease. *Experimental Biology and Medicine*, 247(6), 453–461. <https://doi.org/10.1177/15353702211061883>
- Lillie, L. E., Temple, N. J., & Florence, L. Z. (1996). Reference values for young normal Sprague-Dawley rats: Weight gain, hematology and clinical chemistry. *Human & Experimental Toxicology*, 15(8), 612–616. <https://doi.org/10.1177/096032719601500802>
- Liu, C.-T., & Brooks, G. A. (2012). Mild heat stress induces mitochondrial biogenesis in C2C12 myotubes. *Journal of Applied Physiology*, 112(3), 354–361. <https://doi.org/10.1152/japplphysiol.00989.2011>
- Maechler, M., Rousseeuw, P., Stuyf, A., Hubert, M., & Hornik, K. (2021). *cluster: Cluster Analysis Basics and Extensions* (R package version 2.1.2). <https://CRAN.R-project.org/package=cluster>
- Mahat, D. B., Salamanca, H. H., Duarte, F. M., Danko, C. G., & Lis, J. T. (2016). Mammalian Heat Shock Response and Mechanisms Underlying Its Genome-wide Transcriptional Regulation. *Molecular Cell*, 62(1), 63–78. <https://doi.org/10.1016/j.molcel.2016.02.025>
- Marin, T. L., Gongol, B., Zhang, F., Martin, M., Johnson, D. A., Xiao, H., Wang, Y., Subramaniam, S., Chien, S., & Shyy, J. Y.-J. (2017). AMPK promotes mitochondrial biogenesis and function by phosphorylating the epigenetic factors DNMT1, RBBP7, and HAT1. *Science Signaling*, 10(464), eaaf7478. <https://doi.org/10.1126/scisignal.aaf7478>
- Marra, N. J., Romero, A., & DeWoody, J. A. (2014). Natural selection and the genetic basis of osmoregulation in heteromyid rodents as revealed by RNA-seq. *Molecular Ecology*, 23(11), 2699–2711. <https://doi.org/10.1111/mec.12764>

- Masser, A. E., Ciccarelli, M., & Andréasson, C. (2020). Hsf1 on a leash – controlling the heat shock response by chaperone titration. *Experimental Cell Research*, 396(1), 112246. <https://doi.org/10.1016/j.yexcr.2020.112246>
- McMillan, D. R., Christians, E., Forster, M., Xiao, X., Connell, P., Plumier, J.-C., Zuo, X., Richardson, J., Morgan, S., & Benjamin, I. J. (2002). Heat Shock Transcription Factor 2 Is Not Essential for Embryonic Development, Fertility, or Adult Cognitive and Psychomotor Function in Mice. *Molecular and Cellular Biology*, 22(22), 8005–8014. <https://doi.org/10.1128/MCB.22.22.8005-8014.2002>
- McMillan, D. R., Xiao, X., Shao, L., Graves, K., & Benjamin, I. J. (1998). Targeted Disruption of Heat Shock Transcription Factor 1 Abolishes Thermotolerance and Protection against Heat-inducible Apoptosis. *Journal of Biological Chemistry*, 273(13), 7523–7528. <https://doi.org/10.1074/jbc.273.13.7523>
- Mixed-Effects Models in S and S-PLUS*. (2000). Springer-Verlag. <https://doi.org/10.1007/b98882>
- Nakatsuka, A., Yamaguchi, S., Eguchi, J., Kakuta, S., Iwakura, Y., Sugiyama, H., & Wada, J. (2021). A Vaspin–HSPA1L complex protects proximal tubular cells from organelle stress in diabetic kidney disease. *Communications Biology*, 4(1), 373. <https://doi.org/10.1038/s42003-021-01902-y>
- Nitta, M., Okamura, H., Aizawa, S., & Yamaizumi, M. (1997). Heat shock induces transient p53-dependent cell cycle arrest at G1/S. *Oncogene*, 15(5), 561–568. <https://doi.org/10.1038/sj.onc.1201210>
- Ohnishi, T., Wang, X., Ohnishi, K., Matsumoto, H., & Takahashi, A. (1996). P53-dependent Induction of WAF1 by Heat Treatment in Human Glioblastoma Cells. *Journal of Biological Chemistry*, 271(24), 14510–14513. <https://doi.org/10.1074/jbc.271.24.14510>
- Oi, N., Yamamoto, H., Langfald, A., Bai, R., Lee, M.-H., Bode, A. M., & Dong, Z. (2017). LTA4H regulates cell cycle and skin carcinogenesis. *Carcinogenesis*, 38(7), 728–737. <https://doi.org/10.1093/carcin/bgx049>

- Osilla, E. V., Marsidi, J. L., & Sharma, S. (2023). Physiology, Temperature Regulation. In *StatPearls*. StatPearls Publishing. <http://www.ncbi.nlm.nih.gov/books/NBK507838/>
- Osowski, C. M., & Urano, F. (2011). Measuring ER Stress and the Unfolded Protein Response Using Mammalian Tissue Culture System. In *Methods in Enzymology* (Vol. 490, pp. 71–92). Elsevier. <https://doi.org/10.1016/B978-0-12-385114-7.00004-0>
- Park, H. G., Han, S. I., Oh, S. Y., & Kang, H. S. (2005). Cellular responses to mild heat stress. *Cellular and Molecular Life Sciences*, 62(1), 10–23. <https://doi.org/10.1007/s00018-004-4208-7>
- Peterson, R., A. (2021). Finding Optimal Normalizing Transformations via bestNormalize. *The R Journal*, 13(1), 310. <https://doi.org/10.32614/RJ-2021-041>
- Prastowo, S., Adzdzakiy, M. M., Vanessa, R., Pambuko, G., Purwadi, Susilowati, A., & Sutarno. (2021). Polymorphism scanning of HSP90AB1 gene in local Friesian Holstein as molecular marker for heat stress resistance. *E3S Web of Conferences*, 306, 05016. <https://doi.org/10.1051/e3sconf/202130605016>
- Protsiv, M., Ley, C., Lankester, J., Hastie, T., & Parsonnet, J. (2020). Decreasing human body temperature in the United States since the Industrial Revolution. *ELife*, 9, e49555. <https://doi.org/10.7554/eLife.49555>
- Refinetti, R. (2020). Circadian rhythmicity of body temperature and metabolism. *Temperature*, 7(4), 321–362. <https://doi.org/10.1080/23328940.2020.1743605>
- Rocha, J. L., Godinho, R., Brito, J. C., & Nielsen, R. (2021). Life in Deserts: The Genetic Basis of Mammalian Desert Adaptation. *Trends in Ecology & Evolution*, 36(7), 637–650. <https://doi.org/10.1016/j.tree.2021.03.007>
- Saadeldin, I. M., Swelum, A. A.-A., Tukur, H. A., & Alowaimer, A. N. (2019). Thermotolerance of camel (*Camelus dromedarius*) somatic cells affected by the cell type and the dissociation method. *Environmental Science and Pollution Research*, 26(28), 29490–29496. <https://doi.org/10.1007/s11356-019-06208-5>

- Sajjanar, B., Aalam, M. T., Khan, O., Tanuj, G. N., Sahoo, A. P., Manjunathareddy, G. B., Gandham, R. K., Dhara, S. K., Gupta, P. K., Mishra, B. P., Dutt, T., & Singh, G. (2023). Genome-wide expression analysis reveals different heat shock responses in indigenous (*Bos indicus*) and crossbred (*Bos indicus* X *Bos taurus*) cattle. *Genes and Environment*, 45(1), 17. <https://doi.org/10.1186/s41021-023-00271-8>
- Salt, I., Celler, J. W., Hawley, S. A., Prescott, A., Woods, A., Carling, D., & Hardie, D. G. (1998). AMP-activated protein kinase: Greater AMP dependence, and preferential nuclear localization, of complexes containing the  $\alpha 2$  isoform. *Biochemical Journal*, 334(1), 177–187. <https://doi.org/10.1042/bj3340177>
- Sarkar, D. (2008). *Lattice: Multivariate data visualization with R*. Springer.
- Serre, V., Rozanska, A., Beinat, M., Chretien, D., Boddaert, N., Munnich, A., Rötig, A., & Chrzanowska-Lightowlers, Z. M. (2013). Mutations in mitochondrial ribosomal protein MRPL12 leads to growth retardation, neurological deterioration and mitochondrial translation deficiency. *Biochimica et Biophysica Acta (BBA) - Molecular Basis of Disease*, 1832(8), 1304–1312. <https://doi.org/10.1016/j.bbadis.2013.04.014>
- Shandilya, U. K., Sharma, A., Sodhi, M., & Mukesh, M. (2020). Heat stress modulates differential response in skin fibroblast cells of native cattle ( *Bos indicus* ) and riverine buffaloes ( *Bubalus bubalis* ). *Bioscience Reports*, 40(2), BSR20191544. <https://doi.org/10.1042/BSR20191544>
- Shapiro, S. S., & Wilk, M. B. (1965). An analysis of variance test for normality (complete samples). *Biometrika*, 52(3–4), 591–611. <https://doi.org/10.1093/biomet/52.3-4.591>
- Sheil, D., & Kirkby, A. E. (2018). Observations on Southern White Rhinoceros *Ceratotherium simum simum* Translocated to Uganda. *Tropical Conservation Science*, 11, 194008291880680. <https://doi.org/10.1177/1940082918806805>

- Shelton, D. S., & Alberts, J. R. (2018). Development of behavioral responses to thermal challenges. *Developmental Psychobiology*, 60(1), 5–14.  
<https://doi.org/10.1002/dev.21588>
- Sherr, C. J., & Roberts, J. M. (1999). CDK inhibitors: Positive and negative regulators of G1-phase progression. *Genes & Development*, 13(12), 1501–1512.  
<https://doi.org/10.1101/gad.13.12.1501>
- Siddiqui, S. H., Subramaniyan, S. A., Kang, D., Park, J., Khan, M., Choi, H. W., & Shim, K. (2020). Direct exposure to mild heat stress stimulates cell viability and heat shock protein expression in primary cultured broiler fibroblasts. *Cell Stress and Chaperones*, 25(6), 1033–1043. <https://doi.org/10.1007/s12192-020-01140-x>
- Singh, A. K., Upadhyay, R. C., Chandra, G., Kumar, S., Malakar, D., Singh, S. V., & Singh, M. K. (2020). Genome-wide expression analysis of the heat stress response in dermal fibroblasts of Tharparkar (zebu) and Karan-Fries (zebu × taurine) cattle. *Cell Stress and Chaperones*, 25(2), 327–344. <https://doi.org/10.1007/s12192-020-01076-2>
- Stetler, R. A., Gan, Y., Zhang, W., Liou, A. K., Gao, Y., Cao, G., & Chen, J. (2010). Heat shock proteins: Cellular and molecular mechanisms in the central nervous system. *Progress in Neurobiology*, 92(2), 184–211. <https://doi.org/10.1016/j.pneurobio.2010.05.002>
- Stoddart, M. J. (Ed.). (2011). *Mammalian Cell Viability: Methods and Protocols* (Vol. 740). Humana Press. <https://doi.org/10.1007/978-1-61779-108-6>
- Stolwijk, J. A. (1977). Responses to the thermal environment. *Federation Proceedings*, 36(5), 1655–1658.
- Su, K.-H., Dai, S., Tang, Z., Xu, M., & Dai, C. (2019). Heat Shock Factor 1 Is a Direct Antagonist of AMP-Activated Protein Kinase. *Molecular Cell*, 76(4), 546-561.e8.  
<https://doi.org/10.1016/j.molcel.2019.08.021>
- Sun, G., Guzman, E., Balasanyan, V., Conner, C. M., Wong, K., Zhou, H. R., Kosik, K. S., & Montell, D. J. (2017). A molecular signature for anastasis, recovery from the brink of



- apoptotic cell death. *Journal of Cell Biology*, 216(10), 3355–3368.  
<https://doi.org/10.1083/jcb.201706134>
- Tabuchi, Y., Takasaki, I., Wada, S., Zhao, Q.-L., Hori, T., Nomura, T., Ohtsuka, K., & Kondo, T. (2008). Genes and genetic networks responsive to mild hyperthermia in human lymphoma U937 cells. *International Journal of Hyperthermia*, 24(8), 613–622.  
<https://doi.org/10.1080/02656730802140777>
- Tang, H. L., Tang, H. M., Mak, K. H., Hu, S., Wang, S. S., Wong, K. M., Wong, C. S. T., Wu, H. Y., Law, H. T., Liu, K., Talbot, C. C., Lau, W. K., Montell, D. J., & Fung, M. C. (2012). Cell survival, DNA damage, and oncogenic transformation after a transient and reversible apoptotic response. *Molecular Biology of the Cell*, 23(12), 2240–2252.  
<https://doi.org/10.1091/mbc.e11-11-0926>
- Tang, H. M., & Tang, H. L. (2018). Anastasis: Recovery from the brink of cell death. *Royal Society Open Science*, 5(9), 180442. <https://doi.org/10.1098/rsos.180442>
- Tang, J., Chen, X., Cai, J., & Zhao, H. (2018). *Up-regulation of several selenoproteins*.
- Thompson, L. G. (2010). Climate Change: The Evidence and Our Options. *CLIMATE CHANGE*.
- Thompson, S. M., Callstrom, M. R., Butters, K. A., Knudsen, B., Grande, J. P., Roberts, L. R., & Woodrum, D. A. (2014). Heat stress induced cell death mechanisms in hepatocytes and hepatocellular carcinoma: In vitro and in vivo study: HEAT STRESS INDUCED CELL DEATH MECHANISMS. *Lasers in Surgery and Medicine*, 46(4), 290–301.  
<https://doi.org/10.1002/lsm.22231>
- Towler, M. C., & Hardie, D. G. (2007). AMP-Activated Protein Kinase in Metabolic Control and Insulin Signaling. *Circulation Research*, 100(3), 328–341.  
<https://doi.org/10.1161/01.RES.0000256090.42690.05>
- Trinklein, N. D., Murray, J. I., Hartman, S. J., Botstein, D., & Myers, R. M. (2004). The Role of Heat Shock Transcription Factor 1 in the Genome-wide Regulation of the Mammalian Heat Shock Response□D. *Molecular Biology of the Cell*, 15.

- Vancamp, P., & Demeneix, B. A. (2020). Is the Observed Decrease in Body Temperature During Industrialization Due to Thyroid Hormone-Dependent Thermoregulation Disruption? *Frontiers in Endocrinology*, 11, 470.  
<https://doi.org/10.3389/fendo.2020.00470>
- Vispo, C. R., & Bakken, G. S. (1993). The Influence of Thermal Conditions on the Surface Activity of Thirteen-Lined Ground Squirrels. *Ecology*, 74(2), 377–389.  
<https://doi.org/10.2307/1939300>
- Vujanac, M., Fenaroli, A., & Zimarino, V. (2005). Constitutive Nuclear Import and Stress-Regulated Nucleocytoplasmic Shuttling of Mammalian Heat-Shock Factor 1: Regulated Nucleocytoplasmic Traffic of HSF1. *Traffic*, 6(3), 214–229.  
<https://doi.org/10.1111/j.1600-0854.2005.00266.x>
- Wang, X., Xie, W., Yao, Y., Zhu, Y., Zhou, J., Cui, Y., Guo, X., Yuan, Y., Zhou, Z., & Liu, M. (2020). The heat shock protein family gene *Hspa1l* in male mice is dispensable for fertility. *PeerJ*, 8, e8702. <https://doi.org/10.7717/peerj.8702>
- Wang, Y., Han, X., Yang, Y., Qiao, H., Dai, K., Fan, Q., & Tang, T. (2016). Functional differences between AMPK  $\alpha 1$  and  $\alpha 2$  subunits in osteogenesis, osteoblast-associated induction of osteoclastogenesis, and adipogenesis. *Scientific Reports*, 6(1), 32771.  
<https://doi.org/10.1038/srep32771>
- Wang, Z., Cotney, J., & Shadel, G. S. (2007). Human Mitochondrial Ribosomal Protein MRPL12 Interacts Directly with Mitochondrial RNA Polymerase to Modulate Mitochondrial Gene Expression. *Journal of Biological Chemistry*, 282(17), 12610–12618.  
<https://doi.org/10.1074/jbc.M700461200>
- Warner, A., Rahman, A., Solsjö, P., Gottschling, K., Davis, B., Vennström, B., Arner, A., & Mittag, J. (2013). Inappropriate heat dissipation ignites brown fat thermogenesis in mice with a mutant thyroid hormone receptor  $\alpha 1$ . *Proceedings of the National Academy of Sciences*, 110(40), 16241–16246. <https://doi.org/10.1073/pnas.1310300110>

- Warnes, G. R. (2013). *gregmisc: Greg's Miscellaneous Functions* (R package version 2.1.5/r1689). <https://R-Forge.R-project.org/projects/r-gregmisc/>
- Warnes, G. R., Bolker, B., Bonebakker, L., Gentleman, R., Huber, W., Liaw, A., Lumley, T., Maechler, M., Magnusson, A., Moeller, S., Schwartz, M., & Venables, B. (2022). *gplots: Various R Programming Tools for Plotting Data* (R package version 3.1.3). <https://CRAN.R-project.org/package=gplots>
- Warnes, G. R., Bolker, B., Lumley, T., & Johnson, R. C. (2022). *gmodels: Various R Programming Tools for Model Fitting* (R package version 2.18.1.1). <https://CRAN.R-project.org/package=gmodels>
- Warnes, G. R., Gorjanc, G., Magnusson, A., Andronic, L., Rogers, J., MacQueen, D., & Korosec, A. (2023). *gdata: Various R Programming Tools for Data Manipulation* (R package version 2.19.0). <https://CRAN.R-project.org/package=gdata>
- Welch, W. J., & Suhan, J. P. (1985). Morphological study of the mammalian stress response: Characterization of changes in cytoplasmic organelles, cytoskeleton, and nucleoli, and appearance of intranuclear actin filaments in rat fibroblasts after heat-shock treatment. *The Journal of Cell Biology*, 101(4), 1198–1211. <https://doi.org/10.1083/jcb.101.4.1198>
- Wickham, H. (2007). *Reshaping data with the reshape package* (21(12)). <https://www.jstatsoft.org/v21/i12/>
- Woo, S. H., Oh, S. Y., Han, S. L., Choi, Y. H., Kang, K. I., Yoo, M. A., Kim, H. D., & Kang, H. S. (2000). Involvement of putative heat shock element in transcriptional regulation of p21<sup>WAF1/CIP1/SDI1</sup> by heat shock. *Korean Journal of Biological Sciences*, 4(2), 181–186. <https://doi.org/10.1080/12265071.2000.9647543>
- Wu, H., Guang, X., Al-Fageeh, M. B., Cao, J., Pan, S., Zhou, H., Zhang, L., Abutarboush, M. H., Xing, Y., Xie, Z., Alshanqeeti, A. S., Zhang, Y., Yao, Q., Al-Shomrani, B. M., Zhang, D., Li, J., Manee, M. M., Yang, Z., Yang, L., ... Wang, J. (2014). Camelid genomes reveal

- evolution and adaptation to desert environments. *Nature Communications*, 5(1), 5188.  
<https://doi.org/10.1038/ncomms6188>
- Xu, H.-Z., Wang, Z.-Q., Shan, H.-Z., Zhou, L., Yang, L., Lei, H., Liu, B., & Wu, Y.-L. (2018). Overexpression of Fbxo6 inactivates spindle checkpoint by interacting with Mad2 and BubR1. *Cell Cycle*, 17(24), 2779–2789. <https://doi.org/10.1080/15384101.2018.1557488>
- Yan, J. (2016). *som: Self-Organizing Map* (R package version 0.3-5.1). <https://CRAN.R-project.org/package=som>
- Yang, Q., Ma, Q., Xu, J., Liu, Z., Zou, J., Shen, J., Zhou, Y., Da, Q., Mao, X., Lu, S., Fulton, D. J., Weintraub, N. L., Bagi, Z., Hong, M., & Huo, Y. (2021). Prkaa1 Metabolically Regulates Monocyte/Macrophage Recruitment and Viability in Diet-Induced Murine Metabolic Disorders. *Frontiers in Cell and Developmental Biology*, 8, 611354.  
<https://doi.org/10.3389/fcell.2020.611354>
- Yin, J., Ren, W., Huang, X., Deng, J., Li, T., & Yin, Y. (2018). Potential Mechanisms Connecting Purine Metabolism and Cancer Therapy. *Frontiers in Immunology*, 9, 1697.  
<https://doi.org/10.3389/fimmu.2018.01697>
- Zargarian, S., Shlomovitz, I., Erlich, Z., Hourizadeh, A., Ofir-Birin, Y., Croker, B. A., Regev-Rudzki, N., Edry-Botzer, L., & Gerlic, M. (2017). Phosphatidylserine externalization, “necroptotic bodies” release, and phagocytosis during necroptosis. *PLOS Biology*, 15(6), e2002711. <https://doi.org/10.1371/journal.pbio.2002711>
- Zhu, H., Guo, F.-J., Zhao, W., Zhou, J., Liu, Y., Song, F., & Wang, Y. (2012). ATF4 and IRE1 $\alpha$  inhibit DNA repair protein DNA-dependent protein kinase 1 induced by heat shock. *Molecular and Cellular Biochemistry*, 371(1–2), 225–232.  
<https://doi.org/10.1007/s11010-012-1439-z>

## Curriculum Vitae

Janessa Montenegro

E-mail: [janessamonte@gmail.com](mailto:janessamonte@gmail.com)

### Professional Objective

My short-term goal is to receive an M.S. in Cellular and Molecular Biology to help advance my education and prepare me for achieving my long-term goal of receiving a Ph.D. within the same track and using this degree to join a leading wildlife conservation organization. I am an aspiring graduate student interested in conservation for the purpose of preserving biodiversity and genetic diversity, restoring diminished ecosystems, and advancing the science of preventing future extinctions.

### Education

University of Nevada, Las Vegas; M.S. Program - Cellular and Molecular Biology

Anticipated Graduation Date: Summer 2023

- Research: To understand, at a cellular level, the mechanisms of stressor resilience and sensitivity in a variety of mammalian species to extreme, environmental heat conditions
- Taught BIOL 191L with a Graduate Assistant (GA) position
- Gained skills and experience in immunofluorescence imaging, Western Blots, qPCR, and Lactate Dehydrogenase Assays
- Acquired knowledge and skills regarding cell culturing
- Gained basic bioinformatic skills

University of Nevada, Las Vegas; B.S. Degree - Cellular and Molecular Biology

Graduation Date: December 15, 2020

- Improved communication and teaching skills as a UTA for BIOL 197
- Procured and improved mentoring skills in the Louis Stokes Alliances for Minority Participation (LSAMP) program
- Acquired peer leadership skills in group activities in National Society Leadership and Success (NSLS)
- Gained laboratory skills in undergraduate research provided by LSAMP program

Southwest Career and Technical Academy in Las Vegas, NV

Hospitality and Tourism [2013 – 2017]

- Advanced Honors Diploma
- Gained problem-solving skills via case scenarios in hospitality mock settings
- Conducted school-wide projects with colleagues to gain and improve teamwork and communication skills
- Distributive Education Clubs of America (DECA) Program – Focused interest in marketing, entrepreneurship, finance, hospitality and management

## **Teaching and Mentoring Experience**

Teaching Assistant

The University of Nevada, Las Vegas [Fall 2020 and Spring 2021]

- Instructed BIOL 191L with a Graduate Assistant (GA) position

## Undergraduate Teaching Assistant

University of Nevada, Las Vegas [Summer 2018]

- Assisted the Teacher's Assistant (TA) with any requested tasks
- Lectured one lab session to the class
- Proctored during quizzes/exams, helped set up microscopes and materials for quizzes and lectures
- Assisted students with questions

## LSAMP

University of Nevada, Las Vegas [Fall 2019 – Fall 2020]

- Mentored freshman and sophomore undergraduate students
- Directed students to appropriate support services at UNLV
- Guided students with any questions or concerns
- Encouraged students to conduct undergraduate research

## Undergraduate Research Experience

Undergraduate Research Provided by LSAMP

University of Nevada, Las Vegas [Summer-Fall 2020]

- PCR and DNA sequencing
- Managed and cleaned DNA sequence data using Sequencher program

## Animal Training

University of Nevada, Las Vegas [Fall 2020]

- Mouse restraint training

## **Publications**

- Constructed a manuscript regarding my undergraduate research
  - Montenegro, J. (2020). The Population Genetics of *Apodemus* in the Country of Georgia. Department of Life Sciences, University of Nevada, Las Vegas.

## **Poster Presentations**

- Presented undergraduate research project on the 21<sup>st</sup> Undergraduate Research Symposium
  - Montenegro, J. (2020). The Population Genetics of *Apodemus* in the Country of Georgia. Department of Life Sciences, University of Nevada, Las Vegas.
- Presented poster regarding Master's thesis project at the American Physiological Society Oct. 2022 conference
  - Montenegro, J. (2022). Cellular heat responses of desert mammals promote survival in extreme conditions. Department of Life Sciences, University of Nevada, Las Vegas.

## **Field Work**

Tule Springs Fossil Beds National Monument



Las Vegas, NV [Sept. 2020]

- Assisted Dr. Neiswenter with setting traps for a small mammal survey

## **Clinical Experience**

Intern/Assistant

Mai Orthodontics, Las Vegas, NV [Summer 2016]

- Mentored and taught by Dr. Mai and staff
- Assisted with small tasks on patients
- Conducted x-ray shots
- Managed front desk responsibilities that included maintaining schedule book and contacting patients
- Cleaned equipment and utensils

## **Skills**

- Technical: Scientific tasks, project planning, task management
- Interpersonal: Communication, teamwork, and leadership skills
- Laboratory: Standard PCR, gel electrophoresis, western blots, qPCR, cytotoxicity assays

Achievements

- Certification in the Hospitality and Tourism industry
  - SWCTA, Las Vegas, NV Summer 2017

- Certification from National Society of Leadership and Success (NSLS)
  - UNLV, Las Vegas, NV December 2018
- Nevada INBRE Scientific Core Service Award
  - UNLV, Las Vegas, NV December 2022